

CLIMATE PREDICTABILITY AND SIMULATION  
WITH A GLOBAL CLIMATE MODEL

by

ALAN DAVID ROBOCK

B.A., University of Wisconsin  
(1970)

S.M., Massachusetts Institute of Technology  
(1974)

SUBMITTED IN PARTIAL FULFILLMENT OF THE  
REQUIREMENTS FOR THE DEGREE OF

DOCTOR OF PHILOSOPHY

at the

MASSACHUSETTS INSTITUTE OF TECHNOLOGY

May, 1977

Signature of Author.....  
Department of Meteorology, May 1977

Certified by.....  
Thesis Supervisor

Accepted by.....  
Chairperson, Departmental Committee on Graduate Students

**WITHDRAWN**  
**FROM** MASS. INST. TECH. Lindgren  
**MIT LIBRARIES** JUN 11 1977

CLIMATE PREDICTABILITY AND SIMULATION  
WITH A GLOBAL CLIMATE MODEL

by

ALAN DAVID ROBOCK

Submitted to the Department of Meteorology on May 5, 1977 in partial fulfillment of the requirements for the Degree of Doctor of Philosophy

ABSTRACT

Various theories of both internal and external causes of climate change on the time scale of 100 years are critically examined. Volcanic dust; solar variation; anthropogenic carbon dioxide, aerosols and heat; and stochastic variability (almost intransitivity) are all considered plausible. Data on the past variations of these forcings are collected. Observational data on climate change during the past are also assembled, and the sources of error in the data are evaluated.

A seasonal, zonally-averaged, vertically-averaged, highly-parameterized numerical model, similar to that of Sellers (1973, 1974) is used to test the above theories of climate change. The model simulates the present climate fairly well, but several improvements are suggested for further studies with the model. These include more accurate formulations of cryospheric and other seasonal variations, radiative flux, and oceanic heat flux and mixed layer depth variations.

Results show that volcanic dust and the natural atmospheric variability are sufficient to explain the observed Northern Hemisphere climate change of the past 100 years. Solar variation may have contributed to the Little Ice Age, but its influence is not evident during the past 100 years. Anthropogenic carbon dioxide has a much larger effect than anthropogenic heat, and is just now becoming important enough to cause climate change. Anthropogenic aerosols are insufficiently understood to determine their effects, but may cancel out the warming effects of carbon dioxide and heat.

Thesis Supervisor: Edward N. Lorenz

Title: Professor of Meteorology

#### ACKNOWLEDGEMENTS

I thank my thesis supervisor, Edward Lorenz, for suggesting that I study climate, for suggesting the random perturbation experiments, and for continued guidance and support throughout the writing of this thesis. I feel privileged to have been able to work with him. I also benefited greatly from discussions with many students and faculty in the department, whom I also thank.

I thank Stephen Schneider of NCAR for his valuable discussions of climate modeling theory, and Abraham Oort of GFDL and J. Murray Mitchell of NOAA for providing me with unpublished data.

I thank Miffi Bedrick for her love, support, and general putting up with me as I worked on this thesis, and for helping to plot some of the figures.

I thank Isabelle Kole for her beautiful job in drafting most of the figures and Cheri Pierce for her excellent and fast typing job during a beautiful weekend when she would have rather been outside. I also thank Eve Sullivan for typing most of the rough draft.

The National Science Foundation supported me financially during the writing of this thesis with a Graduate Fellowship and through grant OCD 74-03969, and the National Aeronautics and Space Administration provided me with computer time at the Goddard Institute for Space Studies.

"The answer, my friend, is blowin' in the wind;  
the answer is blowin' in the wind."

- Bob Dylan

TABLE OF CONTENTS

TITLE PAGE .....	1
ABSTRACT .....	2
ACKNOWLEDGEMENTS .....	3
DYLAN QUOTE .....	4
TABLE OF CONTENTS .....	5
CHAPTER I. Introduction .....	8
CHAPTER II. Climate theory .....	11
A. Past climate .....	12
1. The data .....	12
2. The quality of the data .....	21
B. Causes of climate change .....	25
1. External causes .....	26
a. Sunspots and other solar forcing .....	26
b. Volcanic dust .....	40
c. Anthropogenic carbon dioxide .....	46
d. Anthropogenic aerosols .....	49
e. Anthropogenic heat .....	53
f. Other anthropogenic effects .....	54
2. Internal causes (almost-intransitivity) .....	55
3. Ice age time scale causes .....	60
a. Intergalactic dust .....	61
b. Orbital variations .....	61
c. Continental drift .....	62
d. Internal causes .....	63
e. Ice age simulations .....	63
C. Climate feedback mechanisms .....	63
1. The hydrological cycle .....	64
a. Water vapor-greenhouse .....	65
b. Ice (or snow)-albedo .....	66
c. Clouds .....	66
2. Ocean-atmosphere coupling .....	67
3. Temperature-radiation .....	69
4. Radiative-dynamic coupling .....	69
5. Temperature-lapse rate .....	69
D. Different modeling approaches .....	70
1. Model classification .....	70
2. Choice of a model .....	74
a. Advantages of the model .....	74
b. Disadvantages of the model .....	76
3. Previous simulation attempts .....	77

CHAPTER III. The model .....	79
A. General description .....	79
B. The equations .....	80
1. Thermodynamic energy equation .....	80
2. Vertical profiles .....	87
3. Dynamical fluxes .....	90
a. Mean wind fluxes .....	90
b. Atmospheric eddy fluxes .....	92
c. Oceanic eddy fluxes .....	93
4. Surface heat storage .....	94
5. Solar radiation .....	94
6. Terrestrial radiation .....	97
C. Numerical method .....	99
D. Differences between my model and Sellers' .....	103
1. Infrared formulation .....	103
2. Number of time steps .....	105
3. Seasonal forcing .....	106
4. Smoothing .....	106
5. Minor differences .....	107
E. The balanced model climate and comparison with real data ..	108
1. The data .....	109
2. Temperature .....	112
3. Sea ice .....	118
4. Wind .....	118
5. Radiation .....	118
6. Horizontal heat fluxes .....	135
7. Summary .....	144
F. Parameter sensitivity .....	147
1. Changing parameters by 1 % .....	147
2. Different parameterizations .....	151
G. Suggestions for future model improvements .....	156
CHAPTER IV. Results .....	160
A. External causes .....	160
1. Design of the experiments .....	160
2. Solar forcing .....	165
3. Volcanic dust .....	167
4. Anthropogenic effects .....	174
B. Internal causes .....	178
1. Design of the experiments .....	178
2. Results .....	180
C. Geographical sensitivity .....	187
CHAPTER V. Conclusions .....	190
APPENDIX A. Derivation of geopotential height equation (21) .....	193
APPENDIX B. Derivation of a coefficients, equations (24)-(34) .....	194

APPENDIX C. IR model .....	200
APPENDIX D. Random number generator .....	205
REFERENCES .....	206
BIOGRAPHICAL NOTE .....	219

## Chapter I. Introduction

This thesis is an attempt to better understand the causes of climate change during the period of observational record - approximately the last 100 years. Climate can be defined as a set of statistics of atmospheric variables taken over a long, but finite, time interval and a specified space domain. The time interval should be longer than a few weeks to eliminate the day-to-day changes of the weather, and it can extend all the way to ice-age time scales ( $10^4 - 10^6$  years). The statistics can include higher moments as well as means.

The atmospheric variable that is used in this thesis to represent climate is 1000 mb or surface temperature. This is for several reasons. For more than 20 years ago, surface data is the only observational data available. It is also the most easily deduced data from pre-instrumental time. Temperature has an advantage over precipitation in that it has a much smoother distribution in time and space, so that fewer observations are necessary to represent its field. Furthermore, the energy balance equation makes it an easy variable to calculate. And it must be calculated in any case in order to calculate important responses of the climate system, for instance heat storage in the oceans and the ice-albedo feedback.

An understanding of climate change is important to society for several reasons. Seasonal forecasting would allow more efficient use of scarce energy resources and would allow farmers to plan the proper crops to increase agricultural production. In the longer term, it is



important to be able to separate the natural fluctuations from those inadvertently caused by man, to allow us to modify our activities to prevent unwanted climate changes. Along the same line, suggestions are already being made as to how man could advertently modify the climate. Much more study and understanding of the complex nature of the system and all its feedbacks is necessary before such actions should be considered.

The approach of this thesis is to use a numerical model to try to simulate the observed climate changes of the past 100 years, forcing it according to the different plausible theories of climate change. The model is the global, seasonal, highly-parameterized, energy-balance climate model of Sellers (1973, 1974), modified and corrected for use in this thesis. It had been newly developed at the time this thesis was begun, and had not been applied to the problem of time-dependent climate change.

The first step was to collect and analyze the data on past climate change. This is done in Chapter II. This chapter also contains a detailed analysis of the possible causes of climate change during the past 100 years, and the data describing these forcings. The next chapter describes the model and the changes made in it, and compares its seasonal cycles and annual average fields of temperature, radiation and heat fluxes to the available observations. Suggestions are made as to how the model might be improved to correct the deficiencies noted in the data comparison, but the derivation of new parameterizations is beyond the scope of this thesis. Chapter IV presents the results of the simulation attempts with the model, and also examines internally

caused climate change, which relates to climate predictability.

Chapter V is the conclusion.

The model does quite a good job of simulating the present annual averaged climate, and the seasonal cycle. Certain parameterizations need to be improved, however, before further studies are done with it. The most important and obvious ones are the seasonal cycle of ice and snow, zenith angle albedo effects, and the ocean heat flux. Once these corrections are made, the model shows great promise for further use in simulating climate change.

The model simulation experiments allow the climate change of the past 100 years to be completely explained by volcanic dust and natural variability. Solar forcing does not play a role, and anthropogenic effects are not yet of a magnitude to be observable. These statements are subject to the limitations of an imperfect model, data inadequate both in coverage and accuracy, and lack of understanding, or inclusion, of processes which may be important.

## Chapter II. Climate Theory

In order to understand the significance of the work done in this thesis, it is important to know what the past climate has been and what the present state of the theory of climate is. This chapter will review our present knowledge of the past climate and the quality of these observations. It will discuss possible causes of climate change and analyze the data available on the variations of these forcings over the past 100 years. It will describe climate feedback mechanisms and the different approaches to climate modeling. Finally, it will explain why the model used in this thesis was chosen.

Several comprehensive survey articles are available on climate modeling. The best of these is the one by Schneider and Dickinson (1974). It discusses many aspects of climate modeling, but does not give a very detailed view of past climate change. Included topics are definition of climate, climatic predictability, internal versus external causes of climate change, ingredients of a theory of climate, modeling methodology, and an extensive discussion of current modeling efforts of all types. The article includes an extensive bibliography.

Two other surveys were also published in 1974. One of these is the GARP (1974) report. It includes observed variability of the climate system, the physical basis of climate and climate modeling, the design of climate models, and the design of an observational program for climate. The Gates and Mintz (1974) report covers much the same areas and includes a detailed plan for a National Climatic Research Program and a

detailed summary of our present knowledge of past climatic variations.

The SMIC (1971) report presents a summary of past climate, the theory of climate and climate models, as well as indicating various ways in which man's activities may influence the climate of the future.

#### A. Past climate

##### 1. The data

The earth is approximately 4.5 billion years old. During almost 90% of this time, there is no direct evidence for the climate of the earth. During the past billion years there is evidence for three major glaciations of the earth: at least one from 800 million to 600 million years ago, called the Late Precambrian Glacial Age(s); one from 320 million to 250 million years ago, called the Permo-Carboniferous Glacial Age; and our present glacial age, which began only 10 million years ago. Higher organized life began on the earth about 550 million years ago, and during 90% of the time since then the poles have been ice-free, so in this time frame, we are now in an anomalously cold period of our earth's history. During the Permo-Carboniferous Glacial Age the continents were joined in one super-continent (Pangaea) and were yet to drift to their present locations. This summary of the distant past is by way of perspective, as this thesis will deal with time scales on the order of 100 years into the past. The best source for climatic history is "A Survey of Past Climates", Appendix A, pp. 179-276 of Gates and Mintz (1974).

Figure 1 gives a summary of our climatic history on the longest known time scales. Continental drift played a major part in the

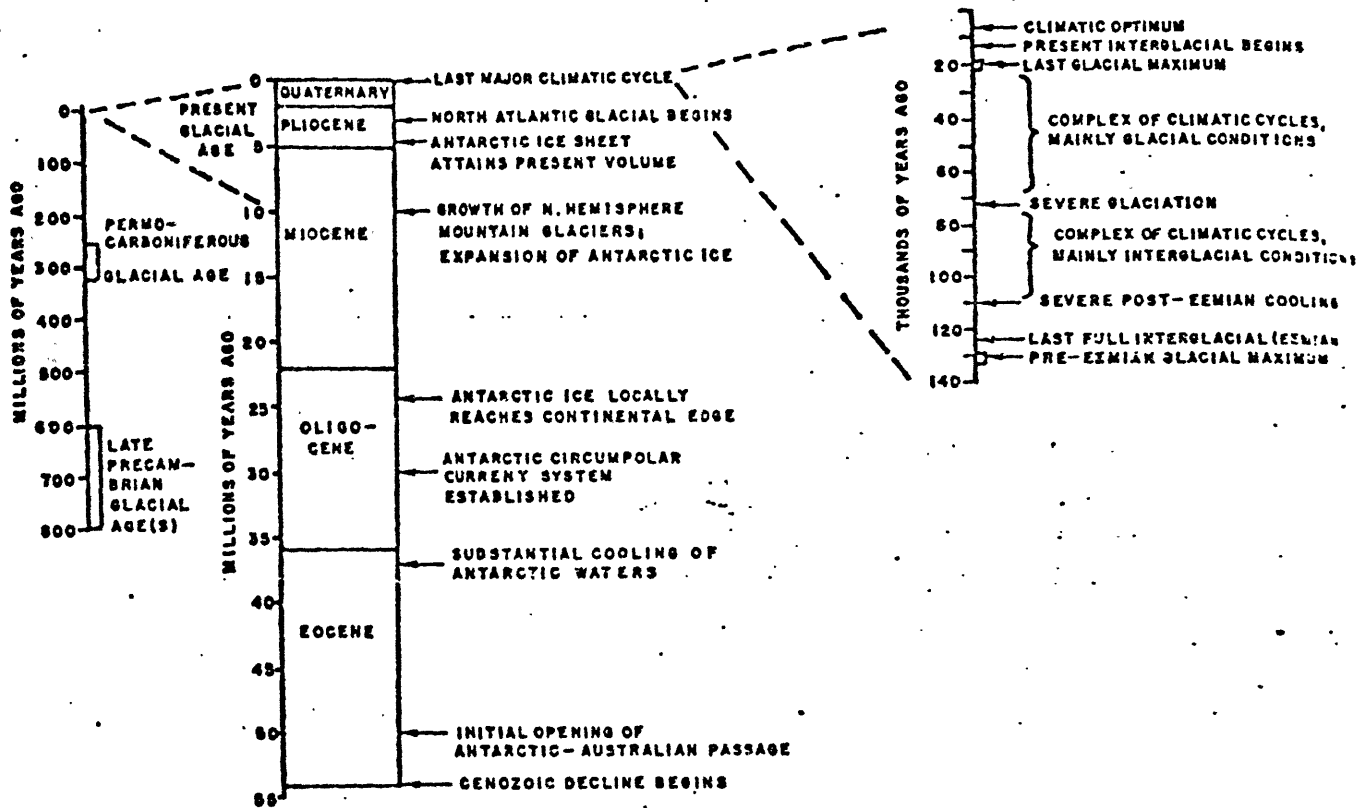


Fig. 1 --History of glacial ages over the last 1,000,000,000 years. Intervals when extensive polar ice sheets occurred are indicated as glacial ages on the left. An outline of significant events in the Cenozoic climate decline is given in the middle, and the significant climatic events during the last major glacial-interglacial cycle is given on the right.

This figure is from Gates and Mintz (1974).

development of the present glacial age. For the purpose of this thesis, however, the continents will be assumed to be fixed in their present locations as part of the fixed external system. During the last 500,000 years, warm interglacials have been occurring approximately every 100,000 years. This can be seen in Figure 2e. Looked at from this perspective, we are now in an anomalously warm period between glacial maxima. The last interglacial period was approximately 125,000 years ago, and since then there have been complex variations and a gradual cooling and ice advance until 10,000 years ago when the present interglacial began. This can be seen in Figure 1 and Figure 2(d and c). The Milankovitch hypothesis has received much support recently as an explanation of climate change on this time scale. See section II.B.3 for further discussion of the causes of ice age time scale climate changes.

The present interglacial began about 10,000 years ago, and has been basically warm with several cold intervals which did not result in large-scale glaciation. The last cold interval occurred from 1430 to 1850 A.D. and was called the Little Ice Age. It had cold maxima about 1450 and 1650 A.D. See figures 2b and 3. The climate then warmed and continued warming until about 1940 after which there has been a cooling.

All of the previous record comes from direct evidence of temperature related phenomena, in historical records when available, and before that and in addition, from evidence such as tree ring growth, oxygen isotope ratios in ice cores, tree-line and glacier margin fluctuations, pollen records from soil cores and fossil plankton records from deep-sea cores. As one goes farther and farther back in time,

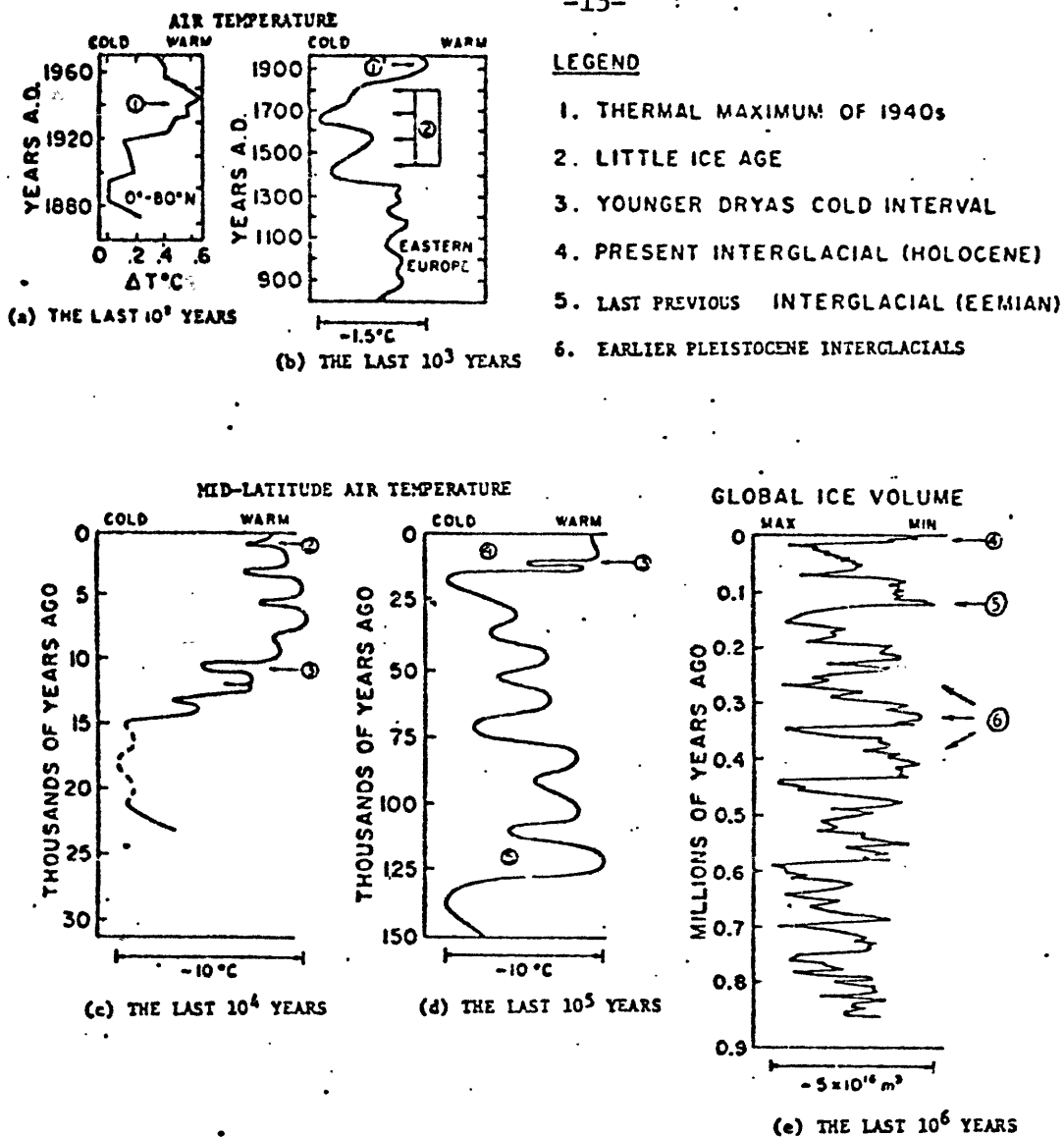
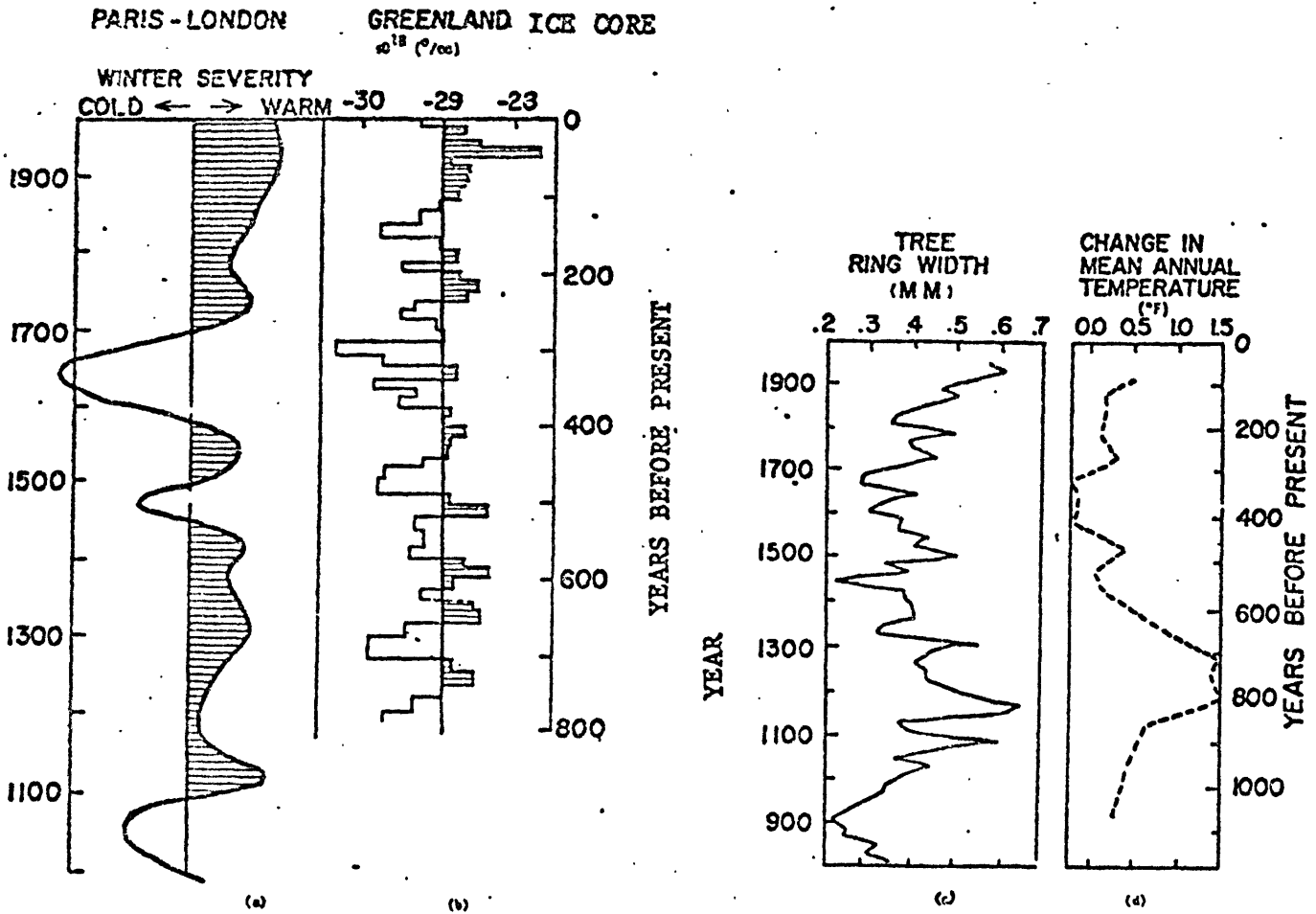


Fig. 2 --Generalized trends in global climate: the past million years. (a) Changes in the five-year average surface temperatures over the region 0 - 80 N during the last 100 years (Mitchell, 1963). (b) Winter severity index for eastern Europe during the last 1000 years (Lamb, 1969). (c) Generalized mid-latitude Northern Hemisphere air-temperature trends during the last 15,000 years, based on changes in tree-lines (LaMarche, 1974), marginal fluctuations in alpine and continental glaciers (Denton and Karlén, 1973), and shifts in vegetation patterns recorded in pollen spectra (van der Hammen *et al.*, 1971). (d) Generalized Northern Hemisphere air-temperature trends during the last 100,000 years, based on mid-latitude sea-surface temperature and pollen records, and on worldwide sea-level records (see Fig. A13). (e) Fluctuations in global ice-volume during the last 1,000,000 years as recorded by changes in isotopic composition of fossil plankton in deep-sea core V28-238 (Shackleton and Opdyke, 1973). See legend for identification of symbols (1) through (6).

This figure from Gates and Mintz (1974).



g. 3.---Climatic records of the past 1000 years. (a) The 50-year moving average of a relative index of winter severity compiled for each decade from documentary records in the region of Paris and London (Lamb, 1969). (b) A record of  $\delta^{18}O$  values preserved in the ice core taken from Camp Century, Greenland (Dansgaard *et al.*, 1971). (c) Records of 20-year mean tree growth at the upper treeline of bristlecone pines, White Mountains, California (LaMarche, 1974). At these sites tree growth is limited by temperature with low growth reflecting low temperature. (d) The 50-year means of observed and estimated annual temperatures over central England (Lamb, 1966).

; figure is from Gates and Mintz (1974).



more and more of the detailed fluctuations are lost and the evidence is more and more speculative. Only the last 100 years of this climatological record have been documented with instrumental observations and only in the last 25 years has there been adequate coverage of the Northern Hemisphere continents. Both the Southern and Northern Hemisphere oceans still lack adequate data coverage.

From 1880 to 1940 the annual mean Northern Hemisphere temperature rose about 1°C and since then has fallen about 0.5°C. This trend is superimposed on highly variable inter-annual changes. This can be seen in Figure 4, which shows the data of Budyko (1969), Asakura (Gates and Mintz, 1974) and Angell and Korshover (1977). The same trend can be seen in the data of Mitchell (1961) (Figure 5), which is given in five-year averages, for four different latitude bands (0-80°N, 0-60°N, 0-60°S and 40-70°N) for both annual and winter averages, and for 30°S-30°N for annual averages only. [One would not expect the tropics to exhibit winter behavior different from annual behavior.]

The above two collections of data represent the extent and quality of instrumental observations of climate change on the time scale of 100 years. Several much shorter (5-30 years) data sets exist, which include upper air and not just surface data. Starr and Oort (1973) studied the temperature change during the five-year period 1958 to 1963 from 10°S to 75°N and found an 0.6°C decrease in the mass-weighted temperature from the surface to 50 mb. During this same time their surface temperature rose by 0.26°C. This change involved a considerable lapse rate change. The next 10 years of data have been collected by Oort (personal communication) but have not yet been published. This

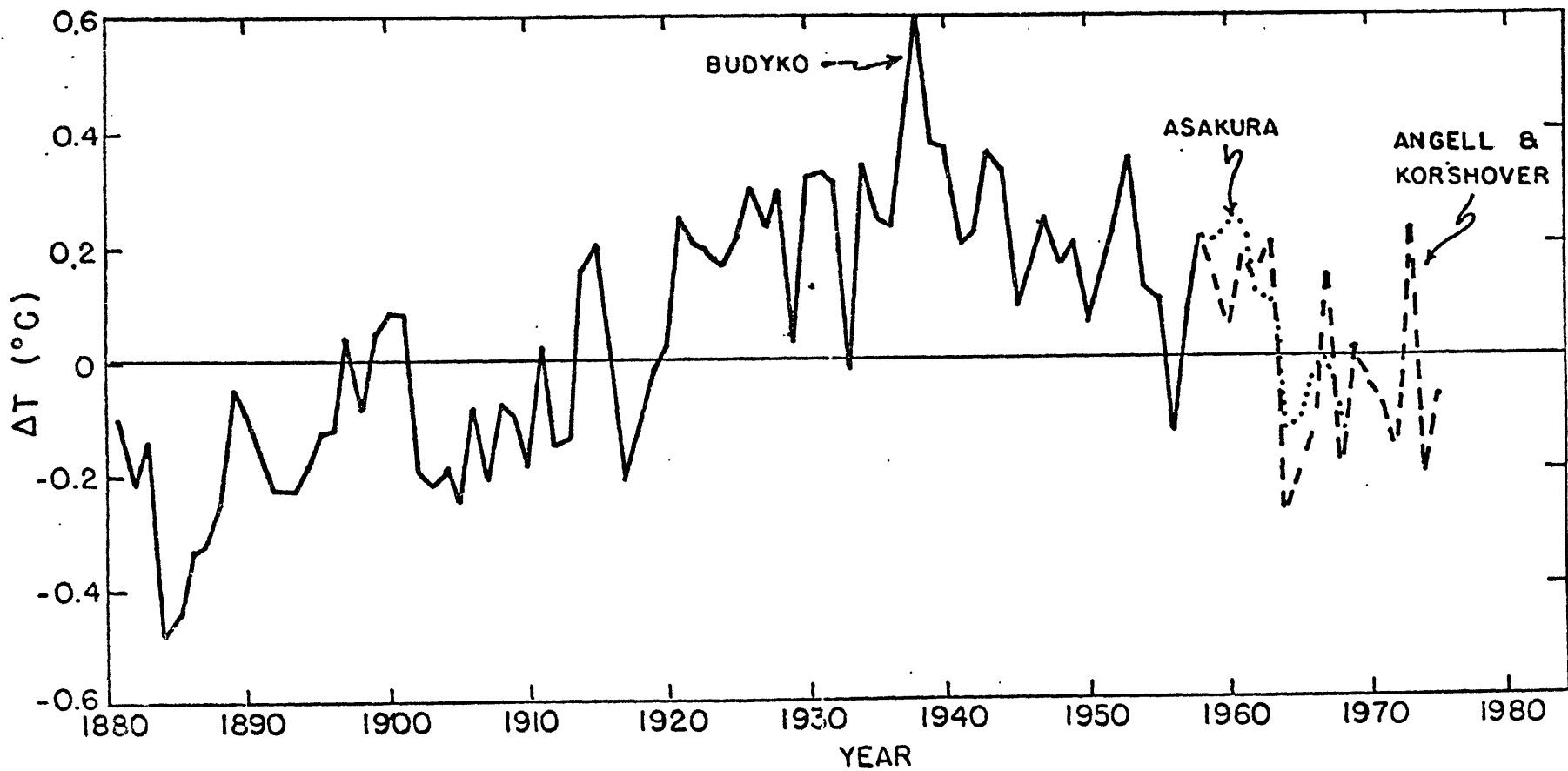


Figure 4. Annual mean temperature of the Northern Hemisphere for 1881-1975, from Budyko (1969), Asakura (Gates and Mintz, 1974), and Angell and Korshover (1977).

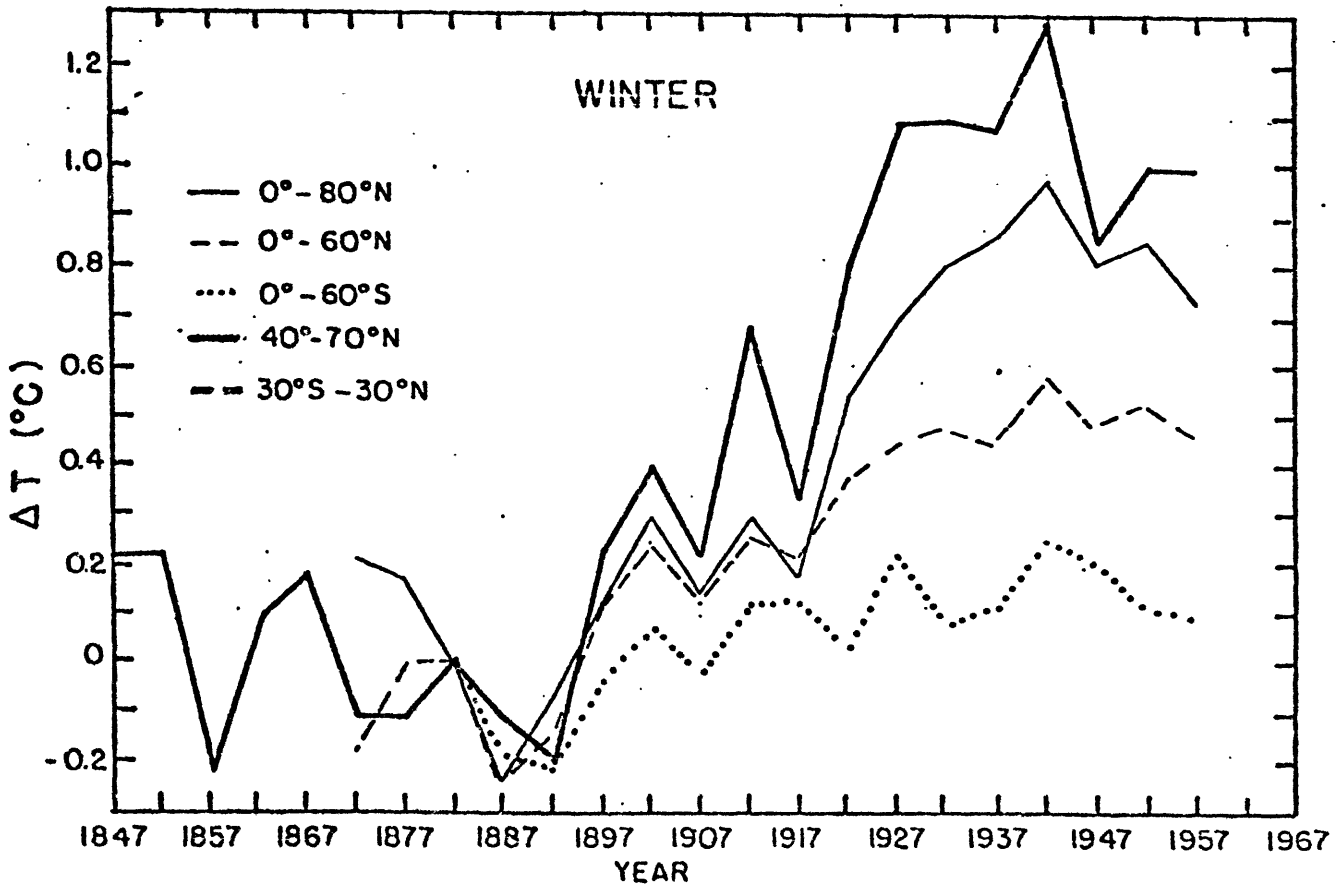
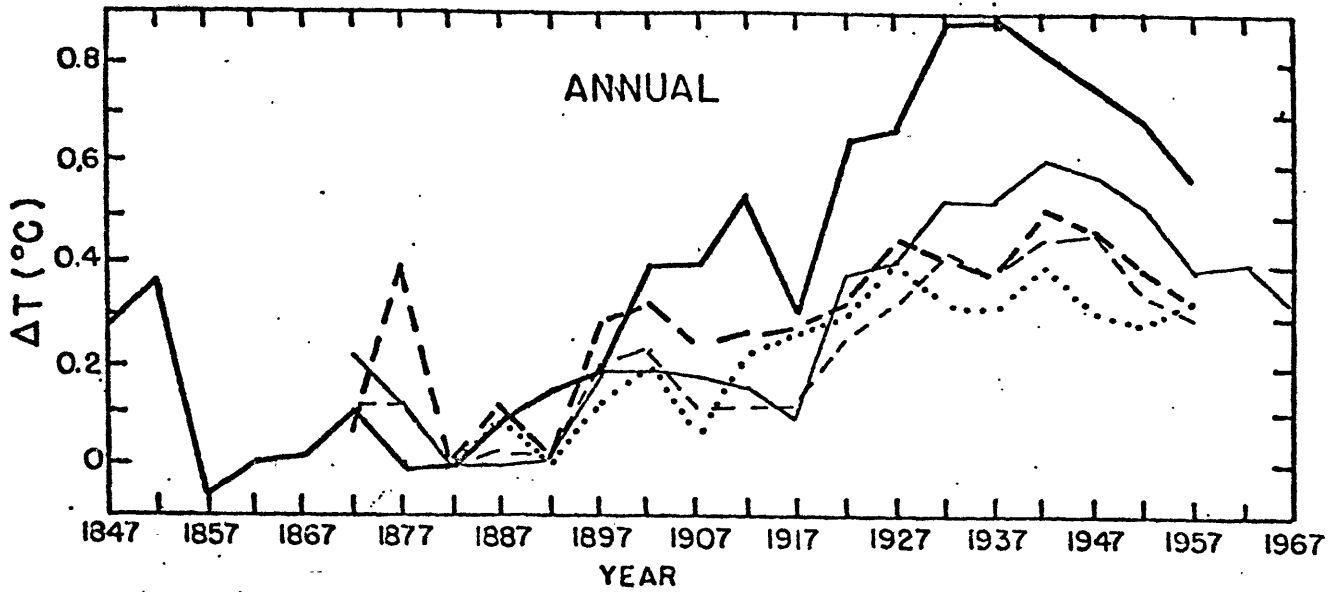


Figure 5. Five-year average temperatures by latitude bands, from Mitchell (1961). The 0°-80°N annual record is updated by Reitan (1974). The center of the five-year averaging periods are indicated on the abscissa.

collection includes the entire world-wide radiosonde network for these latitudes with sophisticated error detection and correction, so cannot be dismissed due to inaccuracy of the data. Yet on the time scale of climate change, five years is a very short time, and a longer record needs to be collected and studied before the complex changes observed during this five year period can be interpreted as typical of climate change, or as part of the random natural variability of the atmosphere.

Angell and Korshover (1975) collected sets of 300 mb and 700 mb temperatures for six different latitude bands from six fairly evenly spaced stations around each band for the time period 1958-1973. The representativeness of these few data points at only two levels remains open to question as indicative of global climate change, especially since Starr and Oort found rather unrelated changes in the upper atmosphere and at the surface, yet their results are suggestive. They found quite different changes at different latitude bands and opposite changes in the two hemispheres. They also found lapse rate changes associated with mean temperature changes.

A more comprehensive collection (Angell and Korshover, 1977) will soon be published which includes data from the surface to 100 mb for a more extensive, but still sparse, global network of 63 stations, for 1958 to 1975. They found complex changes in the vertical structure and horizontal distribution of temperature changes. Their data for Northern Hemisphere surface temperature agree surprisingly well with those of Yamamoto, et al. (1975) who used 343 stations in the Northern Hemisphere, an order of magnitude more. These data of Angell and Korshover, combined with those of Budyko in Figure 4, provide a 95 year record of the

Northern Hemisphere average surface temperature, the only one with annual average values. Borzenkova, et al. (1976) have also published an analysis of Northern Hemisphere surface temperatures for 1881 to 1975, but only for latitude circles 20°N to 85°N.

Damon and Kunen (1976) studied a very sparse set of surface data for the Southern Hemisphere for the years 1943 to 1974. The lack of land area, population, and therefore, weather observing stations makes data collection for this hemisphere especially difficult. They found that during the post World War II period, while the Northern Hemisphere surface temperatures were falling (see Figures 4 and 5), the Southern Hemisphere temperatures were rising!

All the above collections, including Mitchell's, have found a larger temperature change in the polar regions than in the hemisphere as a whole. This observation, which is well simulated by the model used in this thesis as well as all other climate models incorporating a latitudinal variation, will be explained later in terms of the ice-albedo feedback mechanism, including the thermal inertia effect of the ice.

Very long surface temperature records (Gordon and Wells (1976) analyzed a 250 year record for central England.) exist for certain locations, but these are not necessarily representative of other than their immediate locality.

## 2. The quality of the data

Several problems arise when trying to measure zonal averages of surface temperature. The first is getting consistent, long records of

measurements at each station. Errors inherent in these measurements include observational errors (+ or - effect on observed temperature), movement of the thermometer either at one location or to another location in the same city (+ or -), changes in the observing equipment (+ or -), urbanization around the observing station (+), and breaks in the record due to warfare, loss of funding or loss of records. The second is getting enough stations with a long period in a given averaging area. Only recently, in the last 25 years, have world-wide land observing stations been established. Oceanic data coverage is still very sparse. This leads to the next problem, that of getting a good geographical spread of stations within an averaging area. The fourth and last problem is errors introduced in deciding how to average the sparse data, and what types of corrections to make for missing data.

The combination of these problems can lead to large errors in the reported climate "observations". Mitchell tried to correct for some of these errors, and estimate the magnitude of others. As for measurement errors, he eliminated from the data changes from one five year period to the next during which the station locations changed (personal communication), but Budyko did not mention any such correction. Mitchell (1967) estimated the urbanization effect for the Northern Hemisphere in general as  $+0.15^{\circ}\text{C}$  from 1850 to 1960, but did not correct the data for this. Damon and Kunen calculated the urbanization effect to be  $+0.2^{\circ}\text{C}$  for cities larger than 750,000 inhabitants for the Southern Hemisphere data for 1943 to 1974, during which Mitchell found no effect in the Northern Hemisphere. Budyko did not mention the effect. Urbanization, then, seems to have had an important

effect on temperature measurements, but without detailed information about each thermometer location, correction is not possible, and has not been done.

The second problem, that of not enough stations with long records, makes the first part of Mitchell's and Budyko's records questionable, especially Mitchell's 40°N-70°N record (personal communication), since Mitchell (1963) showed that records for individual stations are not well correlated with global averages.

The third problem, that of geographical representativeness of the data, may not be that much of a problem if an attempt is made to evenly space the stations in a zonal direction and area-weight zonal averages when computing hemispheric averages. Mitchell (1963) did this and found that the warming from 1880 to 1940 was significant for the hemisphere as a whole, and that the cooling since then was probably significant. Budyko and Borzenkova, et al. used analyzed maps of observations and then read evenly spaced data from grid points on the maps, also correcting for the geographical unevenness of the observations. Angell and Korshover (1977) used evenly spaced data points and Yamamoto et al. used a very dense network. Budyko also properly area-weighted the zonal averages, as did Mitchell, Angell and Korshover, Yamamoto, et al. and Borzenkova, et al. Damon and Kunen, however, did not area-weight their data, and the warming they found was exaggerated by measurements from the South Polar region.

An idea of the magnitude of error introduced by the fourth problem can be obtained as follows. Figure 6 is a comparison of five-year averages of Budyko's Northern Hemisphere record with Mitchell's 0°-80°N

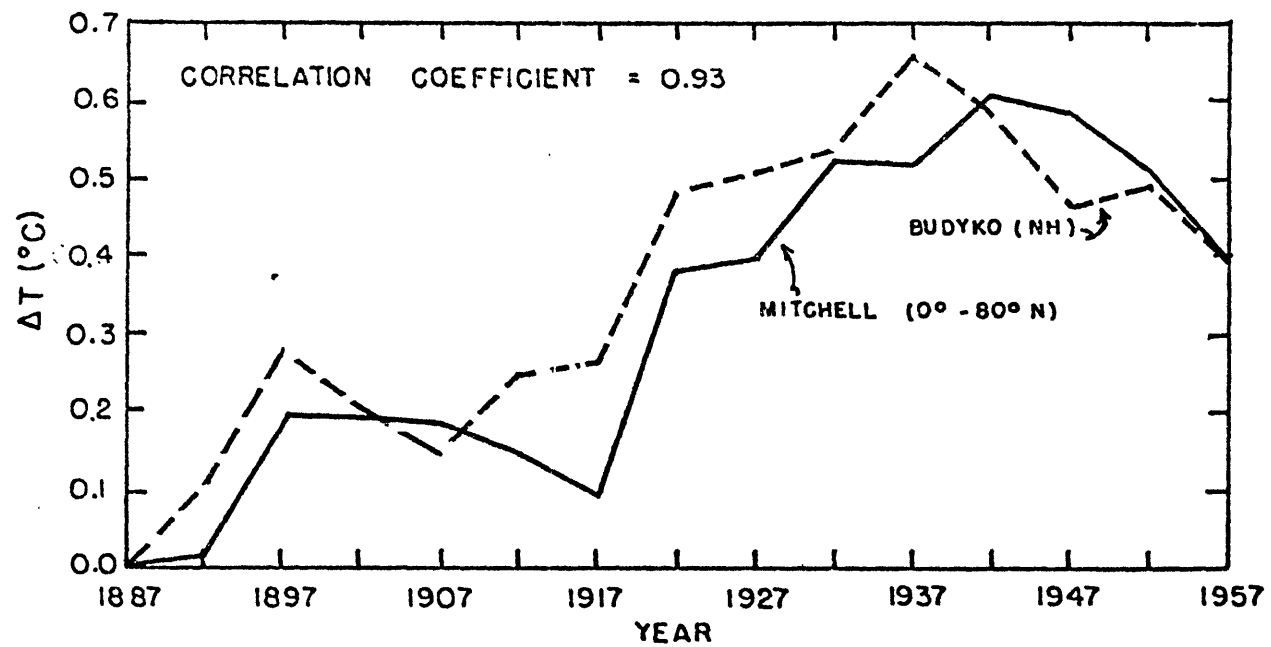


Figure 6. Budyko-Mitchell correlation of five-year average Northern Hemisphere temperature record.



annual (as opposed to winter) record. They are supposedly records of the same thing, since there are no observations north of 80°N, but there are large discrepancies in the two records. The correlation coefficient of the two curves is 0.93.

Although there are many possible sources of error, of unknown magnitude, in the climate records of Budyko and Mitchell, they are the only records that exist for the last 100 years. [Mitchell's 40°N-70°N record is the most complete of these, extending back to 1840 and with the densest data coverage, because North America and Europe are in this region. But still there are large portions of ocean in this region for which data had to be interpolated, and few stations during the earlier part of the record.] So these records will be used to compare to model simulation results. A perfect agreement should not, however, be expected. It may be possible, with this model or others (see Bryson and Dittberner, 1976) to adjust parameters so that the model results closely coincide with the climate record. But with the uncertainties in the climate record, this is not a useful exercise.

#### B. Causes of climate change

Many causes have been suggested for climate change. This section will discuss these various theories, indicating which ones are important for the time scale considered in this thesis (100 years), and which ones will be tested with a numerical model. A critical analysis of the validity of the various theories, and of the existing data on the extent, magnitude and variation of the forcings on the 100-year time scale is also included.

The causes of climate change are either natural or anthropogenic. In the past, variations of climate were due only to natural causes, but now human activities may be reaching the level where they will have a measurable impact on the climate. The causes of climate change can also be classified as either external to the system, such as changing the incoming radiation, the atmospheric composition or the earth's surface; or internal, such as stochastic forcing or almost-intransitivity. The discussion in this section will be organized according to this latter classification.

### 1. External causes

#### a. Sunspots and other solar forcing

Radiation from the sun, with its unequal distribution horizontally and vertically within the atmosphere and on the surface of the earth, produces weather and drives the climate system. Due to the tilt of the earth's axis, solar radiation is also unevenly distributed in time and produces the well-known seasonal cycle. The amount of radiation reaching a surface perpendicular to the radiation at the mean earth-sun distance is known as the "solar constant". Its value, as best known by present observation, is 1.94 ly/min., or  $1354 \text{ W/m}^2$ .

If the solar constant were truly constant, in both total radiation and spectral distribution, it could not cause the climate to change. But it has been postulated that the solar constant does change, and that these changes are related to the well-observed (since 1750) 11-year sunspot cycle, or to other harmonics of the cycle. Ulrich (1975) has noted that the solar luminosity can be theoretically

variable, since present models of a constant sun have been invalidated by the lack of solar neutrinos reaching the sun. Lockwood (1975) observed brightness changes in Uranus, Neptune and Titan that were correlated over a four-year period, indicative of either solar brightness changes or solar induced albedo changes. Solar physics theory is not yet advanced enough, however, to explain the cause or magnitude of solar constant variation, if any.

General discussions of the sunspot-solar constant relationships include those of Dickinson (1975), Gribbin (1973), Gribbin and Plagemann (1974), and Meadows (1975). These speculations have been encouraged and promoted by the large number of authors who have claimed to have found 11 year periodicities in observations of various meteorological phenomena. They include Berger (1971) - temperature extremes at Omaha, Nebraska; Cohen and Sweetser (1975) - Atlantic tropical cyclones; Currie (1974) - surface air temperature; King (1973) - length of the growing season in Scotland, global mean temperature, wet and dry seasons in England, 500 mb heights, and Beirut rainfall; King et al. (1974) - rainfall, temperature, and agricultural production; Wood and Lovett (1974) - Addis Ababa rainfall; and Willett (1974), who uses the double sunspot cycle to explain past climate change and predict the future. Mock and Hibler (1976) found a twenty-year oscillation in eastern North American temperature records until 1960, which may either be interpreted by proponents of the theory as a double-sunspot cycle, or by opponents as evidence of lack of a cycle since the period was 20 years and not 22 years, and the cycle stopped in 1960. Monin and Vulis (1971), on the other hand, have computed the

spectra of a large number of meteorological elements and other geophysical parameters and found no significant 11- or 22-year components.

The existence of an 11-year solar signal at the surface is, therefore, still very much in doubt. If such a signal exists it would be of the correct time scale to be of interest in this thesis, and easy to test with the model. The questions that need to be answered concerning this hypothesis are:

1) What are the observations of sunspots and their cycles, and how well can they be predicted?

2) Have there been any direct measurements of a changing solar constant?

3) Through what physical mechanisms might sunspots be related to a changing solar constant? Through what mechanisms might spectral variations in the solar output be perceived at the surface as a changing solar constant?

4) What meteorological variables have definitely been observed to be related to solar emissions?

5) Which of the theories of solar variability, related or unrelated to sunspots, seem the most valid, and which will be tested by the model?

These questions are answered as follows:

1) A sunspot is a dark area on the surface of the sun associated with magnetic disturbances. Areas brighter than the average solar disk also appear and are called faculae. At the maximum of the solar cycle, spots cover about 0.1 % of the surface of the sun, while faculae cover 5 to 6 times this area. A measure of the total level of sunspot

activity was developed by Wolf in the 19th century and is still in use today. It is called the Wolf relative sunspot number and is defined as  $W = h (10g + f)$ , where  $f$  is the total number of spots,  $g$  is the total number of sunspot groups, and  $h$  is a variable used to correct for differences in observers, sites and instruments (Eddy, 1976).

Counts of sunspots have been made since Galileo invented the telescope in 1610. Figure 7 is a graph of the Wolf sunspot number from 1610 to the present and also includes predictions by Sleeper (1975) to 1989 and by Willett (personal communication) until 2001. The numbers for the 1600's and early 1700's are not as reliable as the later ones, and for the early 1600's are interpolated from the data of Eddy (1976). Table 1 contains the numbers used in the figure. The period from 1645 to 1715 is known as the Maunder minimum and was a period of very low sunspot activity. Since then the sunspot number has exhibited a rather regular variation with an 11-year period but variable amplitude. The predicted values of the Wolf number should be considered speculative. No skill has yet been demonstrated in forecasting the details of the sunspot cycle. The predictions are included for completeness, as simulation runs with the model will be carried out to the year 2000.

Cohen and Lintz (1974) have performed a maximum entropy spectral analysis of the cycle and found periods of 90 and 11 years. Schove (1955) found periods of 11 and 78 years. Sleeper (1972) and Gribbin (1973) have claimed that the gravitational field in the solar system, mainly influenced by the orbits of Saturn and Jupiter, but also in accordance with the orbits of the minor planets, exhibits a 180-year periodicity with minor periods of 11 and 22 years, and with the 180-

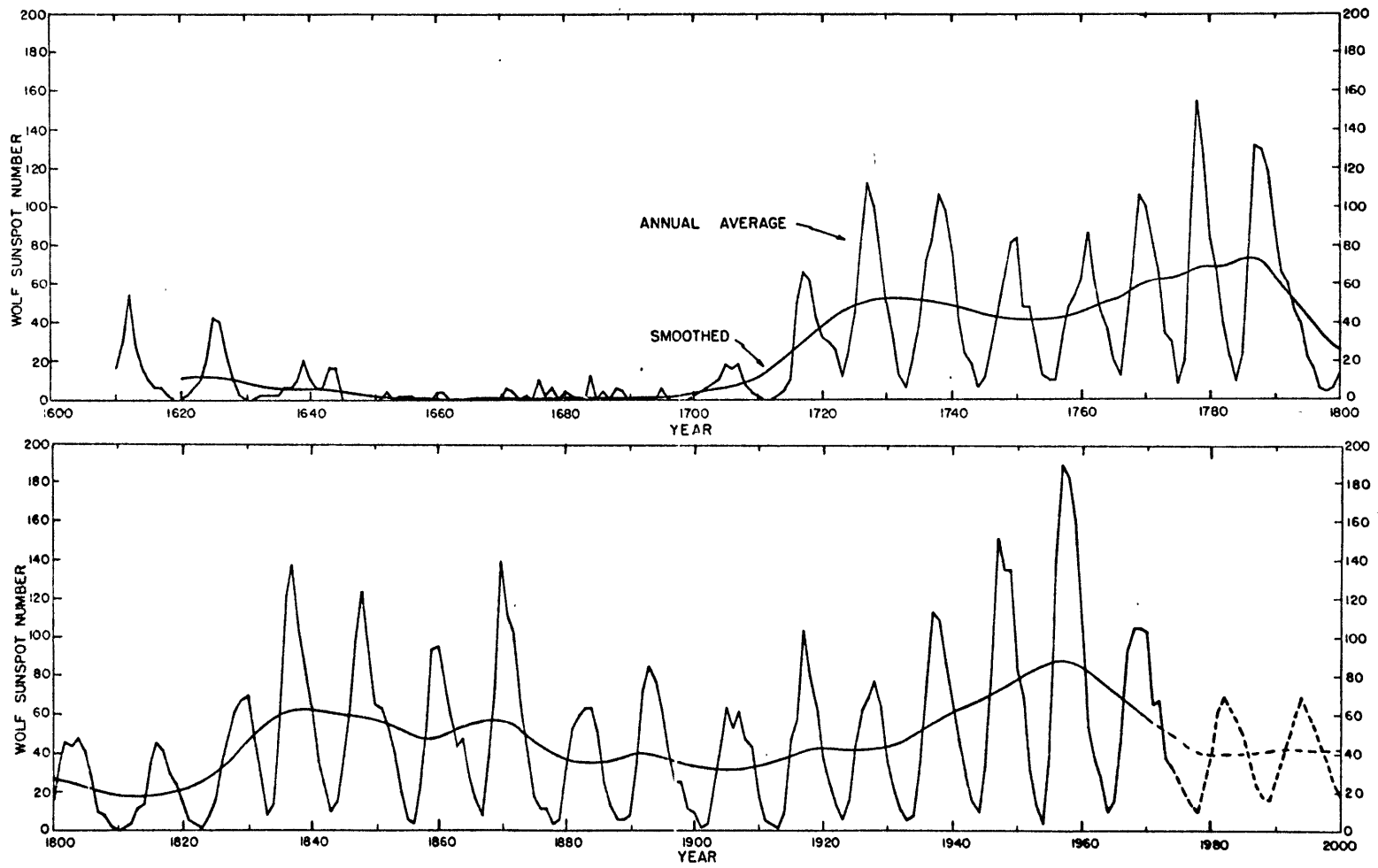


Figure 7. Graph of Wolf sunspot number, 1610-2001. See text for data sources.

Table 1. Wolf sunspot numbers, 1610 - 2001. Annual average (A) and smoothed (S) values are listed. See text for data sources.

Year	1610		1650		1690		1730	
	A	S	A	S	A	S	A	S
0	15		0	1.97	0	1.77	50	52.49
1	30		0	1.67	0	1.62	31	52.50
2	53		3	1.45	0	1.55	12	52.45
3	28		0	1.23	0	1.57	6	52.60
4	15		2	1.06	0	1.66	20	52.89
5	10		1	0.98	6	1.90	37	53.06
6	5		2	1.02	0	2.26	72	53.02
7	5		0	1.02	0	2.76	82	52.50
8	2		0	1.02	0	3.36	106	51.81
9	0		0	1.02	0	3.99	98	50.96
10	0	11.79	4	1.02	2	4.68	75	50.00
11	2	11.70	4	1.00	4	5.36	44	48.82
12	5	11.72	0	0.95	6	5.98	23	47.72
13	10	11.92	0	0.90	8	6.52	18	46.75
14	20	12.40	0	0.89	9	6.95	6	45.68
15	41	12.81	0	0.88	18	7.31	12	44.65
16	40	12.70	0	0.98	15	7.79	25	43.66
17	22	12.06	0	1.09	18	8.61	44	42.83
18	10	11.17	0	1.27	8	9.64	62	42.26
19	2	10.33	0	1.45	3	10.89	81.08	41.79
20	0	9.55	0	1.67	2	12.35	83.25	41.38
21	0	8.82	6	1.90	0	14.01	47.67	41.11
22	2	8.13	4	2.07	0	15.89	47.83	41.18
23	2	7.56	0	2.20	2	17.91	30.75	41.20
24	2	7.12	2	2.42	3	20.14	12.25	41.19
25	2	6.74	0	2.61	10	22.74	9.58	41.31
26	5	6.48	10	2.83	50	25.92	10.00	41.41
27	5	6.48	2	2.89	65	29.34	32.42	41.75
28	10	6.73	6	2.96	62	32.64	47.58	42.35
29	20	6.99	0	2.96	42	35.68	53.92	43.40
30	10	7.01	4	2.96	31	38.50	62.92	44.90
31	5	6.88	2	2.89	29	41.10	85.92	46.71
32	6	6.69	0	2.79	25	43.33	61.17	48.34
33	16	6.40	0	2.74	12	45.20	45.00	49.63
34	15	5.88	11	2.73	24	47.03	36.33	50.83
35	0	5.13	0	2.58	43	48.79	20.92	51.75
36	0	4.42	4	2.45	80	50.46	11.42	52.58
37	0	3.73	0	2.25	112	51.57	37.83	54.06
38	0	3.07	5	2.13	100	52.12	70.00	56.28
39	0	2.46	4	1.95	75	52.36	106.08	58.65

Table 1. (continued)

Year	1770		1810		1850		1890	
	A	S	A	S	A	S	A	S
0	100.67	60.36	0.0	18.76	66.58	56.06	7.08	39.17
1	81.67	61.42	1.42	18.40	64.42	55.20	35.58	39.75
2	66.42	61.96	4.92	18.16	54.17	54.29	73.00	40.05
3	34.75	62.31	12.17	18.15	39.08	53.15	85.00	39.80
4	30.67	62.67	13.83	18.37	20.50	51.95	78.08	38.98
5	7.00	63.09	35.50	18.86	6.50	50.76	64.08	37.92
6	19.83	64.39	45.83	19.45	4.17	49.71	41.75	36.78
7	92.42	66.62	41.00	20.05	22.67	49.00	26.17	35.88
8	154.33	68.49	30.42	20.72	54.75	48.72	26.83	35.17
9	126.00	69.11	24.00	21.52	93.92	48.96	12.08	34.48
10	84.83	68.96	15.67	22.58	95.75	49.83	9.33	33.80
11	68.17	68.84	6.58	23.79	77.08	50.83	2.75	33.07
12	38.50	68.93	4.08	25.13	59.08	51.94	4.92	32.38
13	22.75	69.43	1.75	26.48	44.08	53.16	24.42	31.91
14	10.17	70.45	8.50	27.95	47.08	54.46	42.00	31.72
15	24.00	71.77	16.58	29.85	30.58	55.45	63.50	31.93
16	82.92	73.07	36.33	32.60	16.33	56.20	53.83	32.21
17	132.00	73.12	49.75	36.18	7.33	56.83	62.00	32.99
18	130.92	71.17	62.42	40.17	37.42	57.41	48.67	33.75
19	118.17	67.89	67.00	44.18	73.83	57.60	43.92	34.45
20	89.83	64.05	70.92	47.86	139.08	57.29	18.50	34.95
21	66.58	60.05	47.83	50.87	111.08	55.90	5.67	35.47
22	60.08	56.01	27.58	53.41	101.83	53.97	3.50	36.09
23	46.92	51.91	8.67	55.64	66.25	51.51	1.42	36.72
24	40.92	47.74	13.25	57.89	44.58	48.98	9.50	37.51
25	21.42	43.43	57.00	60.27	17.17	46.50	47.42	38.70
26	16.08	39.08	121.50	62.28	11.25	44.34	57.08	39.99
27	6.33	34.75	138.33	63.23	12.17	42.35	103.83	41.43
28	4.00	31.07	103.25	63.23	3.25	40.35	80.50	42.24
29	6.92	28.43	86.00	62.72	6.00	38.41	63.67	42.77
30	14.50	26.76	63.25	61.86	32.42	36.73	37.67	42.95
31	34.08	25.83	36.83	61.03	54.25	35.43	26.17	43.04
32	45.00	25.13	24.08	60.64	59.58	34.98	14.25	42.94
33	43.00	24.34	10.67	60.56	63.75	35.17	5.75	42.70
34	47.42	23.44	15.17	60.70	63.50	35.79	16.58	42.47
35	42.17	22.44	40.17	60.72	52.25	36.44	44.42	42.27
36	28.17	21.46	61.50	60.22	25.33	36.94	63.83	42.08
37	10.17	20.54	98.50	59.36	13.00	37.38	69.08	42.16
38	8.17	19.83	124.25	58.33	6.83	37.92	77.83	42.48
39	2.42	19.23	95.92	57.17	6.17	38.54	64.92	43.11



Table 1. (continued)

Year	1930		1970	
	A	S	A	S
0	35.67	43.89	104.92	58.52
1	21.25	44.99	66.67	55.93
2	11.17	46.41	68.83	53.75
3	5.58	47.80	38.17	51.39
4	8.67	49.39	34	49.18
5	36.00	51.16	27	47.05
6	79.67	53.23	19	44.87
7	114.33	55.61	13	42.70
8	109.50	57.75	10	40.84
9	88.75	59.77	23	39.72
10	67.67	61.66	39	39.30
11	47.50	63.54	62	39.42
12	30.58	65.20	70	39.78
13	16.25	66.63	63	40.02
14	9.50	67.93	57	40.36
15	33.17	69.43	49	40.59
16	92.58	71.62	38	40.72
17	151.50	74.15	24	40.81
18	136.17	76.37	17	40.96
19	135.25	78.58	15	41.14
20	84.17	80.39	26	41.14
21	69.50	81.99	37	41.14
22	31.33	83.31	48	41.14
23	13.83	84.74	59	41.14
24	4.42	86.27	70	41.14
25	38.00	88.00	61	41.14
26	141.75	89.55	53	41.14
27	189.83	89.82	44	41.14
28	184.58	88.58	36	41.14
29	158.42	86.42	25	41.14
30	112.33	83.64	17	41.14
31	53.92	80.67	10	41.14
32	37.67	78.07		
33	27.83	75.73		
34	10.17	73.48		
35	15.17	71.40		
36	46.75	69.26		
37	93.67	66.77		
38	106.08	63.98		
39	105.58	61.20		

year period broken into 100- and 80-year periods. Willett (1974) uses all these periods, emphasizing the 22-year period, to find correlations with past climate change and make forecasts for the future. He points out that during the first 11-year cycle of the double cycle sunspot pairs are led by spots of one polarity as they travel around the sun, and during the second cycle the polarity reverses. At the end of the 80- and 100-year portions of the 180-year cycle, the polarity does not reverse between 11-year cycles. This conjecture, however, has yet to be observed. Sleeper (1974, 1975) uses these past variations to make forecasts into the future of the sunspot cycle.

To summarize, the sunspot number shows an obvious 11-year periodicity superimposed on what some have claimed are 22-, 80-, 100-, and 180-year periods. Yet during the Maunder minimum very few sunspots were observed. Observations of sunspots are quite good since 1750, and fairly good from 1610 to 1750. Based on past periodicities, predictions of the cycle have been made for 25 years into the future, but they must be considered speculative.

2) The longest series of observations of the solar constant were made by the Smithsonian Institution under the direction of Charles Greeley Abbott, from 1905 to 1952 (Abbot; 1963, 1966). During this period they made observations of the solar constant from the earth's surface, making theoretical and observational corrections for the atmospheric attenuation of the solar radiation. The largest atmospheric effects are due to the changing concentrations of water vapor and ozone. From 1905 to 1920 they spent about six months each year making observations from Mt. Wilson. Mountain top stations were used to lessen

the effects of the atmosphere. Using Langley's "long method" they calculated the solar constant. During the early 1920's a new "short method" was developed to rapidly calculate the solar constant, and from 1923 to 1952 daily measurements were made from several mountain top observatories in both the Northern and Southern Hemispheres.

Abbott claimed to have found a variation in the solar constant in phase with the 22 year, 9 month, double sunspot cycle with an amplitude of 3 %. He also claimed to have found 27 harmonics of this cycle, all with periods that are exact fractions of the basic 273 month period. Later analysis of Abbott's data (Foukal et al., 1977) also showed a secular trend of 0.17 % during the 30 years that Abbott took his data, but found that this was probably due to changing calibration techniques, which overemphasized solar constant values that were high. The validity of Abbott's results has been the subject of much criticism. The inexactness of the atmospheric corrections may have resulted in spurious values. Furthermore, changes in the observers and instruments over a 30-year period probably introduced errors as large as the changes measured in the solar constant.

Kondratyev and Nikolsky (1970), from a series of about 8 balloon measurements made during the mid-1960's from altitudes of about 30 km, also measured large changes in the solar constant, and related them to the sunspot number by the empirical formula:

$$SC = 1.903 + 0.011 W^{.5} - 0.0006 W \quad \text{ly/min}$$

where SC is the solar constant and W is the Wolf sunspot number. Yet their measurements were taken during a period of atmospheric nuclear

testing and injection into the stratosphere of large quantities of dust by the eruption of Gunung Agung in Bali in 1963, and although they tried to correct for these effects, their measurements are open to serious question, as they readily admit.

The problems of atmospheric effects associated with these attempts at measuring the solar constant strongly suggest that a better way would be measurements from satellites above the atmosphere. So far there has been no long-term program of measurement of the solar constant by satellite. This has been partially a problem of reliable instruments not being available that can maintain a calibration for a long time, and partially the lack of interest in, or realization of the importance of, or belief at all in, the variation of the solar constant by NASA. But with the Space Shuttle to aid in the calibration and the clamor for such measurements by people studying climate, a program such as this is sure to be started in the near future.

Three space vehicles launched by the United States have had instruments which measured the solar constant: Nimbus F and Mariner 6 and 7 (Foukal et al., 1977). Each of these had a large day to day instrumental drift of about 0.03 %/day so were useless for measuring long-term changes in the solar constant. Yet these data were useful in investigating short-term variations associated with sunspots and faculae. Foukal found a maximum variation of the solar constant of 0.03 % associated with magnetic solar variations, much less than that expected due to the darkening and brightening of the sun produced by the magnetic variations. He concluded that the darkness and brightness of sunspots and faculae do not cause solar constant changes.

Foukal also decided to search in Abbott's data for a variation in the solar constant associated with the maximum and minimum value of facular area and sunspot number during each month. He found no relationship with sunspots, but did find an average 0.05 % variation in the solar constant from minimum to maximum facular area in each month. The average monthly facular area variation is half the average variation during a solar cycle, so Foukal concludes that there may be a 0.1 % variation in the surface observations of solar constant of Abbott, associated with facular area changes, which correspond to the sunspot cycle. Since no such relationship was observed in the spacecraft data, he concludes that this must have been an atmospheric effect, most probably that of ozone, as discussed in the next section. Yet Abbott tried to correct his measurements for ozone variation! So Abbott's uncorrected values should show an even larger effect, of, at present, unknown magnitude.

Eddy (1976) as a result of his study of the Maunder minimum and cosmic ray variation has theorized that there may be a long-term variation of the solar constant that is unrelated to the variations within each 11-year sunspot cycle. The magnitude of this solar constant change would be indicated by the overall envelope of sunspot numbers, with the 11-year cycle filtered out. He supports this theory with the fact that this envelope was very low during the Maunder minimum, which corresponded to the Little Ice Age. An 11-year running mean was applied twice to the annual average sunspot data to produce a smoothed sunspot value to test this theory. The smoothed data are shown in Table 1 and Figure 7 with the annual average data.

3) Although changes in the solar constant related to the sunspot cycle are very small, if they exist at all, changes in certain shortwave frequencies have been well documented and large. At  $0.2 \mu$  there is a 1 % modulation in the solar flux by faculae and at smaller wavelengths, the modulation can be more than ten times this effect (Foukal et al., 1977). Less than 0.1 % of the energy of the total solar flux is in wavelengths smaller than  $0.2 \mu$ , but an indirect mechanism exists which may affect the amount of solar radiation reaching the surface. Ozone is created in the upper stratosphere at wavelengths between  $0.18$  and  $0.21 \mu$  and Willett (1962) found a highly significant correlation between ozone concentration and the sunspot number. Ruderman and Chamberlain (1975) point out that cosmic rays reaching the earth also vary with the sunspot cycle, and that they affect the  $\text{NO}_x$  concentration. During sunspot maximum, the cosmic rays are less, lowering the  $\text{NO}_x$  concentration, which in turn lowers the catalytic destruction of ozone. These two mechanisms work together to increase the ozone concentration during sunspot maximum. The combined radiation effects of these ozone and  $\text{NO}_x$  changes have been studied by Ramanathan et al. (1976) with a one-dimensional radiation model. They found that surface temperatures go up as ozone concentration goes up. The  $\text{NO}_x$  radiative effects partly compensate for this temperature rise. Angione et al. (1976) also suggested that this variation of ozone causes ozone to act as a shutter, modulating solar radiation by absorbing it in the Chappuis band ( $0.5 - 0.7 \mu$ ) in the center of the visible spectrum. The ozone observations are not yet good enough and the above theoretical interactions are too poorly understood to indicate the magnitude of the total effect, but it

could produce variations of sufficient magnitude to cause climate change.

The evidence therefore points to a possible indirect mechanism, through ozone, of a relationship between sunspot number, an indicator of faculae, and the amount of solar radiation reaching the ground. This effect was filtered out quite well by Abbott, so only a small signal is detectable in his data, yet a much larger effect may exist.

4) One other short-term effect of the sun on the atmosphere has been well documented. It has been shown that the vorticity area index, a measure of the relative area of low pressure systems, is related, with a time lag, to passages of the earth through solar magnetic sector boundaries. This effect has been measured for the Northern Hemisphere only in the winter, when storms are strong. It has been documented by Schuurmans (1969), Roberts and Olson (1973), Hines and Halevy (1975), Wilcox (1976), Wilcox et al. (1976), and Shapiro (1976). No long-term effects have been measured, since passages of the magnetic sector boundary can only be measured by satellites above the atmosphere, and these measurements have only been made for a few years. It is interesting to note that McGuirk and Reiter (1976) have found a significant vacillation in atmospheric energy parameters with a mean period of about 24 days. This period is almost the same as that of the rotation of the sun. Although they did not mention the sun as a cause of the observed vacillation, it may possibly be. Care should be taken not to make conclusions solely on the basis of similar periods, as this has been done extensively with 11-year periodicities observed on earth. A further study relating McGuirk and Reiter's parameters to the vorticity area index or to

magnetic sector boundary passages may prove fruitful.

5) It is conceivable that there may be variations in the solar constant perceived at the earth's surface, probably through the ozone shutter mechanism. It is also conceivable that there may be a long-term drift in the solar constant related to the envelope of the sunspot number. Short-term variations of the weather may also be related to the sun. All these theories will be tested by the model used in this thesis. Details of how they will be incorporated into the model will be discussed later, after the model is described.

One globally averaged model (Schneider and Mass, 1975) has been used to test the Kondratyev and Nikolsky theory, and got a large unreal 11-year cycle in predicted temperature. For more details see section II.D.3.

#### b. Volcanic dust

When large volcanoes erupt, they inject aerosol particles into the stratosphere. These particles interact with radiation in the atmosphere with the net effect of blocking some of the solar radiation and cooling the earth. Newell and Weare (1976) have shown that the eruption of Gunung Agung in Bali in March, 1963, produced a temporary 0.5°C cooling of the tropical troposphere. Dyer (1974) also studied the Agung eruption and showed that its effects disappeared after 8 years. Thus volcanoes produce climate changes of a time scale important to the subject of this thesis. Periods of increased volcanism may have produced climate change on ice-age time scales also. Ninkovitch and Donn (1976) have studied ocean cores and have concluded that there is



still not enough evidence at this time to determine whether long enough periods of increased volcanism existed to modify climate. Roosen et al. (1976), however, claim to have found a relation between earth tides, volcanism and the temperature record of the Greenland ice cores to explain part of the ice-age temperature change. Bray (1974, 1976) also claims to have found evidence that ice-age glacial advances were synchronous with periods of increased volcanism. In any case, if it can be shown that volcanoes do produce cooling, even though volcanic eruptions cannot at this time be forecast, a massive eruption could be used to forecast climate change for the succeeding 10 years.

Lamb (1970) has compiled a list of volcanic eruptions since the year 1500. The evidence for the earlier of these is based on anecdotal historical records and as such is not very reliable. Also, records for the Southern Hemisphere do not exist until the nineteenth century. Nevertheless, Lamb has assigned magnitudes to the various eruptions and indicated the relative effect each would have on the Northern and Southern Hemispheres. His volcanic dust veil index (Table 2) is his estimate of the relative stratospheric dust load produced by volcanoes for the Northern Hemisphere for each year since 1600. The values in 1975-1978 were added to account for the Fuego eruption. Russell and Hake (1977) have shown that this dust veil was less extensive than that of Agung in Central America. Mitchell (1970) has used Lamb's raw data to produce his own estimate of the global dust load for 1850 to the present (Table 3). He also includes eruptions during the present century that Lamb excluded as being too small, and therefore his record is more detailed and accurate. One must be careful when using this data as



Table 3. Volcanic dust veil index for Northern Hemisphere, from Mitchell (1970).

Year	1850	1890	1930	1970
0	10	50	-	20
1	10	20	-	-
2	-	60	-	-
3	-	40	-	-
4	-	20	-	-
5	140	10	-	80
6	240	-	-	40
7	160	-	-	20
8	50	-	-	10
9	20	-	-	
10	10	-	-	
11	50	-	-	
12	40	170	-	
13	20	340	-	
14	10	240	-	
15	-	100	-	
16	-	50	-	
17	-	70	50	
18	-	50	40	
19	-	20	20	
20	-	20	10	
21	-	10	10	
22	10	50	-	
23	10	40	50	
24	-	30	50	
25	20	20	30	
26	50	10	70	
27	40	-	50	
28	20	-	30	
29	10	-	10	
30	-	-	10	
31	-	-	10	
32	-	10	-	
33	500	10	160	
34	340	-	140	
35	180	-	60	
36	140	-	80	
37	90	-	60	
38	130	-	70	
39	90	-	50	

input to a climate model with latitudinal resolution, for it assumes uniform hemispheric or global concentration of dust. Cadle et al. (1976), using a two-dimensional dispersion model of the atmosphere, show that for simulated eruptions of Agung and Bezymianny that the resulting stratospheric ash cloud was limited in latitudinal extent (see Figures 8 and 9). This implies that the latitude as well as the magnitude of volcanic eruptions should be used as input to a model testing volcanic forcing of climate change. However, since no such chronologies have been published, although Bryson and Dittberner (1976) refer to one by Hirschboeck which has not yet been published, and since the model is in need of further improvement, as indicated in Chapter 3, this theory will be tested in this thesis with forcing only by Lamb's and Mitchell's averaged data.

Since stratospheric aerosols not only scatter solar radiation, but also absorb both solar and infrared radiation and emit infrared radiation, it is not obviously clear that their net effect is to cool the earth. Many detailed one-dimensional radiation models have been used to study this problem, however, and they all indicate that these aerosols would have a net cooling effect. These include the studies of Barrett (1971), Mitchell (1971), Dickinson (1974), Pollack and Toon (1974), Herman et al. (1976) and Luther (1976). Cadle and Grams (1975) and Toon and Pollack (1976) have provided detailed analyses of the aerosols found in the stratosphere to use as inputs to these models.

It would be nice not to have to make detailed radiation calculations in a simple climate model to simulate volcanic aerosols. Fortunately, MacCracken and Potter (1975) and Coakley and Grams (1976) have

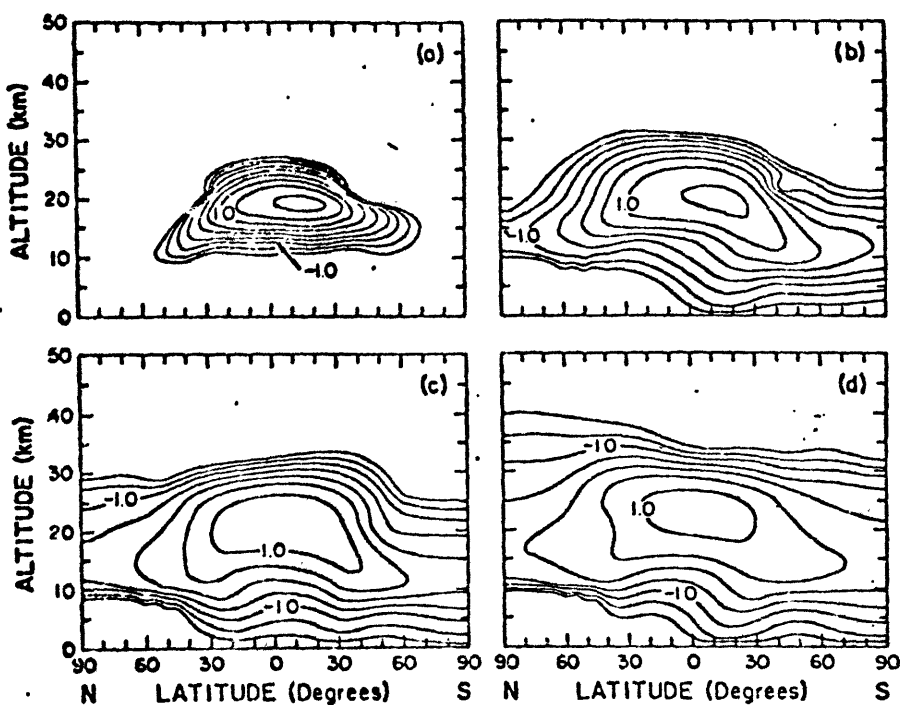


Fig. 8. Log concentration isopleths for fine ash (in parts per billion by mass) from the model for the Agung eruption. Intervals are 0.5 log ppbm. Days following the eruption are (a) 60, (b) 195, (c) 300, and (d) 495.

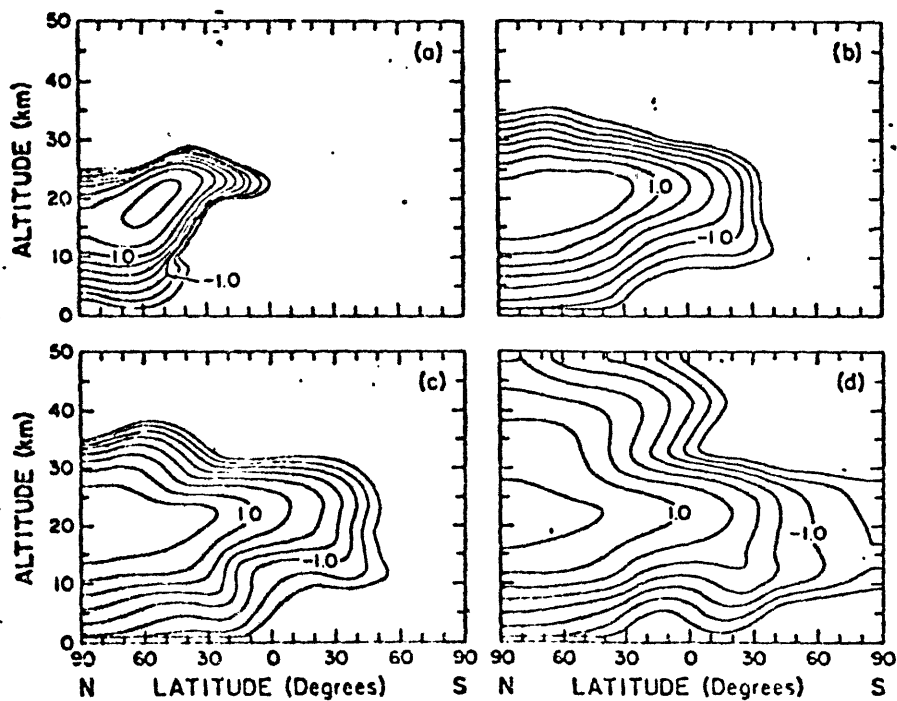


Fig. 9. Log concentration isopleths for fine ash (parts per billion by mass) from the model for the Bezymianny eruption. Intervals are 0.5 log ppbm. Days following the eruption are (a) 60, (b) 195, (c) 300, and (d) 495. It is assumed that the emissions were the same as those from Agung.

Above figures from Cadle, et al. (1976).

shown with completely different detailed models that lowering the solar constant or increasing the stratospheric aerosol loading have very similar effects on the radiation reaching the surface. Therefore, in this study, the solar constant will be lowered by an amount proportional to the volcanic dust veil to simulate its effect on climate.

A few attempts have been made to include volcanic dust in globally- or hemispherically-averaged climate models. These were done by Schneider and Mass (1975); Pollack et al. (1975) and Bryson and Dittberner (1976). Oliver (1976) also studied the hemispheric temperature response to volcanic dust with an empirical curve-fitting approach. All got reasonably good agreement with Mitchell's 0°-80°N or Budyko's NH temperature records, although Schneider and Mass's response is overshadowed by the sunspot effect. See section II.D.3.

At present it is not possible to forecast volcanic eruptions. Future research, along the lines of Press and Briggs (1975) may, however, increase our understanding of this and other related geological and tectonic features of the earth and allow forecasts of volcanoes to be made.

#### c. Anthropogenic carbon dioxide

The burning of fossil fuels (such as oil, coal and natural gas) by man adds carbon dioxide (CO<sub>2</sub>) to the atmosphere. The increase in CO<sub>2</sub> concentration since the beginning of the present century is well documented, and forecasts have been made, continuing the presently observed growth rate, to the end of the century. Mitchell (1972), Machta and Telegadas (1974) and Broecker (1975) have all published

such forecasts. The forecast of Broecker (Figure 10) is used in this thesis, and assumes constant  $\text{CO}_2$  concentrations before 1880, observed increases to the present, and approximately a 3 % growth rate into the future. Forecasting human and societal activities is a very inexact procedure, so this forecast of future growth should not be considered very reliable.

Carbon dioxide is well mixed in the atmosphere, so any change in its concentration should have global effects, unlike anthropogenic aerosols which have more local effects. The surface layer of the ocean acts as a sink for  $\text{CO}_2$ . Approximately half of all anthropogenic  $\text{CO}_2$  produced is no longer in the atmosphere, and is assumed to have been dissolved in the oceans. This process, especially its biological components, is very poorly understood, and changes in it may affect the  $\text{CO}_2$  forecast. Seasonal cycles in  $\text{CO}_2$  concentrations have also been observed (Machta and Telegadas, 1974) due to biological activity of plants on land, and this process may have an important influence on the seasonal climate cycle. These  $\text{CO}_2$  cycles may have a maximum amplitude in the mid-latitudes of the Northern Hemisphere, where the strongest biological seasonal cycle exists, or the mixing in the atmosphere may spread them over the whole globe. This process has not been adequately studied.

Additional  $\text{CO}_2$  acts to warm the atmosphere through the so-called greenhouse effect, although greenhouses are heated in addition by inhibition of convection.  $\text{CO}_2$  absorbs terrestrial radiation and reradiates it to warm the atmosphere. Although the direction of the effect is agreed upon, the magnitude is a subject of controversy. Depending on

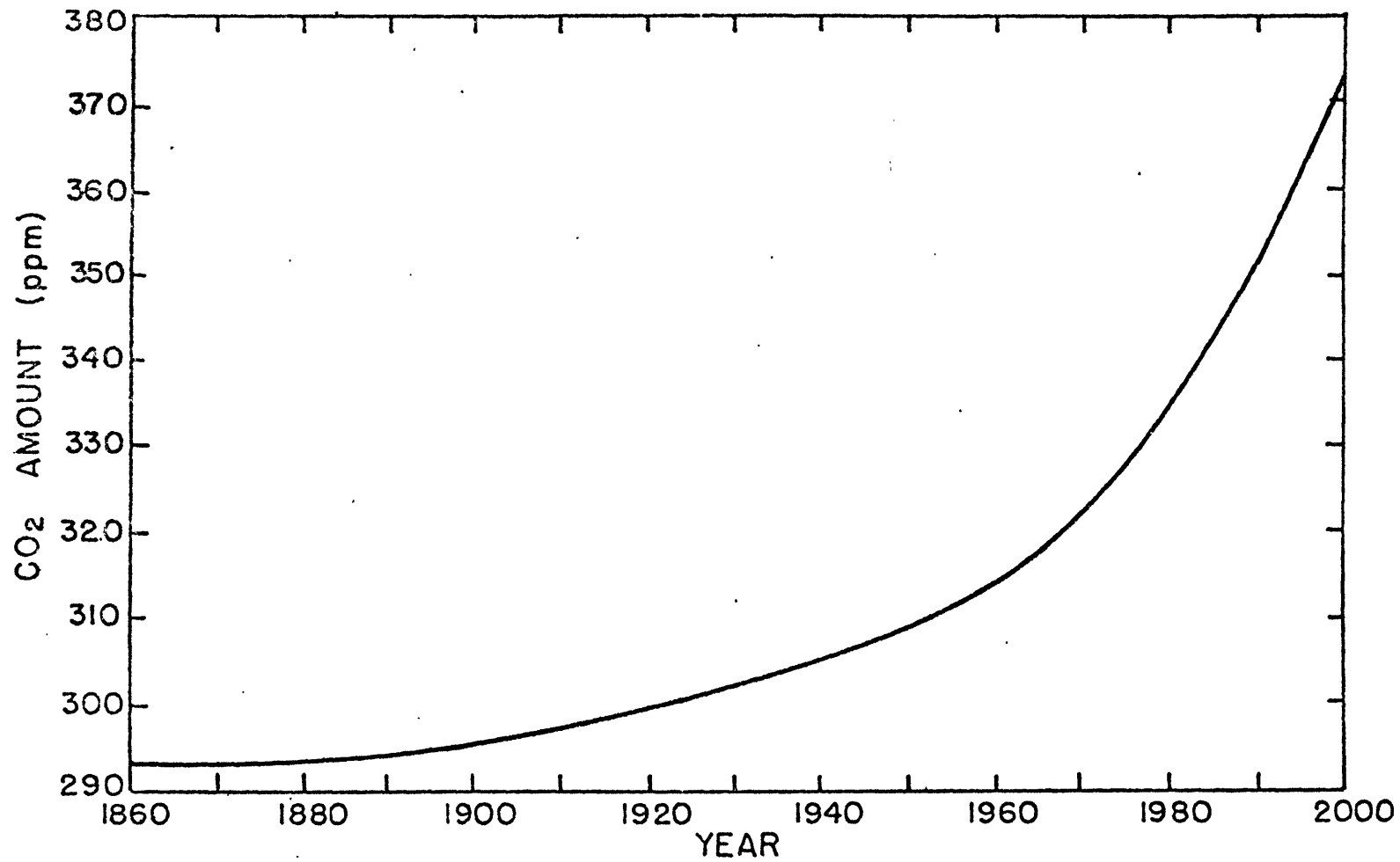


Figure 10. Atmospheric carbon dioxide content, from Broecker (1975). It was constant at 293 ppm before 1880.



the assumptions made in the model used, and the type of model, order of magnitude variation is found in the estimates of the temperature effect of a doubling of the CO<sub>2</sub> concentration. This subject is well reviewed by Schneider (1975). Mitchell (1977) and Budyko and Vinnikov (1976) have used these estimates to forecast future climate based on the projected anthropogenic CO<sub>2</sub> effects.

d. Anthropogenic aerosols

The most visible form of man's pollution of the atmosphere is the addition of aerosols. Man's urban and industrial activities, as well as certain agricultural practices, inject large amounts of smoke, dust and particulates into the air. Some pollution released as gases also reacts chemically in the atmosphere to form aerosols. The effects of these aerosols on climate are produced through interactions with both solar and terrestrial radiation, and, when they are of the proper size and composition to serve as condensation nuclei, through modification of cloud and precipitation formation mechanisms. A good general discussion of these effects is contained in Schneider (1972) and Schneider and Kellogg (1973).

Data about the amount, composition, distribution, rate of change with time, and fraction that is anthropogenic of aerosols is very sparse. Aerosols differ from CO<sub>2</sub> in that they have a relatively short lifetime in the troposphere of approximately one week, because they are rained out and washed out. They are therefore more highly concentrated near their sources than elsewhere. Aerosols in the stratosphere, on the other hand, have a lifetime of several years. The SMIC (1971)

report estimated that between 5 and 45 % of the aerosol load was anthropogenic. Weickman and Pueschel (1974), using other people's data, attempted to estimate the aerosol load of the atmosphere and guessed that 11.5 % was anthropogenic. Bryson and Wendland (1970) give Russian dustfall in the Caucasus data which show an extremely rapid rise after World War II. Bryson and Dittberner (1976) again use this data as input for their climate model, although the data only extends to 1958. The only other report of a time record of aerosols is also contained in Bryson and Dittberner's paper and gives data on leadfall in Greenland up to 1965. The two records do not coincide very well at all.

An alternative way to estimate the distribution and rate of change of anthropogenic aerosols is to assume that Gross National Product is proportional to Gross National Pollution. This was the approach of Kellogg et al. (1975). They also assumed that mean winds would distribute the aerosols and specified an average residence time, and produced maps of the worldwide distribution of aerosols, from which the data in Table 4 was taken. If it is assumed that the anthropogenic portion of aerosols is equal to the excess anthropogenic CO<sub>2</sub> and that it rises at the same rate (Figure 10), then a complete time and space distribution of anthropogenic aerosols is specified. As anti-pollution measures become more widespread, the rate of increase of anthropogenic aerosols will fall behind that of CO<sub>2</sub> and the concentration may even decrease. The timing of this effect remains a matter of speculation, especially since the agricultural portion is not well known and will not behave the same way. The magnitude of the effect remains

Table 4. Worldwide distribution of anthropogenic aerosols and heat, at their 1972 levels. See text for data sources.

Latitude band	Additional optical depth caused by anthropogenic aerosols (= 20% of natural loading (0.3) in most polluted area)		Anthropogenic heat (Total = $8 \times 10^{12}$ W) ( $\times 10^{11}$ W)
	Land	Water	(Land)
80° - 90°N	0	0	0
70° - 80°N	0.0007	0	0.04
60° - 70°N	0.0086	0.0067	3.67
50° - 60°N	0.0326	0.0193	13.82
40° - 50°N	0.0600	0.0107	21.00
30° - 40°N	0.0500	0.0094	16.71
20° - 30°N	0.0300	0.0030	10.40
10° - 20°N	0.0220	0.0053	5.58
0° - 10°N	0.0120	0.0040	2.92
0° - 10°S	0.0113	0.0026	2.65
10° - 20°S	0.0030	0.0001	1.39
20° - 30°S	0.0080	0.0005	1.44
30° - 40°S	0.0040	0.0010	0.37
40° - 50°S	0	0.0002	0.01
50° - 60°S	0	0	0
60° - 70°S	0	0	0
70° - 80°S	0	0	0
80° - 90°S	0	0	0

to be specified, and this is discussed in Chapter 4 with the description of the model experiments. It should be noted that this process of estimating anthropogenic aerosol loads, which is used in this thesis, excludes agricultural aerosols not produced by industrialized countries, but there are no good data on this anyway.

Many studies have been made, with varying degrees of complexity and sophistication, of the radiative effects of aerosol pollution. Depending on the models used, the processes included, and the assumed composition and distribution of the aerosols, it is concluded by different authors that the aerosols cause cooling, or that the aerosols cause warming, or that the net effect depends on the critical absorption to backscatter ratio (which itself depends on the surface albedo only in the simplest formulation, or on as many as three more parameters), or that the system is too complicated or ill-defined to calculate any net effect. Among those claiming cooling are Welch and Zdunkowski (1976) and Zdunkowski et al. (1976) who used a sophisticated boundary layer model and calculated local effects. They found that humidity effects on aerosols were important, and included infrared effects. Bryson and Wendland (1970), Barrett (1971), Rasool and Schneider (1971), and Budyko and Karol (1975) reached the same conclusion with simpler models and reasoning. Mitchell (1971) calculates that the global average effect will be warming, while not considering infrared effects (which would also contribute to warming). Chylek and Coakley (1974), Gribbin (1975a), Herman and Browning (1975), Reck (1975) and Russell and Grams (1975) all also calculate a net warming effect. Among those who give indeterminate results are Mitchell (1970, 1974, 1975), Weare

et al. (1974), Reck (1974), Gribbin (1975b), Fiocco et al. (1976), and Toon and Pollack (1976). It is clear that the net radiative effect of anthropogenic aerosols is not clear.

Twomey (1971), Pruppacher (1973), Hobbs et al. (1974), and Radke and Hobbs (1976) all speculated about hydrological effects of anthropogenic aerosols. Since clouds themselves, and their interaction with climate are not well understood, it is impossible to determine how anthropogenic aerosols could change climate through them.

Bryson and Dittberner (1976) included the radiative effects of anthropogenic aerosols in their model and calculated a cooling effect. Sellers (1973) also used a radiation model in his climate model which produced a net cooling effect due to increased aerosols. These simulation attempts are discussed more fully in section II.D.3.

#### e. Anthropogenic heat

Man's activities at the surface of the earth add heat to the environment. Peterson (1973) estimates that man added  $2.2 \times 10^{20}$  J to the environment in 1970, and SMIC (1971) estimated the amount at  $2.5 \times 10^{20}$  J. For the purpose of this thesis the total amount will be assumed to be  $2.5 \times 10^{20}$  J, in 1972, slightly favoring the SMIC estimate, which is better documented. The growth rate of the heat will be scaled by the  $\text{CO}_2$  increase (Figure 10) since both are assumed proportional to industrial development. The heat, like anthropogenic aerosols, will have a larger effect in the Northern Hemisphere, where the greatest industrial activity is. The latitudinal distribution will be assumed to be the same as that of anthropogenic aerosols, but with the entire

source on land (see Table 4).

One previous attempt at simulating the anthropogenic heat effect is that of Washington (1972). He found that the pollution effect was small, but two assumptions in his model may have led to this result. First, he used the NCAR GCM with fixed ocean temperatures, which limited the temperature response of the rest of the model. Second, he assumed that anthropogenic heat generation was proportional to population, and so introduced a large amount of heat in tropical areas like Bangladesh, India, and Indonesia, where the solar input is large, and the anthropogenic heat effect is overshadowed.

#### f. Other anthropogenic effects

Other activities of man may cause climate to change through modification of the atmospheric composition or the earth's surface. These processes are not well understood or observed, and so will not be tested in this thesis, but will be mentioned here as a warning and further indication of our incomplete understanding of climate and man's effect on it.

Ramanathan (1975) pointed out that freon ( $\text{CF}_2\text{Cl}_2$  and  $\text{CFCl}_3$ , used as a propellant in aerosol cans, as a foaming agent and as a refrigerant) in addition to its well publicized possible effect on the ozone layer, also is a very efficient absorber in the infrared. He calculated, that if its concentration continued to rise at the presently observed rate, it would cause a  $1^\circ\text{C}$  rise in global average surface temperature by the year 2000. This estimate is, of course, as uncertain as the possible effects of  $\text{CO}_2$ , as previously discussed. Wang et al.

(1976) calculated the greenhouse effects due to large numbers of other anthropogenic gases now found in trace quantities and concluded that their overall effect would also be a warming of the earth. What other presently existing or yet to be invented concoctions from a chemistry laboratory will be introduced into the atmosphere by man, and what will be their effects? Hopefully the answer will come from future theoretical research before it comes from observations.

One other gas which man introduces into the atmosphere in large quantities is water vapor. This affects the complex hydrological cycle both through the atmospheric composition and surface characteristics, as discussed in section II.C.1, and the net effect is not clear.

Man's agricultural activities cause the modification of large parts of the earth's surface. The clearing of land and planting of crops cause changes in both the albedo and surface moisture content, and modify the water vapor and CO<sub>2</sub> input into the atmosphere. Overgrazing can result in large local long-term changes, such as the production of deserts (Charney, 1975 and Charney et al., 1975). The large-scale deforestation now taking place in the interior of Brazil could have a large impact on the climate, since this is a region of high solar radiation input. The net large-scale effects of these activities are yet to be well understood.

## 2. Internal causes (almost-intransitivity)

The previous section discusses causes of climate change that are external to the climate system. These forcings are not in turn influenced by the climate changes that they produce. It is possible,

however, that even in the absence of any external forcing a unique climate may not exist. Climate change may be a natural internal feature of the land-ocean-ice-atmosphere (climate) system.

The theory of internal causation of climate change has been developed by Lorenz (1968, 1970, 1976). He suggested that climate change might just be the natural variations due to the complex non-linear interactions among the various components of the climate system. (The system will be fully discussed in section C. of this chapter.) The terminology of mathematical ergodic theory is used to explain this climate theory. A "transitive" system is defined as one in which the very long-term statistics of the variables are independent of the initial conditions. An "intransitive" system is one in which two or more sets of statistics would result in the very long-term, depending on the initial conditions. If, however, the statistics of a system were transitive for a very long-term, but over a shorter term depended on the initial conditions, then it would appear to be intransitive to an observer on this shorter time scale. Lorenz calls this an "almost-intransitive" system, and suggests that the climate may be such a system.

The climate system contains elements that make internal causes of climate change plausible. The first of these is weather. Heat transport from the equator to the poles is accomplished in the mid-latitudes primarily through the mechanism of baroclinic eddies. These eddies are unstable to small perturbations and grow to finite amplitudes before decaying. Although there are preferred locations on the earth for the initiation and dissipation of these storms, and preferred



tracks for them to follow during their lifetimes, no two are exactly alike. In fact searches through past data for matching patterns of the circulation at different times have been remarkably unsuccessful. An indication of the cumulative effect of these random variations in the meridional heat flow can be seen in the data of VonderHaar and Oort (1973) (Table 5, which gives the standard deviations of the annual averages of the heat flow for five years of data). The global average of the standard deviations, for the part of the globe for which the data exist, is 9.9 % of the mean. Admittedly, the data are from a rather small sample, and there may be other possible causes of the observed variations. In fact VonderHaar and Oort originally attributed all the variation to observational errors, and the data were collected during the period in which Starr and Oort (1973) measured a  $0.6^{\circ}\text{C}$  decrease in hemispheric mean temperature, so observational errors plus climate change surely contributed to some of the variation. Independent confirmation of the actual variability of the fluxes, however, comes from the study of McGuirk and Reiter (1976). They found a significant oscillation with a mean period of about 24 days in atmospheric energy parameters during the winter season from 9.5 years of data. Furthermore, they found that during different years, different zonal wavenumbers were favored in the production of the meridional energy flux. So it is reasonable to conclude that a substantial portion of the variation in the flux found by VonderHaar and Oort was a real variation, and Oort now feels that this is the case (personal communication).

Table 5. Atmospheric energy flux (positive northward) and its standard deviation, from five years of data of VonderHaar and Oort (1973). The world mean is calculated from absolute values of the flux, weighted by the length of the latitude circles.

<u>Latitude</u>	<u>Mean</u>	<u>Standard Deviation</u>	
	(x 10 <sup>15</sup> W)	(x 10 <sup>15</sup> W)	(% of mean)
80°N	0.49	0.16	32.4
70°N	1.46	0.08	5.5
60°N	2.80	0.13	4.7
50°N	2.97	0.21	7.1
40°N	2.92	0.13	4.5
30°N	2.69	0.21	7.9
20°N	1.21	0.11	8.8
10°N	0.96	0.10	16.7
EQ	0.17	0.13	76.9
10°S	-1.91	0.32	16.7
World mean:	1.75	0.17	9.9

The other elements needed to complete the scenario for internally caused climate change are the various sources, sinks and transports of energy that operate on different time scales. These include the land and ocean surface, and the snow and ice cover which are variable. Furthermore, the ocean acts to store and release heat through its internal dynamics which include mean and eddy motions of the surface layer, deep ocean currents, and variations of the depth of the surface mixed layer. Variations of salinity and temperature, which are caused by evaporation and precipitation as well, in turn influence the formation and dissipation of ice. All these processes are in turn influenced by the radiation field and the wind field. A more thorough discussion of these feedback mechanisms is included in section II.C. For the present purposes it is sufficient to state that variations in heat fluxes by the winds can influence heat storage in the ocean, that not only has a much larger thermal inertia than the other parts of the system, but can redistribute the heat stored in a certain location. These complex non-linear interactions in turn influence the resulting wind fields, and produce the internal variations that may be perceived as climate change.

It is impossible, just using observations of the climate, to tell whether the climate is transitive, intransitive or almost-intransitive. It is not possible to restart the atmosphere with different initial conditions and observe its behavior. However, very simple mathematical models (Lorenz, 1964, 1976) consisting of only one equation with one parameter have been developed which in attempting to simulate these

internally varying causes of climate change produce almost-intransitivity. In this thesis, an attempt will be made to model this type of climate change with a model containing many of the previously discussed climate features which may produce almost-intransitivity.

For some purposes, it would be nice to distinguish between the natural variability of the system produced by internal stochastic forcing (Mitchell, 1976) which is a part of the signal in a transitive or an intransitive system, and variability due to almost-intransitivity. With a finite record, this distinction is impossible, but there are indicators of almost-intransitivity, such as obvious shifts from one mode to another with little overlap (Lorenz, 1976), and they may be used to suggest its existence.

### 3. Ice-age time scale causes

Climate changes also occur on the order of ice ages ( $10^4$ - $10^6$  years). These will not be studied by this thesis as the model that will be used does not include several processes that are thought to be important on these time scales. These include continental drift, ice sheets, and deep ocean currents. It would be relatively simple to include these processes in the model and use it to study these types of changes, and this would be one of the logical extensions of the research presented here, once the model is sufficiently understood and validated for shorter scale climate changes, as will be discussed later. Certain improvements seem to be necessary to reproduce accurately short term climate changes, before attempts are made to study the longer time scales. A brief description of the postulated causes of ice age time

scale climate changes, that are not important for 100 year time scale changes, follows.

a. Intergalactic dust

Clouds of dust exist at various places in our galaxy and at some times in its orbit around the galactic center the solar system passes through these clouds. The effect of such a passage, however, is not clear. McCrea (1975) suggests that the dust would be accreted into the sun and cause a temporary increase in the sun's radiation. Beigelman and Rees (1976) suggest that the dust would block some of the sun's radiation between the sun and earth, leading to a cooling. The dust may also interact with the earth's atmosphere. The total effect, then, is not clear.

b. Orbital variations

The obliquity of the earth's axis changes with a period of about 41,000 years and precession of the equinoxes (wobble of the pole) has approximately a 21,000 year period. These two changes affect the distribution of solar radiation in time and location in the earth's surface during a seasonal cycle without changing the total amount of radiation. The eccentricity of the orbit also changes, with a period of about 100,000 years, and this change influences the amount of radiation, although its effect is not as large as the first two effects. The effect of these orbital variations on climate was first suggested by Milankovitch in 1941 and is known as the Milankovitch hypothesis.

Several recent research efforts indicate that this indeed is the dominant mechanism of climate change on the time scale of  $10^4$ - $10^5$  years.

Calder (1974) and Chappell (1974) compared ice-core oxygen isotope records and sea level changes with calculated orbital effects and found a good correlation. Hays et al. (1976) performed spectral analyses of 2 deep sea cores and found significant power at Milankovitch frequencies. Gribbin (1976) reports energy calculations which verify the orbital hypothesis. Weertman (1976) used an ice sheet model and Milankovitch radiation and concluded that the variations were large enough to produce ice ages. Suarez and Held (1976) used a simple two-level climate model run to equilibrium every 5000 years with the appropriate radiation and found agreement with the past observed changes.

Because the last interglacial lasted approximately 10,000 years and the present one has lasted for 10,000 years already, people such as Mitchell (1972) and Kukla et al. (1972) have suggested based on similarity with the past that the present interglacial will end very soon. Although orbital variations will not be included in the experiments in this thesis, the magnitude of possible changes due to short-term variations is calculated and the possibility that man's effects will be large enough to counteract natural Milankovitch changes will be evaluated.

### c. Continental drift

Continental drift is thought to be important on time scales of  $10^8$  years. For about 300,000,000 years before the present ice age ( $10^7$  year time scale), there was no ice at the poles. The drift of Antarctica to the South Pole, to allow ice to form on its high land surface, and the surrounding of the Arctic Ocean by North America and

Asia, which prevents warm ocean currents from reaching it and allows ice to exist on its surface, may have caused the present ice covered poles with no external changes in solar radiation. In the present thesis, the continents are fixed, but a future study of this theory could be done with the model used by simply assuming a different land distribution.

d. Internal causes

The oceans have time scales important to ice-age climate changes. These were discussed above in section II.B.2., and are also discussed in II.C.3. as oceanic time scales overlap and are also important for shorter time scale climate changes.

Ice-sheet dynamics also introduces time scales that may be important for internal variations on ice-age time scales.

e. Ice-age simulations

Attempts have been made to simulate the climate at the height of the last ice-age 18,000 B.P. Kraus (1973) and CLIMAP (1976) have published observational studies of surface conditions then. Modeling attempts include those of Williams (1974) and Gates (1976a, 1976b).

C. Climate feedback mechanisms

The climate is a statistical representation of the very complex interactive physical system made up of the earth, oceans, atmosphere and cryosphere (ice and snow). In order to adequately model the climate, all physical processes involving changes within and interactions between the various components on the appropriate scales must be

included. A convenient way to discuss these interactions is in terms of individual feedback relations between surface temperature (which has been defined as the indicator of climate) and the different components of the climate system.

These mechanisms were first described by Schneider and Kellogg (1973) and Schneider and Dickinson (1974). This discussion describes the current state of knowledge concerning them. In some cases a positive feedback relationship exists. If the temperature is changed by some external (to the feedback mechanism) forcing, the system interacts to amplify this temperature change and produce an even greater resulting change. In other cases a negative feedback occurs, and temperature changes are damped. In still other cases, the interactions are so complex that it is not now known in which direction the feedback occurs. From a deterministic point of view, the interaction of all the feedbacks simultaneously, with their different time and space scales, determines the reaction of the entire climate system to external forcings. From a non-deterministic point of view, this complex interaction of the various feedback processes, driven by the random disturbances of baroclinic instability, may produce climate changes with no external forcing. In reality, a combination of these points of view is probably necessary to understand climate change. A discussion of the important climate feedback processes follows.

### 1. The hydrological cycle

The distribution of water in all its three phases is an important determining factor in the climate. In fact MacCracken and Potter (1975)



concluded from their model studies that interactions between temperature, precipitable water and infrared emission were more important than the strong ice-albedo feedback studied by Budyko (1969) and Sellers (1969). The amount of moisture in the soil and the distribution of ice and snow on the ocean and land surface affect the albedo and the thermal inertial of the surface. The distribution both horizontally and vertically of water vapor and clouds (liquid and solid water) are important factors in the atmospheric interaction with both solar and terrestrial radiation. Atmospheric transport of latent heat is an important energy transport process. Precipitation, evaporation and surface runoff are important factors in determining the ocean surface salinity and temperature. These last processes, in addition to currents, will be discussed in the next section on oceans. The resulting feedbacks involving water include the following:

a. Water vapor - greenhouse

This is a positive feedback mechanism. If the surface temperature is raised, more water will evaporate from the surface (assuming it is not completely dry) into the atmosphere. This additional water will absorb terrestrial radiation and through the greenhouse mechanism increase the temperature of the air more than if this water had not evaporated. This increased air temperature will cause the surface temperature to increase even further, resulting in the positive feedback. If the atmosphere is assumed to have a constant relative humidity (rather than absolute humidity) in a model, then this feedback will be included.

b. Ice (or snow)-albedo

This is a strong positive feedback mechanism, as demonstrated by the simple climate models of Budyko (1969) and Sellers (1969). Assuming that the ice or snow cover is related to temperature, if temperature increases, for instance, the ice cover will shrink, thereby decreasing the surface albedo. The surface will then absorb more solar radiation, further increasing the temperature, resulting in the positive feedback.

c. Clouds

The relationship between clouds and surface temperature is complex and not well understood. On the one hand increased temperature leads to increased evaporation which increases the moisture available for clouds. Simplistic reasoning would indicate that there would then be more clouds, but whether this would mean deeper clouds with the same total cloud cover, or greater cover with the same thickness, is unclear. On the other hand, recent studies by Sellers (1976) and Roads (1977) have shown that increasing surface temperatures produce more cumuliform and less stratiform cloudiness with a resulting decrease in total cloud cover. The resulting change in cloud cover, depth or type then interacts with both the solar and terrestrial radiation fields to produce temperature changes. These effects, which are highly dependent on surface albedo, are fairly well known, given the above information about the cloud changes. But the reaction of clouds to temperature changes is not well understood, so the overall feedback direction is not known. The role of vertical and horizontal motion fields on clouds is an additional complicating factor and this

interaction with temperature must also be accounted for. The overall effect is probably not very strong in either direction, or it would have been discovered by now with observational studies. Additional discussions of various aspects of this problem have been made by Cess (1974, 1975, 1976).

## 2. Ocean-atmosphere coupling

The ocean plays an important role in the climate system. Heat, moisture and momentum are exchanged across the ocean-atmosphere interface. The processes that control these exchanges and their temporal and spatial variation, as well as those that control the transport of heat and momentum within the ocean, are not well understood. Some of the important components of this interaction, however, will be mentioned.

Heat is transported within the oceans by means of surface currents and eddies and deep currents. Strong western boundary currents, such as the Gulf Stream, accompanied by weaker, broader eastern return flows, are indicative of the surface mean motions. These motions are important on time scales short compared to climate and are an important component in the equator to pole heat flux. The above statement also applies to the recently discovered MODE eddies. Deep ocean currents, which are very slow, also transport heat, but are important on time scales of ten years or longer. Several theories of ice age climate change (see Weyl, 1968 and Newell, 1974) depend on changing transport over long time scales by the deep ocean currents. Recent observational evidence (Pisias et al., 1975; Sachs, 1976 and Ledbetter and Johnson,

1976) seems to support these theories. Attempts have been made to numerically model both the surface and deep ocean circulations, but no consistent quantitative results have been obtained. The total north-south energy transport by the oceans is not even very well known, as discussed in section III.E.1.

The depth of the surface mixed boundary layer determines the thermal inertia of the ocean to short-term energy fluxes at the surface, including horizontal transports. The depth is in turn determined by the sign of the heating at the surface, the magnitude of turbulent mixing produced by the winds, and heat transport from below through the thermocline. The depth is relatively constant in the tropics throughout the year, but experiences a large seasonal variation at mid and high latitudes with surface cooling causing sinking and increased mixing, and deepening the layer, and surface warming heating only the top surface and producing a new shallow mixed layer at the top.

The role of sea surface temperature anomalies in producing atmospheric circulation changes has been discussed by Sawyer (1964) and Namias (1970) and their link to cloudiness has been discussed by Otterman (1975). Numerical studies using the NCAR GCM by Houghton et al. (1974) and Chervin et al. (1976) have shown local effects due to sea surface temperature perturbations, but no significant downstream effects.

Salinity of the ocean water and formation of ice on the surface also play an interactive role in modifying circulation and mixed layer changes in the ocean. Because of the complex nature of the ocean and all its interactions with the atmosphere, no direct temperature

feedback relationship has been established.

### 3. Temperature-radiation

This is an obvious direct negative feedback mechanism. As the temperature of the surface is increased, the radiation leaving the surface increases proportional to the fourth power of the temperature. This acts to cool the surface and decrease the initial temperature change. In the same way, cooling the surface strongly reduces the outgoing radiation, lessening the effect of the cooling.

### 4. Radiative-dynamic coupling

As with dynamics in the ocean, atmospheric dynamics act to redistribute radiatively imposed heating. The heating at the same time acts to modify the dynamics. Again the situation is too complex to specify a direct feedback relationship. Methods of including dynamic fluxes in climate models will be discussed in the next chapter describing the numerical model used for this thesis.

### 5. Temperature-lapse rate

If the atmospheric lapse rate changes in a specified way in response to surface temperature changes, the changes in temperature averaged throughout the atmosphere (which changes in the surface  $T$  are often assumed to represent) can either be larger or smaller than the surface temperature changes. Observations of Angell and Korshover (1975) from 15 years of upper air data showed a tendency for increase of lapse rate during warming, however their data did not extend down to the surface. From Figure 2 of Starr and Oort (1973) it can be

calculated that the 1000 mb temperature actually rose by 0.26°C while the vertical average temperature fell by 0.6°C, showing an increase of lapse rate during warming of the surface and during cooling of the entire atmosphere. Cess (1975), on theoretical grounds, found that climate is quite insensitive to lapse rate as a feedback mechanism. Stone (1973), also theoretically, showed that the assumption of a constant static stability during climate changes was a good one.

The response of lapse rate to surface temperature changes remains unclear as to both its direction and magnitude. The question should properly be included as a subset of the previous section, as complex dynamical processes, including the competing effects of vertical heat flux by large scale eddies and moist convective processes (Schneider and Dickinson, 1974), act to determine the lapse rate, and their relationship to surface temperature is not clear.

#### D. Different modeling approaches

##### 1. Model classification

A large variety of numerical models have been used to study the climate. They each have different features and cover a broad spectrum of approaches to the problem, but attempts have been made to classify them. Detailed descriptions of these various models classified in different ways can be found in the review papers of SMIC (1971), GARP (1974), Gates and Mintz (1974) and Schneider and Dickinson (1974). Without going into detail about the different models, the different approaches taken will be discussed according to four different classification schemes (see Figure 11).

## CLASSIFICATION OF CLIMATE MODELS

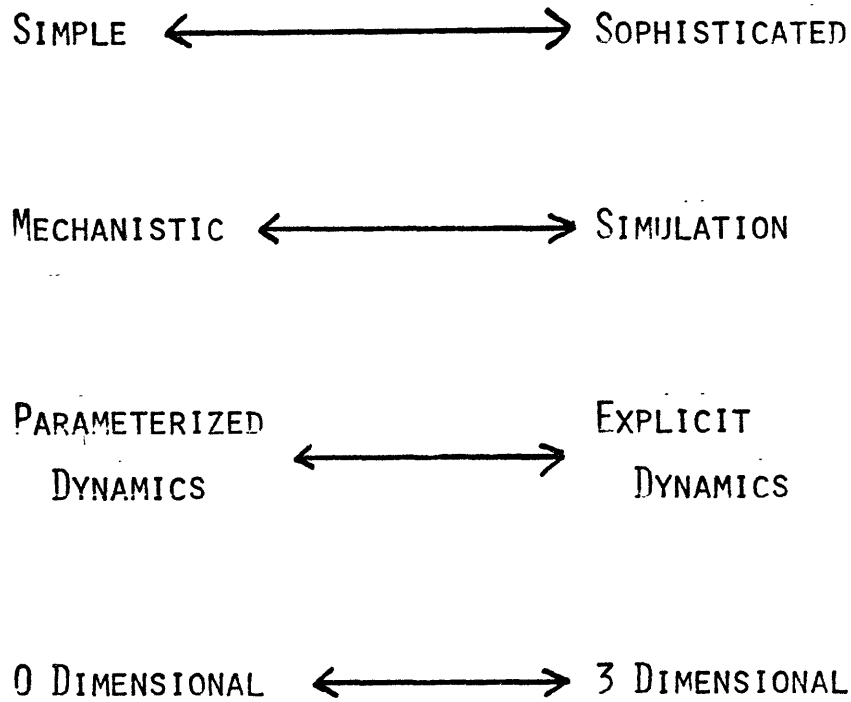


Figure 11.

a) The simplest models look at only one equation describing a certain climate relationship, and solve this equation to understand the relationship that it describes. Sophisticated models solve many equations simultaneously to calculate the results of the many complex interactions described in the equation.

b) Mechanistic models look at only a small number (one or two) of climate feedback mechanisms (see section II.C.) and try to understand the behavior of each mechanism individually without the complex simultaneous interactions of the other mechanisms. These types of models cannot realistically reproduce the behavior of the complete climate system. Simulation models attempt to do this. They include as many of the interacting feedbacks as possible and actually try to reproduce past climate changes. In this context, simulation will be taken to mean simulation of the time response of the climate system, rather than simulation of the instantaneous spatial characteristics of the system, such as Gates and Schlesinger (1977).

c) Dynamical fluxes are an important complex component of the climate system. Some models attempt to calculate atmospheric motions explicitly by solving the equations of motion. This approach is very realistic but the spatial and temporal resolution needed makes it very costly in terms of computer time. In order to get around this problem, some models simulate the averaged effects of the atmospheric motions using simple parameterizations relating the motions directly to mean temperature gradients or other variables predicted by the model. This procedure eliminates a lot of the complex behavior of the atmosphere, especially the random nature of the motions produced by baroclinic



instability, that can be simulated by the explicit models, but can make the model many orders of magnitude faster on the computer, allowing runs which model climatic time scales.

d) The number of spatial dimensions explicitly included in the model is another factor which determines its complexity. Typical zero-dimensional models average the domain vertically throughout the atmosphere and horizontally over the whole globe (Schneider and Mass, 1975) or over one hemisphere (Bryson and Dittberner, 1976). Typical one-dimensional models consider either the vertical dimension (Manabe and Wetherald, 1967) or the y-dimension (north-south) (Sellers, 1969) explicitly and average over the other dimensions. Typical two-dimensional models consider explicitly the x-y plane (Sellers, 1976) or the y-z plane (MacCracken and Potter, 1975). General circulation models (e.g., Somerville, et al., 1974) consider all three dimensions explicitly. If the time dimension is also considered, these models can be further classified; some models are designed to calculate equilibrium conditions while others are designed to simulate time-dependent changes.

Any given model may fall at different places along the scale of each classification scheme, thus preventing a single comprehensive classification scale. Still, certain generalizations can be made about models which lie mostly to the left or right along the scales in Figure 11. Models which lie generally to the left have the advantages of being fast on the computer, and thus allowing simulation of many years of real time, or many separate runs with different conditions. They also have the advantage of allowing the interaction of various physical processes to be more easily understood, due to the lack of

complexity. Models lying to the right of the classification scales, however, can more realistically simulate the complex interactions of the real climate system.

## 2. Choice of a model

The choice of a model to study the climate is dictated by its intended uses. For the purposes of this thesis, a model was desired that would be able to simulate climate changes of the past 100 years and be sophisticated enough to include as many feedback processes as possible, and yet be fast enough on the computer to allow many different runs testing different theories of climate change and different mechanisms of the model itself. The model chosen was one based on the model of Sellers (1973, 1974), modified for the intended purposes. A detailed description of the model, including an analysis of the parameterizations used, the feedback mechanisms included, and its ability to reproduce the present climate, is the subject of the next chapter. The advantages of using this model, as well as the disadvantages, are the subject of this section.

### a. Advantages of the model

At the time this research was begun, no attempts had been made to simulate the climate of the past 100 years. (Since then, several simulations have been attempted, as discussed in the next section.) Although the model was formulated to calculate the time-dependent change of the climate, Sellers only used it to calculate equilibrium states resulting from different external conditions. An indication of the time-dependent nature of the model response is given in Figure 9 of

Sellers (1973), but Sellers (1974) did his best to eliminate this feature from his studies. The model, then, seemed ideally designed for time-dependent simulation, and had not been used for this purpose.

Physical processes of the climate system are highly parameterized in the model. This produces two advantages of the model. First, it is possible to include a large number of feedback mechanisms in the model, thus allowing it to attempt to simulate the complexity of the real climate system. Second, this allows the model to run extremely fast on the computer, easily allowing many runs simulating 100 years of real time.

The complexity of the model allows many different postulated causes of climate change to be explicitly included in the model. The causes studied in this thesis include solar variability, volcanic dust, anthropogenic carbon dioxide, aerosols and heat, and almost-intransitivity. Simple inclusion of processes thought to be important on ice-age time scales, such as ice-sheet dynamics and deep ocean currents, would allow the model to be used to simulate these scale climate changes also.

The model includes the simulation of the seasonal cycle. One common criticism of highly parameterized climate models like this one is that they are constrained to simulate present day climate (because the parameterizations are based on current observations), and it cannot be known whether during changes of climate, the parameters chosen are valid for the new climate regime. The ability of the model to simulate seasonal changes, which are much larger than any observed climate changes of the last 100 years, gives an added measure of confidence in

the parameterization.

The spatial resolution of the model includes explicit consideration of the area of sea surface and of land in each ten-degree latitude band. This allows explicit calculation of the separate thermal inertia of each area as well as heat transports from each land or water area to each adjacent one. Explicit modeling of the land and water areas allows more realistic simulation of effects of the earth's real geography.

b. Disadvantages of the model

Although the model reproduces the present climate, because it is highly parameterized it is not certain that the interactions of the parameterized processes accurately model the interactions in the real world. The accurate reproduction of the present climate may be a fortuitous combination of unrealistic parameterizations.

Although the grid used explicitly considers separate land and ocean areas in each latitude band, longitudinal variations within each of these areas have been observed to be as large as variations between the areas. These variations within the grid areas are averaged out and not considered explicitly.

The model lacks an explicit hydrological cycle and thus certain processes such as ice and snow formation are very artificially parameterized. Clouds and relative humidity are assumed fixed at latitudinal annual averages, and feedbacks between them and other processes are excluded.

Ocean circulations are very artificially parameterized and deep ocean circulations are ignored.

The first two disadvantages are necessitated by computational restraints, and the last two by lack of understanding of the complex processes involved. Correction of these problems may alter the model results.

### 3. Previous simulation attempts

Although no simulation of the climate had been attempted when this research was begun, three attempts have been published since then. Schneider and Mass (1975) used a zero-dimensional, global, annual average model to simulate the forcing due to Kondratyev and Nikolsky's hypothesized solar variations, volcanic dust and anthropogenic carbon dioxide. Pollack, et al. (1975) used a one-dimensional (in the vertical) radiation model to calculate changes due to volcanic dust and carbon dioxide. They did not include time-dependence, but calculated equilibrium states. Bryson and Dittberner (1976) used a zero-dimensional hemispheric model without seasons and forced it with volcanic dust, and anthropogenic aerosols and carbon dioxide. Pollack, et al. and Bryson and Dittberner compared their results to Mitchell's 0°-80°N temperature record and found qualitative agreement. Bryson and Dittberner also found quantitative agreement, but their forcings were carefully calibrated ahead of time to produce the desired result. Schneider and Mass, although presenting the past observations, declined to explicitly compare them to their model results, due to the admitted crudity of their model and the postulated forcings.

None of the models considered explicitly the latitudinal variation of climate or included dynamical fluxes of heat. Seasonal changes were not modeled. Furthermore, only a few deterministic (external) causes of climate change were considered by each study, and no non-deterministic (internal) causes were considered. This study will improve on these previous attempts by comprehensively correcting all the above indicated shortcomings.

### Chapter III. The model

To study the climate, I used a numerical model based on the model of Sellers (1973), hereafter referred to as S. This model was updated by Sellers (1974), hereafter referred to as S'. I made several changes to correct errors in the original model, and to allow the model to be used in a time-dependent simulation mode. I did not attempt to develop new parameterizations. This chapter will first give a general description of the model, derive all the equations used in the model, and describe the numerical method used. Next, the differences between my model and that of Sellers will be discussed explicitly. The balanced climate produced by the model will then be compared with the available real data to see how well it simulates the present climate. Next the sensitivity of the model results to changes of the parameters and the parameterizations will be investigated. Finally, several possible future improvements to the model will be discussed.

#### A. General description

The model I used is a global, seasonal, highly-parameterized, energy-balance, numerical model of the climate. The variable which is being predicted, and which is used in this study as a description of the climate, is 1000 mb air temperature ( $\bar{T}_0$ ).  $\bar{T}_0$  is assumed to represent the horizontally averaged temperature over each grid area, to be described next. It is also a time average, the time step being  $\sim 15$  days (24 time steps/year). In addition,  $\bar{T}_0$  is assumed to be

representative of the entire atmosphere-land or -ocean column of the grid area, as the vertical profile is specified. The basic governing equation of the model is the thermodynamic energy equation. All terms in the equation are parameterized in terms of  $\bar{T}_0$  and its gradient.

The surface of the earth is divided into 18  $10^\circ$  latitude bands, and each band is divided into a land and ocean surface area, giving an 18 x 2 grid, or 35 grid areas, since there is no ocean south of  $80^\circ\text{S}$ . This grid is shown in Figure 12. The land areas in each latitude band are offset relative to each other so that the land-land, land-ocean and ocean-ocean portion of each latitude circle is equal to the observed value. A typical grid area is shown in Figure 13, with all the heat fluxes, to be described later, shown across the proper boundaries.

## B. The equations

In this section the equations used in the final version of the model used for simulations in this thesis will be described. The changes from the original S, S' model will be explicitly discussed in section D. Critical evaluation of the validity of the various model assumptions is included in sections D, F and G.

### 1. Thermodynamic energy equation

The thermodynamic energy equation, the basic equation which is solved at each grid area at each time step, is:

$$\bar{R} = \frac{1}{g} \int_0^{p_0} \frac{d}{dt} (Lq + c_p T_A + gh) dp + c \int_0^d \frac{d\bar{T}_E}{dt} dz \quad (1)$$



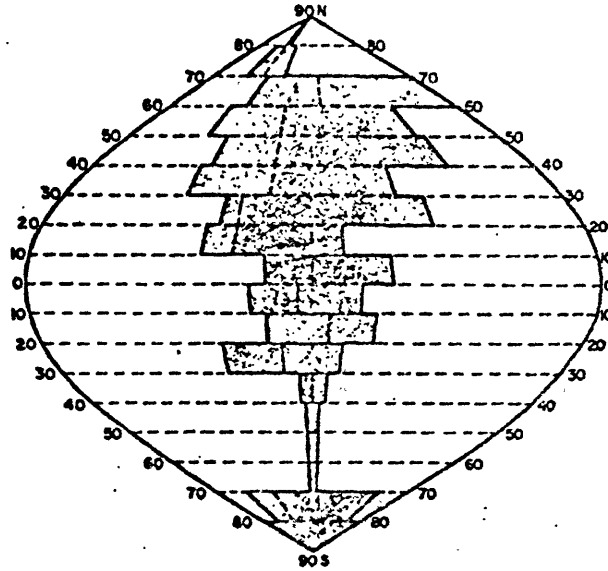


Fig. 12. The idealized continent-ocean system used in this study. The vertical dashed lines separate the land masses of the western and eastern hemispheres.

This figure is from Sellers (1973).

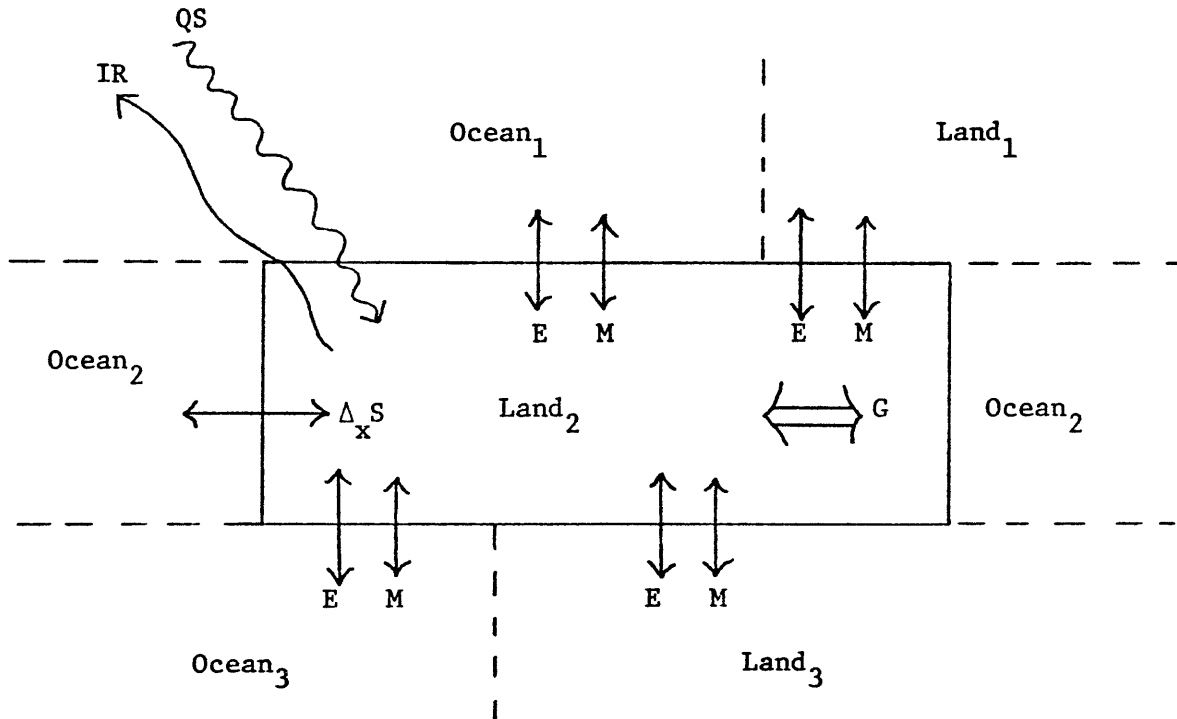


Figure 13. A typical land grid area. Ocean grid areas are exactly the same, but have an additional North-South eddy flux of heat across ocean-ocean boundaries due to oceanic circulation.

- E = atmospheric eddy heat flux
- M = atmospheric heat flux due to mean winds
- $\Delta S_x$  = East-West heat flux by mean wind
- QS = solar radiation
- IR = terrestrial radiation
- G = heat storage

where  $\bar{x} = \frac{1}{t'} \int_0^{t'} x dt$

$t'$  = time step = 15 days = 365.2422/24 days

$R$  = net available radiation for a column from the top of the atmosphere to a depth  $d$  in the soil or water, below which the vertical energy flux is negligible =  $QS - IR$

$QS$  = net solar radiation

$IR$  = net terrestrial radiation

$g$  = acceleration of gravity  $\approx 9.8 \text{ m/sec}^2$

$p_0$  = surface pressure = 1000 mb over oceans,  
and see Table 6 for land values

$L$  = latent heat of condensation = 2500 J/gm

$q$  = specific humidity

$c_p$  = specific heat of air at constant pressure = 1.005 J/(gm °C)

$T_A$  = air temperature

$h$  = height above sea level

$c$  = heat capacity of soil or water

$T_E$  = soil or water temperature

Each of the total derivatives under the first integral on the right-hand side of (1) may be expanded as

$$\frac{d\bar{s}}{dt} = \frac{\partial \bar{s}}{\partial t} + \frac{\partial}{\partial x} \bar{u} \bar{s} + \frac{\partial}{\partial y} (\bar{v} \bar{s} + \overline{v' s'}) + \frac{\partial}{\partial p} \bar{\omega} \bar{s} \quad (2)$$

where  $s$  = either latent heat ( $Lq$ ), sensible heat ( $c_p T$ ) or potential energy ( $gh$ )

$u$ ,  $v$  and  $\omega$  = three components of the wind

Table 6. Model parameter values.

Latitude band	$p_o$ (land) (mb)	$A_L'$	$r_L$ (%)	$r_W$ (%)	$n$ (%)	$\alpha_L$ (%)	$\alpha_W$ (%)	Latitude circle	$b$	$d$ (m)
80° - 90°N	998	1.00	84	88	62.4	16	12.4	80°N	1.16	40
70° - 80°N	991	1.75	82	87	67.5	16	12.1	70°N	1.10	45
60° - 70°N	992	1.53	80	85	65.5	16	11.9	60°N	0.96	50
50° - 60°N	976	1.54	77	82	63.5	16	9.5	50°N	0.86	60
40° - 50°N	961	1.36	72	78	57.3	15	8.1	40°N	0.95	70
30° - 40°N	940	1.67	62	78	47.3	16	7.2	30°N	1.10	80
20° - 30°N	976	1.08	57	80	40.8	18	6.7	20°N	1.19	85
10° - 20°N	964	1.29	64	84	43.8	13	6.3	10°N	1.17	90
0° - 10°N	943	1.60	76	86	51.3	8	6.2	EQ	1.16	90
0° - 10°S	966	1.75	76	86	49.0	8	6.2	10°S	1.17	90
10° - 20°S	930	2.33	64	84	47.3	13	6.3	20°S	1.19	85
20° - 30°S	956	2.00	57	80	48.0	18	6.7	30°S	1.10	80
30° - 40°S	978	2.00	68	78	54.1	16	7.2	40°S	0.95	70
40° - 50°S	1000	1.00	78	78	65.5	15	8.1	50°S	0.86	60
50° - 60°S	1000	1.00	82	82	77.6	16	9.5	60°S	0.96	50
60° - 70°S	1000	1.00	85	85	74.0	16	11.9	70°S	1.10	45
70° - 80°S	930	1.26	82	87	56.6	16	12.1	80°S	1.16	40
80° - 90°S	784	1.00	84		45.5	16	12.4			

The  $\overline{u's'}$  term is small due to the grid shape and therefore neglected.  $\overline{v's'}$  is approximated as  $-K_s \frac{\partial \bar{s}}{\partial y}$ ;  $K_s$  is the eddy diffusivity. This term represents the combined effects of standing and transient eddies.

Each term obtained when (2) is inserted into (1) may be written as follows where  $G_s$  is the heat storage term,  $S_T$  is the total north-south heat transport,  $M_s$  is the mean meridional portion,  $E_s$  is the eddy portion, and the "o" subscript refers to surface values:

$$G_s = \frac{1}{g} \int_0^{P_0} \frac{\partial \bar{s}}{\partial t} dp = \frac{1}{g} a_{cs} \frac{\partial \bar{s}_o}{\partial t} P_0 \quad (3)$$

$$\begin{aligned} \Delta_x S &= \frac{1}{g} \int_0^{P_0} \frac{\partial}{\partial x} \bar{\mu} \bar{s} dp = \frac{1}{g} \int_0^{P_0} \bar{\mu} \frac{\partial \bar{s}}{\partial x} dp \\ &= \frac{1}{g} a_{xs} \bar{\mu}_o \frac{\partial \bar{s}_o}{\partial x} P_0 A_L' \end{aligned} \quad (4)$$

$$\begin{aligned} \Delta_y S_T &= \frac{1}{g} \int_0^{P_0} \frac{\partial}{\partial y} (\bar{v} \bar{s} - K_s \frac{\partial \bar{s}}{\partial y}) dp \\ &= \frac{1}{g} \frac{\partial}{\partial y} \int_0^{P_0} (\bar{v} \bar{s} - K_s \frac{\partial \bar{s}}{\partial y}) dp \end{aligned} \quad (5)$$

$$M_s = \frac{1}{g} \int_0^{P_0} \bar{v} \bar{s} dp = \frac{1}{g} a_{ms} \bar{v}_o \bar{s}_o P_0 \quad (6)$$

$$E_s = - \frac{1}{g} \int_0^{p_0} K_s \frac{\partial \bar{s}}{\partial y} dp = - \frac{1}{g} a_{ES} K_s \frac{\partial \bar{s}_0}{\partial y} p_0 \quad (7)$$

$$S_T = M_s + E_s \quad (8)$$

$$\frac{1}{g} \int_0^{p_0} \frac{\partial}{\partial p} \bar{\omega} \bar{s} dp = 0 \quad (9)$$

When these equations apply to potential energy,  $\bar{h}_0 = R_d \bar{T}_0 / g$ , the scale height of an isothermal atmosphere, and  $R_d$  is the gas constant for dry air = 0.287 J/(gm°C). In equation (4),  $A'_L = A_L / A_{LM}$ , when  $A_L$  is the fraction of the given latitude belt occupied by land and  $A_{LM}$  is the fraction of the belt occupied by the largest single land mass. This factor takes account of the number of land-ocean boundaries in a zonal direction in each latitude belt, and is the effective width of the belt. Its value is always between 1 and 2.33 and is tabulated in Table 6.

The coefficients in (3), (4), (6) and (7) relate the integrals of temperature, wind speed and humidity to their surface values. They are discussed and evaluated in the next section.

The second integral in (1) may be written for land,

$$c_L \int_0^d \frac{d\bar{T}_L}{dt} dz = c_L \int_0^d \frac{\partial \bar{T}_L}{\partial t} dz = G_L \quad (10)$$

and for water,

$$\begin{aligned} c_w \int_0^d \frac{d\bar{T}_w}{dz} dz &= c_w \int_0^d \frac{\partial \bar{T}_w}{\partial t} dt - c_w \frac{\partial}{\partial y} \int_0^d K_w \frac{\partial \bar{T}_w}{\partial y} dz \\ &= G_w + \Delta y F \end{aligned} \quad (11)$$

$$\text{where } F = - c_w \int_0^d K_w \frac{\partial \bar{T}_w}{\partial y} dz = - c_w a_F K_w \frac{\partial \bar{T}_w}{\partial y} d \quad (12)$$

F is discussed in section B.3.c and  $G_L$  and  $G_W$  are discussed in section B.4.

## 2. Vertical profiles

In order to evaluate the coefficients in (3), (4), (6) and (7), vertical profiles of temperature, wind speed, and humidity were assumed, in a manner similar to Saltzman and Vernekar (1971):

$$\bar{T} = \bar{T}_o - (p_o - p) \frac{\partial \bar{T}}{\partial p} \quad (13)$$

$$\bar{u} = \bar{u}_o + (p - p_o) \frac{\partial \bar{u}}{\partial p} \quad (14)$$

$$\bar{v} = \bar{v}_o \left( \frac{2p - p_o}{p_o} \right) \quad (15)$$

$$\bar{q} = \bar{q}_o (p/p_o)^{a1} \quad (16)$$

It is assumed that 1)  $\frac{\partial \bar{T}}{\partial p} = 0.12^\circ\text{C}/\text{mb}$ , a value similar to that of Saltzman and Vernekar, and 2) except at the equator

$$\frac{\partial \bar{u}}{\partial p} = \frac{R_d}{f p_a} \frac{\partial \bar{T}_p}{\partial y} \quad (17)$$

where  $p_a = 500$  mb and  $f$  is the Coriolis parameter. At the equator it is assumed that  $\partial \bar{u} / \partial p = 0$ .

In (16), the exponent  $a_1$  may be determined by integrating (16) from  $p_0$  to the top of the atmosphere. This gives

$$1 + a_1 = \frac{0.622 e_0}{g w_a} \quad (18)$$

where  $w_a$  is the precipitable water vapor in the column and  $\bar{e}_0$  is the surface vapor pressure

$$\bar{e}_0 = p_0 \bar{q}_0 / 0.622 = r \bar{e}_0^* \quad (19)$$

$r$  is the relative humidity, assumed constant in time at the climatological average value for each latitude band separately for land and water, as given in Table 6.  $\bar{e}_0^*$  is the saturation vapor pressure at temperature  $\bar{T}_0$  and is obtained from the Clausius-Clapeyron equation. The precipitable water vapor  $\bar{w}_a$  [cm] was empirically related to the surface vapor pressure  $\bar{e}_0$  [mb] by S using observed data:

$$\bar{w}_a = (0.123 + 0.152 \bar{e}_0) \frac{p_0}{1000} \quad (20)$$

From the hydrostatic equation and (13), it follows that

$$\bar{h} = \frac{R_d}{g} \left[ (\bar{T}_0 - p_0 \frac{\partial \bar{T}}{\partial p}) \ln \frac{p_0}{p} + \frac{\partial \bar{T}}{\partial p} (p_0 - p) \right] \quad (21)$$

This derivation is given in Appendix A.

In (4), with  $\bar{s} = c_p \bar{T}$ , the integral of  $\bar{u}(\partial \bar{T} / \partial x)$  becomes much too large if the zonal temperature gradient is allowed to maintain its surface value to the top of the atmosphere when zonal velocities are



highest, from (14). Therefore, from observations, it was assumed that this gradient decreases linearly with pressure to zero at 500 mb. That is,

$$\frac{\partial \bar{T}}{\partial x} = \frac{1}{p_0} (2p - p_0) \frac{\partial \bar{T}_0}{\partial x}, \quad p \geq 500 \text{ mb} \quad (22)$$

$$\frac{\partial \bar{T}}{\partial x} = 0, \quad p < 500 \text{ mb} \quad (23)$$

These equations are not consistent with the assumption of a constant temperature lapse rate in (13). However, because the zonal transport terms are small, it is not believed that this is a serious discrepancy.

The a coefficients may now be determined by introducing (13)-(16) and (21)-(23) into (3), (4), (6) and (7) and integrating. The derivations are given in Appendix B. They give

$$a_{GH} = 1.0 \quad (24)$$

$$a_{GP} = 1.0 \quad (25)$$

$$a_{GV} = \frac{1}{1 + a1} \quad (26)$$

$$a_{XV} = \frac{1}{1 + a1} \left( 1 - \frac{1}{2 + a1} \frac{p_0}{\bar{u}_0} \frac{\partial \bar{u}}{\partial p} \right) \quad (27)$$

$$a_{XH} = \frac{1}{4} \left( 1 - \frac{1}{6} \frac{p_0}{\bar{u}_0} \frac{\partial \bar{u}}{\partial p} \right) \quad (28)$$

$$a_{XP} = 0.0966 \left( 1 - 0.319 \frac{p_0}{\bar{u}_0} \frac{\partial \bar{u}}{\partial p} \right) \quad (29)$$

$$a_{MH} = \frac{1}{6} \frac{P_0}{\bar{T}_0} \frac{\partial \bar{T}}{\partial p} \quad (30)$$

$$a_{MV} = \frac{a1}{(1 + a1)(2 + a1)} \quad (31)$$

$$a_{MP} = 2 a_{MH} - 0.5 \quad (32)$$

$$a_{EH} = 1.0 \quad (33)$$

$$a_{EV} = \frac{1}{1 + a1} \quad (34)$$

$$a_{EP} = 0 \quad (35)$$

The value for  $a_{EP}$  follows from the observation of Gort and Rasmusson (1971), among others, that the meridional transport of eddy potential energy is small and can be neglected.

### 3. Dynamical fluxes

#### a. Mean wind fluxes

To evaluate (4) and (6) it is necessary to calculate the surface values of the horizontal wind. Approximate expressions may be derived from the equations of motion applicable to this problem

$$f \bar{v}_0 + \bar{\alpha}_0 \frac{\partial \bar{\tau}_{0x}}{\partial z} = 0 \quad (36)$$

$$f \bar{\mu}_0 - \bar{\alpha}_0 \frac{\partial \bar{\tau}_{0y}}{\partial z} + \bar{\alpha}_0 \frac{\partial \bar{p}_0}{\partial y} = 0 \quad (37)$$

where  $\bar{\alpha}_0$  is the surface specific volume and  $\bar{\tau}_{ox}$  and  $\bar{\tau}_{oy}$  are, respectively, the eastward and northward components of the frictional stress, assumed to vanish at the top of the friction layer. Assuming a logarithmic wind profile near the ground, it follows that

$$-\bar{\alpha}_0 \frac{\partial \bar{\tau}_{ox}}{\partial z} = a |\bar{u}_0| \bar{u}_0 \quad (38)$$

$$-\bar{\alpha}_0 \frac{\partial \bar{\tau}_{oy}}{\partial z} = a |\bar{v}_0| \bar{v}_0 \quad (39)$$

where

$$a = \frac{g}{\bar{\alpha}_0 \Delta p} k^2 \left( \ln \frac{z}{z_0} \right)^{-2}$$

and  $\Delta p$  is the depth of friction layer, assumed to equal 100 mb;  $k$  is the von Karman constant, assumed to equal 0.40 over land and 0.35 over oceans (Tennekes, 1973); and  $z_0$  is the roughness length, assumed to equal 100 cm over land and 0.01 over water.  $Z$  is assumed to equal 10 m, and for each latitude circle, a weighted average of  $a$  is calculated, depending on the portions of the circle that are land-land, land-ocean, or ocean-ocean boundaries.

The pressure gradient term in (37) is the small difference between two large terms of the same sign. That is, from the equation of state,

$$\begin{aligned} \bar{\alpha}_0 \frac{\partial p_0}{\partial y} &= R_d \frac{\partial \bar{T}_0}{\partial y} - \bar{p}_0 \frac{\partial \bar{\alpha}_0}{\partial y} = R_d \frac{\partial \bar{T}_0}{\partial y} - b R_d \frac{\partial \bar{T}_0}{\partial y} \\ &= R_d (1-b) \frac{\partial \bar{T}_0}{\partial y} \end{aligned} \quad (40)$$

Values of the constant  $b \left( = \frac{\bar{T}_o}{\bar{\alpha}_o} \frac{\partial \bar{\alpha}_o}{\partial \bar{T}_o} \right)$  were determined by S from observations and are listed in Table 6.

Equations (28) and (29) now become:

$$f \bar{v}_o - a \left| \bar{u}_o \right| \bar{u}_o = 0 \quad (41)$$

$$f \bar{u}_o + a \left| \bar{v}_o \right| \bar{v}_o + R_d (1 - b) \frac{\partial \bar{T}_o}{\partial y} = 0 \quad (42)$$

Solving for  $\bar{u}_o$  and  $\bar{v}_o$  gives

$$\bar{u}_o = 0, \quad \bar{v}_o = \left( \frac{R_d}{a} (b-1) \frac{\partial \bar{T}_o}{\partial y} \right)^{1/2} \quad \text{at the equator,} \quad (43)$$

$$\bar{u}_o = \frac{R_d (b-1) \frac{\partial \bar{T}_o}{\partial y}}{f \left( 1 + \left| \frac{a \bar{u}_o}{f} \right|^3 \right)}, \quad \bar{v}_o = \frac{a}{f} \left| \bar{u}_o \right| \bar{u}_o \quad \text{elsewhere.} \quad (44)$$

Equation (44) is solved for  $\bar{u}_o$  by Newton's method, since  $\bar{u}_o$  appears on both sides of the equation. In order to increase the stability of the computations, the values of  $\bar{u}_o$  and  $\bar{v}_o$  obtained are smoothed latitudinally using a 1-2-1 smoothing.

#### b. Atmospheric eddy fluxes

Following evidence presented by S and also by Stone (1973), the eddy diffusivities for specific and latent heat are made proportional to the temperature gradient:

$$K_H = K_V = 2.5 \times 10^5 \left| \Delta \bar{T}_o \right| \text{ m}^2/\text{sec} \quad (45)$$

where  $\Delta\bar{T}_0$  is the surface temperature difference between successive  $10^\circ$  latitude belts. These values were smoothed in the same manner as the velocity components.

In order to increase the linear dependence of the solution on the surface temperature, (7) when applied to latent heat was rewritten

$$E_v = -\frac{1}{g} \alpha_{EV} K_v p_0 L \frac{\partial \bar{q}_0}{\partial \bar{T}_0} \frac{\partial \bar{T}_0}{\partial y} \quad (46)$$

$\frac{\partial \bar{q}_0}{\partial \bar{T}_0}$  is still a non-linear function of  $\bar{T}_0$ .

#### c. Oceanic eddy fluxes

The eddy diffusivity  $K_W$  for heat transfer by ocean currents, appearing in (12) is given by

$$K_W = 1.7 \times 10^5 (1 - A_I) A_L \text{ m}^2/\text{sec} \quad (47)$$

where  $A_I$  is the fractional area of the oceans covered by ice. The factor  $A_L$  is introduced to take into account the effect of the continents in channeling the north-south ocean currents. The average value of  $K_W$  is about  $5 \times 10^4 \text{ m}^2/\text{sec}$ , which agrees well with values found in the vicinity of the Gulf Stream, but is about an order of magnitude larger than values considered typical for other parts of the oceans. This discrepancy is intentional, and is an attempt to account partially for the neglected heat transport by vertical circulations. Also, in (12), it is assumed that  $a_F = 1.0$  and that  $d$ , the mixing depth, is equal to the observed value as given by S and as listed in Table 6.

#### 4. Surface heat storage

The rate of heat storage in land ( $G_L$ ) and water ( $G_W$ ) is expressed as a function of the surface temperature using the classical theory of heat transfer in a homogeneous medium under the action of a sinusoidal surface temperature variation. The result is

$$G = \left( \frac{\pi}{P} C \lambda \right)^{1/2} \left( \bar{T}_o - \bar{\bar{T}}_o + \frac{P}{2\pi} \frac{\partial \bar{T}_o}{\partial t} \right) \quad (48)$$

where  $P$  is the period of the oscillation (1 year),  $\bar{\bar{T}}_o$  the mean annual 1000 mb temperature and  $\lambda$  the thermal conductivity of the medium. The product  $(C\lambda)^{.5}$  is called the thermal property by S and equals  $1.67 \times 10^{-5}$  J/(m<sup>2</sup> °C sec<sup>.5</sup>) for land. For water, it depends on the ice cover and is assumed to equal  $(8.37 \times 10^{-4} - 8.16 \times 10^{-4} A_I)$  in the same units.

#### 5. Solar radiation

The net solar radiation is determined by

$$QS = Q (1 - \alpha). \quad (49)$$

The albedo,  $\alpha$ , of the surface-atmosphere system is determined from

$$\alpha = r_* + \frac{t_*^2 \alpha_s}{1 - \alpha_s r_*} \quad (50)$$

where  $\alpha_s$  = surface albedo

$r_*$  = fractional reflection to space

$t_*$  = fractional transmission of atmosphere

These last two terms were determined from a simplified form of a two-stream approximate solution to the multiple scattering problem for a

thin atmosphere, as given by Sagan and Pollack (1967):

$$t_* = 2 / [ \sqrt{3} \tau (2 - \tilde{\omega}_0 - \tilde{\omega}_0 \langle \cos \theta \rangle) + 2 + 3 (1 - \tilde{\omega}_0 \langle \cos \theta \rangle) (1 - \tilde{\omega}_0) \tau^2 ] \quad (51)$$

$$r_* = \frac{\sqrt{3}}{2} \tilde{\omega}_0 (1 - \langle \cos \theta \rangle) \tau t_* \quad (52)$$

where  $\tau$  = optical thickness of the atmosphere

$\tilde{\omega}_0$  = single-scattering albedo

$\langle \cos \theta \rangle$  = assymetry factor, describing the degree of forward scattering

Drawing on information from a number of sources, S determined that  $\tau$ ,

$\tilde{\omega}_0$ , and  $\langle \cos \theta \rangle$  were respectively equal to  $0.0003 p_0$ , 0.95 and 0.64

for clear skies, and  $0.005 p_0$ , 0.99 and 0.84 for cloudy skies,  $p_0$  in

mb. The fractional cloudiness,  $n$ , of each latitude band was set equal

to the observed annual average as given by London (1957), Sasamori et

al. (1972) and Vowinckel and Orvig (1970), and is listed in Table 6.

Surface albedos for snow-free land,  $\alpha_{Lo}$ , are listed in Table 6 and

were taken from observations gathered by S. Annual average values of

ice-free sea surface albedos,  $\alpha_{Wo}$ , are also listed in Table 6. It was

determined from the observations of Payne (1972) that sea surface

albedos for different months and latitudes fit the formula

$$\alpha_{Wo} = 0.06 / \cos \gamma \quad (53)$$

where  $\gamma = (\text{latitude} - \text{solar zenith angle})/1.2$ . These values, which

depend only on solar zenith angle for their time dependence, were used

for each month and season, and their annual average was used in the

model. The albedo of snow was set equal to 0.8 and the albedo of snow-free ice was set equal to 0.6 for temperatures below freezing, and 0.4 for temperatures above freezing, to account for puddles on the ice surface (Chernigovskiy, 1966).

The fractional area of the ocean covered by ice,  $A_I$ , the fractional area of the ice covered by snow,  $A_{IS}$ , and the fractional area of land covered by snow,  $A_S$ , were all empirically determined by S based on observations. The resulting relationships are:

$$A_I = c_1 - c_2 \frac{\bar{T}_S^A}{\bar{T}_{WS}^A} \frac{\bar{T}_{WS}^{(i)}}{\bar{T}_{WS}^A} \quad (54)$$

$$A_{IS} = c_3 - c_4 \frac{\bar{T}_S^A}{\bar{T}_{WS}^A} \frac{\bar{T}_{WS}^{(i)}}{\bar{T}_{WS}^A} \quad (55)$$

$$A_S = c_3 - c_4 \frac{\bar{T}_S^A}{\bar{T}_{LS}^A} \frac{\bar{T}_{LS}^{(i)}}{\bar{T}_{LS}^A} \quad (56)$$

where

$$c_1 = 8.44$$

$$c_2 = 0.00010983$$

$$c_3 = 10.89$$

$$c_4 = 0.00014085$$

$$\bar{T}_S^A = \text{annual average surface temperature}$$

$$\bar{T}_S^{(i)} = \text{surface temperature } i \text{ time steps previous to current one}$$

Previous surface temperatures were used to account for the observed lag between temperature and ice or snow cover. It was found that  $i = 3$  made the resulting net annual radiation closest to zero, since the above



formulations are not in themselves energy consistent. Since the model contains no explicit hydrological cycle, snow or ice persistence was simulated by including the mean annual temperature in the above formulations.

### 6. Terrestrial radiation

A relatively simple two-layer model is used to estimate the net infrared emission to space, IR. Separate calculations were performed for the clear and cloudy fractions of the grid area, and the total IR was the fractional cloud area-weighted sum of the two calculations. The first layer, with a radiating temperature  $\bar{T}_{A1}$ , extends from  $p_0$  to 500 mb. It contains half of the total atmospheric carbon dioxide (234.2 cm for pre-industrial times) and 10% of the total ozone (3 mm). The remainder of these gases is found in the upper layer, which has a temperature  $\bar{T}_{A2}$ . The lower layer contains  $\bar{w}_{A1}$  cm of precipitable water and the upper layer  $\bar{w}_{A2}$  cm. From (16) it follows that

$$\bar{w}_{A2} = \bar{w}_a \left(\frac{500}{p_0}\right)^{1+a_1}, \quad \bar{w}_{A1} = \bar{w}_a - \bar{w}_{A2} \quad (57)$$

The corrected optical depth for each gas is assumed to equal the actual amount multiplied by  $(p_e/p_0)^{k'}$ , where  $p_e$  is the effective pressure of the radiating gas and  $k'$  a constant equal to, following Manabe and Wetherald (1967), 0.7 for water vapor, 0.67 for carbon dioxide and 0.3 for ozone. For  $p_e$ , values of  $0.8 p_0$  for  $H_2O$ , and 750 mb for  $CO_2$  and  $O_3$  were used in layer 1; and 450 mb for  $H_2O$ , 250 mb for  $CO_2$  and 50 mb for  $O_3$  in layer 2. For the cloudy regions, clouds are assumed to occupy an infinitely thin stratum between the two layers and to have a temperature equal to  $[0.5 (\bar{T}_{A1}^4 + \bar{T}_{A2}^4)]^{1/4}$ .

It follows then that

$$IR = (1 - n) IR_{NC} + nIR_C \quad (58)$$

where  $IR_{NC}$  is the IR with no clouds and  $IR_C$  is the IR with clouds:

$$IR_{NC} = (1 - \epsilon_{TNC}) \epsilon_0 \sigma \bar{T}_0^4 + (1 - \epsilon_{2NC}) \epsilon_{1NC} \sigma \bar{T}_{A1NC}^4 + \epsilon_{2NC} \sigma \bar{T}_{A2NC}^4 \quad (59)$$

$$IR_C = 0.5(1 - \epsilon_{2c}) \sigma (\bar{T}_{A1c}^4 + \bar{T}_{A2c}^4) + \epsilon_{2c} \sigma \bar{T}_{A2c}^4 \quad (60)$$

where  $\epsilon_0$ ,  $\epsilon_1$ ,  $\epsilon_2$  and  $\epsilon_T$  are the emissivities, respectively, of the earth's surface (0.9), layer 1, layer 2 and the entire atmospheric column.  $\bar{T}_{A1}$  and  $\bar{T}_{A2}$  are calculated separately for clear and cloudy conditions as functions of  $\bar{T}_0$  using the empirical condition that each layer is cooling radiatively at a rate equal to 1.50 °C/day times its emissivity (which practically always lies between 0.54 and 0.85). The derivations of the equations for  $\bar{T}_{A1}^4$  and  $\bar{T}_{A2}^4$  are given in Appendix C.

Tables given by Staley and Jurica (1970) were used to estimate the various emissivities. For all the gases, from S',

$$\epsilon_T = 1 - (1 - \epsilon_1)(1 - \epsilon_2) \quad (61)$$

For ozone,  $\epsilon_1 = 0.033$  and  $\epsilon_2 = 0.030$ . The emissivity of water vapor is given by the empirical relation, from S',

$$\begin{aligned} \epsilon_{H_2O} = & a' + b' \log w_a' + c' (\log w_a')^2 \\ & + d' (\log w_a')^3 \end{aligned} \quad (62)$$

where  $w_a'$  [cm] is the corrected optical depth and  $a'$ ,  $b'$ ,  $c'$  and  $d'$  are functions of the  $CO_2$  amount, to correct for the overlap between  $CO_2$  and  $H_2O$  absorption bands. Values of  $a'$ ,  $b'$ ,  $c'$  and  $d'$  are given in Table 7 for three different values of  $CO_2$  amount, and were linearly interpolated for intermediate values. The emissivity of carbon dioxide was determined for each layer from the empirical relation

$$\epsilon_{CO_2} = 0.01 \cdot \bar{T}_A h'$$

where  $h' = 0.427 + 0.05 \log m$

$m$  = pressure corrected optical depth of  $CO_2$ , in cm, for each layer

This relationship makes the  $CO_2$  emissivity a function of both layer temperature and  $CO_2$  amount.

### C. Numerical method

Equation (1) can be rewritten for each grid area, using the symbols of (3)-(12) as

$$\begin{aligned} G_T \cdot A_{LOC} = & R \cdot A_{LOC} + XFLUX \cdot A_L \cdot (-1)^{LOC} \\ & + (FLUX)_{LOC, LOC, S} \cdot X_{LOC, LOC, S} \\ & + (FLUX)_{LOC, NLOC, S} \cdot X_{LOC, NLOC, S} \end{aligned}$$

Table 7. Parameter values for equation (62), from S'.

Layer	CO <sub>2</sub> amount (cm)	a'	b'	c'	d'
1	125	0.525	0.154	0.0416	0.0156
	250	0.519	0.147	0.0384	0.0154
	500	0.512	0.140	0.0387	0.0174
2	125	0.552	0.162	0.0425	0.0167
	250	0.548	0.157	0.0388	0.0148
	500	0.544	0.152	0.0365	0.0145

$$\begin{aligned}
 & - (\text{FLUX})_{\text{LOC}, \text{LOC}, \text{N}} \cdot X_{\text{LOC}, \text{LOC}, \text{N}} \\
 & - (\text{FLUX})_{\text{NLOC}, \text{LOC}, \text{N}} \cdot X_{\text{NLOC}, \text{LOC}, \text{N}} \quad (64)
 \end{aligned}$$

where LOC = L or W, depending on whether grid area is land or water

NLOC = L if LOC = W, NLOC = W if LOC = L

L = land

W = water

$$G_T = G_H + G_V + G_P + G_{\text{LOC}}$$

$$X_{\text{FLUX}} = \Delta_x H + \Delta_x V + \Delta_x P$$

$$(\text{FLUX})_{ijk} = (H + V + P + F) \text{ across boundary of length } X_{ijk};$$

with i to north, j to south and along k border of grid area. F = 0 unless i = j = W. For example

$(\text{FLUX})_{L,W,N}$  is the total flux across the portion of the northern boundary of a water grid area that has land to the north.

Boundary conditions are provided by

$$X_{\text{LLN}} = X_{\text{LWN}} = X_{\text{WWN}} = X_{\text{WLN}} = 0, \text{ between } 80^\circ\text{N and } 90^\circ\text{N}, \quad (65)$$

$$X_{\text{LLS}} = X_{\text{LWS}} = X_{\text{WWS}} = X_{\text{WLS}} = 0, \text{ between } 80^\circ\text{S and } 90^\circ\text{S}. \quad (66)$$

Time differencing is by means of a Crank-Nicholson scheme. The time step is taken to be 1/24 of a year. Equation (1) can be rewritten for each land area or each water area combining all the linear terms in temperature of the grid area, temperature of the grid area to the north of the same composition (L or W), and grid area to the south of

the same composition:

$$W_{4\ell} = W_{1\ell} T_{\ell+1}^i + W_{2\ell} T_{\ell}^i + W_{3\ell} T_{\ell-1}^i \quad (67)$$

where  $i$  = time step

$\ell$  = latitude index

$$W_j = \theta W_j^i + (1 - \theta) W_j^{i-1}, \quad j = 1-3$$

$W_4$  = non-linear terms in  $T^i$  plus all other terms not  $f(T^i)$

$$\theta = 0.5$$

An iteration procedure is then used to solve (67) for all grid points as follows. First the temperature of each land or water grid area is estimated as the temperature it had during the same month ("month" is used here to denote time step; there are 24 "months" per year) in the previous year, plus the change of temperature that occurred during the previous month from its value the previous year. Second, using these estimated temperatures,  $W_{1-4}$  are calculated for all the land grid areas. New temperatures for all the land areas are then solved for simultaneously using Gaussian elimination of a tri-diagonal matrix, a very rapid procedure. The new temperatures thus calculated replace the estimated temperatures for land and  $W_{1-4}$  are then calculated for water. The water temperatures (temperatures of the ocean-atmosphere column) are then solved for simultaneously as above. The new water temperatures are then used to calculate  $W_{1-4}$  for land and the iteration proceeds. Iteration continues until the maximum of the temperature difference for any of the grid areas between the new and old temperatures is less than some convergence criterion.

The criterion used is  $0.01^{\circ}\text{C}$ . The minimum number of iterations is 2, that is new temperatures must be calculated for all land and water grid areas to replace the estimates at each time step. If the temperature at any grid area is oscillating from one iteration to the next, a smoothing in time is performed to try to damp the oscillation and lower the needed number of iterations. An arbitrary limit of 20 is imposed on the iterations at any time step. This limit is reached only when large perturbations are imposed every time step, or a few times during the most rapid temperature change when the climate is proceeding into an ice-covered earth. The mean number of iterations per time step with a balanced climate is 2.18. (A complete cycle of calculating land, and then water temperatures is counted as two iterations.) This iteration procedure is explained in a flow chart in Figure 14.

#### D. Differences between my model and Sellers'

Much of the preceding two sections was taken verbatim from S and S'. In order to indicate the changes I made from the original model, they are discussed explicitly in this section. The changes and the reasons for them are explained. The effects on the model output of most of these changes are described in section F.2.

##### 1. Infrared formulation

Calculating the total infrared (IR) emissions first requires that the temperatures of two atmospheric layers be determined based on assumptions about the cooling rate (see Appendix C). These temperatures are then used to calculate the IR emission, using equations

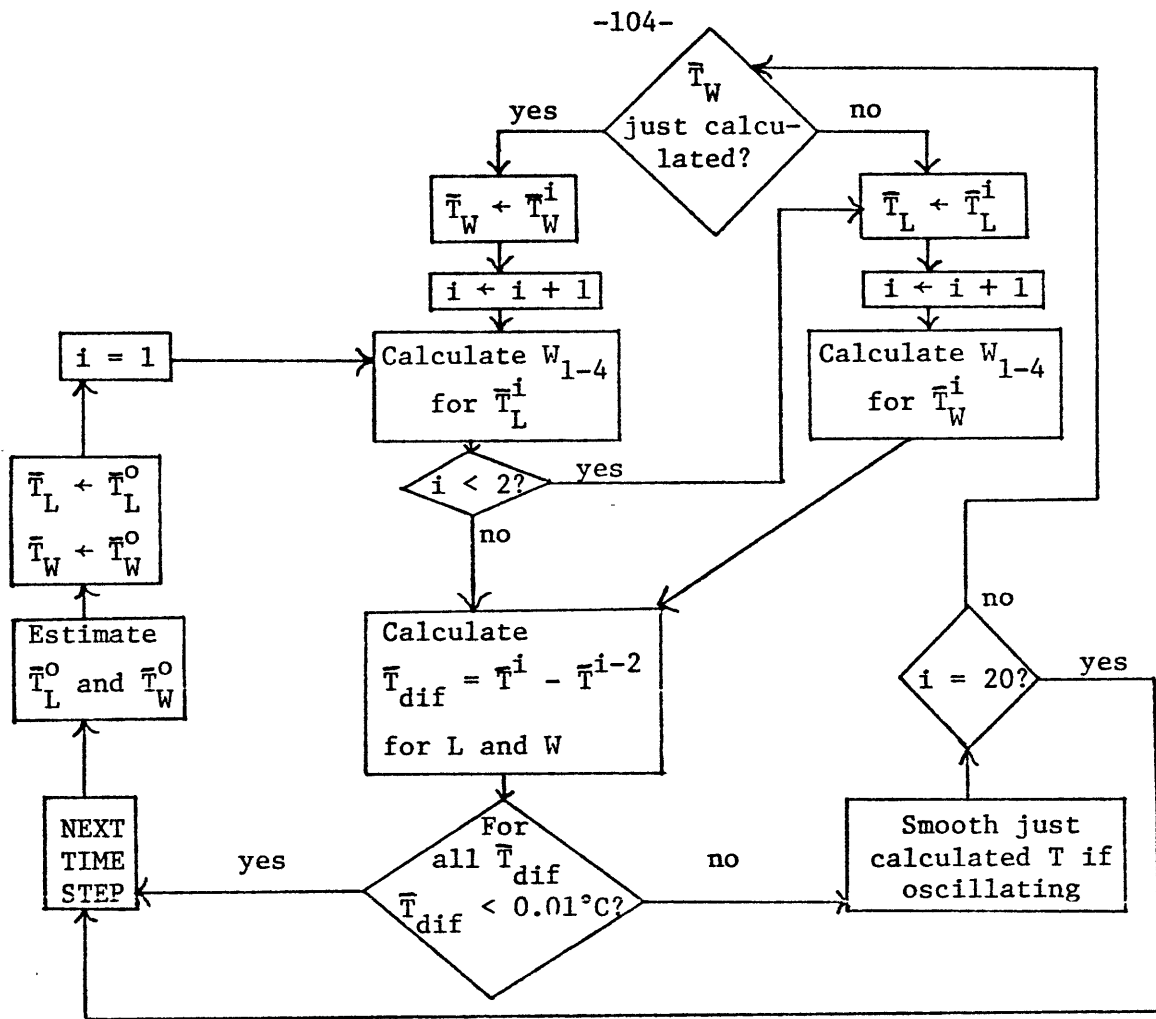


Figure 14. Flow chart for iteration procedure.



(58)-(60). In calculating the atmospheric layer temperatures, S assumed that no clouds were present, and used these calculated temperatures,  $\bar{T}_{A1NC}$  and  $\bar{T}_{A2NC}$ , in both equations (59) and (60) as the atmospheric temperatures in calculating the total IR flux. It seemed to me inconsistent to assume that there were no clouds in calculating the layer temperatures for equation (60), and then imposing clouds when calculating the IR flux, so I assumed clouds existed in both instances.

S assumed a constant carbon dioxide emissivity in time and space. When investigating the effects of changing carbon dioxide concentration, S' imposed a different emissivity initially, and then ran the model until it was balanced to measure the final effect, but did not look at time-dependent forcing or the time-dependent features of the response. I wanted to investigate the effects of anthropogenic carbon dioxide, which is a time-dependent forcing, and so developed formula (63) from the data of Staley and Jurica (1970). This makes the emissivity a function of carbon dioxide amount which changes continuously when simulating anthropogenic effects. It also, more realistically, makes the emissivity a function of temperature, which gives a more accurate spatial distribution, and also includes the feedback effect between temperature and emissivity.

## 2. Number of time steps

S used one month time steps - 12 time steps per year. Using a centered-differencing scheme, this is not enough time steps to accurately resolve the seasonal cycle. I decided to use 24 time steps per year, which is enough to ensure a reasonably small truncation error,

and also is convenient for comparing the model results to monthly data.

### 3. Seasonal forcing

A number of components of the climate system are observed to have seasonal fluctuations. S chose to vary two of them, fractional cloud cover and sea surface albedo, according to their observed seasonal cycles, while keeping all the other components fixed at their annual average values. This seemed to me to be an inconsistent method of investigating the seasonal cycle. I, therefore, chose to keep all the climate components at their observed annual values, and forced the seasonal cycles only by the changing solar input. The components of the climate system which are calculated as functions of temperature, such as winds and cryosphere, of course also change on a seasonal cycle, but the only time-dependent forcing is that of the sun. At a later time, other components, parameterized in terms of temperature, or solar zenith angle (including all the albedo effects, not just sea surface), may be added to attempt a consistent, more accurate simulation of the seasonal cycle.

### 4. Smoothing

S (his equations (47) and (48)) used the following smoothing for water surface temperatures:

$$\bar{T}_{AW} = c_5 \bar{T}_{Wo} + c_6 \bar{T}_{Lo} \quad (68)$$

where, empirically,

$$c_5 = A_W^{1/4} [A_W^{1/4} + A_L^{5/2}]^{-1}, \quad c_6 = 1 - c_5 \quad (69)$$

$A_w$  is the fractional area of the latitude belts covered by ocean, and  $\bar{T}_{AW}$  is the air temperature above the water, which replaces the water temperature ( $\bar{T}_{Wo}$ ) where it appears in all the terms under the first integral on the right-hand side of (1). He imposed this smoothing because he found it was necessary to stabilize the calculations of zonal divergence, which became unrealistically large in the high latitudes of the Southern Hemisphere. I found this smoothing to be unnecessary in my calculations, and so did not include it. I suspect that S's problems may have been due to a programming error. Furthermore, I did not understand how this smoothing would reduce the zonal divergence, since in the region in which he found it necessary,  $A_w$  is very large and  $\bar{T}_{AW}$  is almost equal to  $\bar{T}_{Wo}$ , the number it replaces.

#### 5. Minor differences

S kept the albedo of ice constant at 0.6. I changed it to 0.4 when  $\bar{T}_{Wo}$  was above freezing to correct for meltwater on the ice surface, as observed by Chernigovskiy (1966).

Tennekes (1973) showed that the von Karman constant should be 0.35 over smooth surfaces. I used this value, instead of 0.40 used by S, for ocean surfaces.

I used surface pressure over land equal to the values given in Table 6, rather than 1000 mb as S did, for all calculations involving surface pressure except the a coefficient, equations (27)-(30).

Instead of the observed values of sea surface albedo, I used the parameterization of equation (53). This is important when studying the seasonal cycle and using the monthly values, as is done in section

F.2., so as not to introduce any artificial time dependence into the seasonal forcing. In this way the seasonal cycle is still forced by only changing solar angle.

In equations (54)-(56), S used  $i = 1$  to calculate the ice and snow areas. I found that this introduced a net heat source in the latitudes where the ice and snow were changing during the year. This is because these equations are not energy consistent and the ice and snow were melting too rapidly and forming too rapidly. This, interacting with the ice area-dependent ocean thermal inertia, section B.4., caused the net heat absorption during the year. I found that  $i = 3$  gave the minimum heat anomaly. This clearly is an unsatisfactory, unrealistic solution to the problem created by this parameterization. A better one is discussed in section G.

#### E. The balanced model climate and comparison with real data

The IR cooling rate was adjusted so that the world average, annual average 1000 mb temperature ( $T$ ) for the model was equal to  $14.5^{\circ}\text{C}$ , a value in the middle of the range ( $14^{\circ}\text{C}$ - $15^{\circ}\text{C}$ ) of most estimates of this quantity. The cooling rate (which is multiplied times the emissivities in the IR calculations) which gave this was  $1.50^{\circ}\text{C}/\text{day}$ . The model in a balanced state reproduces the same seasonal cycle year after year. In this section, the balanced climate produced by the model, with no internal or external climate forcing, will be presented and compared to the available observational data. This will give an idea of the accuracy of the model, and indicate components which may need improvement. If the model can accurately simulate the

seasonal cycle, then one would have confidence in its ability to simulate climate changes which are much smaller than the seasonal ones. The quantities considered here include  $\bar{T}_0$ , surface temperature ( $T_S$ ), sea ice extent, horizontal winds, atmospheric and oceanic heat fluxes and radiation at the top of the atmosphere. All quantities are presented as zonal averages. The model output and data are presented in Figures 15-40 and in Table 8.

### 1. The data

The data with which the model results are compared come from a number of sources and are of variable quality and limited extent. Still they are the best available and better model validation awaits future observational studies.

The sources for the temperature data used in Table 8 and Figures 15-20 are Oort and Rasmusson (1971) (O+R), Schutz and Gates (1971, 1972a, 1972b, 1973a, 1973b, 1974a, 1974b) (S+G), and Newell et al. (1972) (N). O+R is the only source with monthly values, but it covers only the Northern Hemisphere. The other two sources cover the whole world, but are only four months: January, April, July and October. (From now on, month will refer to calendar months - 12 per year.) The data suffer from the same problems as discussed in chapter 2, including lack of adequate coverage over the oceans, measurement errors and errors introduced in analysis. An additional problem arises when trying to calculate a time mean state. The different data sets were collected at many different times during the past 50 years. O+R used only five years of data, from 1958 to 1963. These sampling problems

may bias the "average" state that is calculated. This is true for the other data as well.

The sea ice data used in Figure 19 were taken from Alexander and Mobley (1976) (A+M). Data on 50% snow cover does not exist. Wiesnet and Matson (1975) have published Northern Hemisphere winter snowline data from satellites, but this data is hard to compare to the model, which calculates fractional coverage.

The wind data used in Figures 20 and 21 comes from O+R. The data from 10°S to 75°N are from radiosonde measurements and are quite reliable, although for only five years of data, with the associated problems. The data for 65°S to 10°S also come from O+R, but are from a collection of data taken only over the ocean. They would therefore be expected to show stronger winds than a zonal average, which would include slower speeds over land due to stronger friction.

The radiation data used in Figures 22-31 come from satellite measurements of Ellis and VonderHaar (1976) (E+V). They suffer from the same sampling problems as O+R, namely very few samples (1 to 4 per month) and observations taken at the same local time each day. The E+V data were taken daily at the same daylight time, different for each month for each satellite. The O+R data were taken daily at 00Z for all locations. A consideration of these and other possible errors leads them to estimate the total uncertainty of their solar insolation to be  $\pm 1.5\%$  and of their albedo and IR to be  $\pm 5\%$ . They further note large interannual variations in the polar regions.

The surface albedo data in Figure 32 are taken from S+G, who used surface estimates to calculate the albedos, based on observed

fractional coverage of different ground covers. They should be quite reliable, but do not account for feedback or anthropogenic surface albedo changes. The assumed albedos for the various surfaces, however, may be in error.

The horizontal heat flux data for Figures 33-36 come from Oort and VonderHaar (1976) (O+V). They took atmospheric flux data from O+R, which were also used for Figures 37-40, and are quite good, subject to the problems as mentioned above. The radiation data of E+V were used to calculate the total heat flux as that required to balance the radiation. These data sets were then combined to calculate the oceanic flux as a residual. Heat storage from O+R for the atmosphere and from a large variety of ship observations based on all historical data available for the ocean were also used in the calculations. The oceanic flux values must therefore be regarded as the least reliable, being based on residuals of several error-laden data sets. O+V analyzed the errors and found interannual variability to be the dominant source in the radiation and atmospheric flux data. The estimated errors for the ocean fluxes were almost as large as the fluxes themselves.

The observational data are therefore of variable quality. Lack of adequate temporal and spatial coverage affects all the data sets. Some of them are only very recently published. These considerations limited the present study to model validation. Future parameterization improvements, as discussed in section G, will allow more accurate simulation studies to be conducted.

## 2. Temperature

The annual average surface temperature is shown in Figure 15. The model accurately simulates the observations except near the South Pole (SP). This may be due to several causes. The model assumes a constant lapse rate, and cannot simulate surface temperature inversions which are known to exist in this region. Also, the lapse rate used by the model to calculate the surface temperature from 1000 mb temperature on the high Antarctic continent may be in error. Furthermore, horizontal heat fluxes into the SP are assumed to extend throughout the 1000 mb deep atmosphere, and in reality, the high continent prevents this. So the model may be keeping the South Pole artificially warm by calculating too much heat flow into the region.

Figures 16 and 17 show the seasonal cycle of 1000 mb temperature for the Northern Hemisphere (NH) and Southern Hemisphere (SH). In Figure 16, it can be seen that the shape and phase of the seasonal cycle is correctly calculated by the model for the NH, but the amplitude is too small for the polar regions. This can be seen more clearly in Table 8. Monthly values of the SH temperature are not available, but four values per year are. The amplitude, except at the South Pole (SP) is well simulated for the SH. It is smaller than for the NH due to the larger proportion of ocean surface, with its higher thermal inertia and its smaller snow-albedo feedback.

The discrepancies between the model and the data can be more easily seen with north-south plots for four different months, as shown in Figure 18. In April and October the data is well simulated,



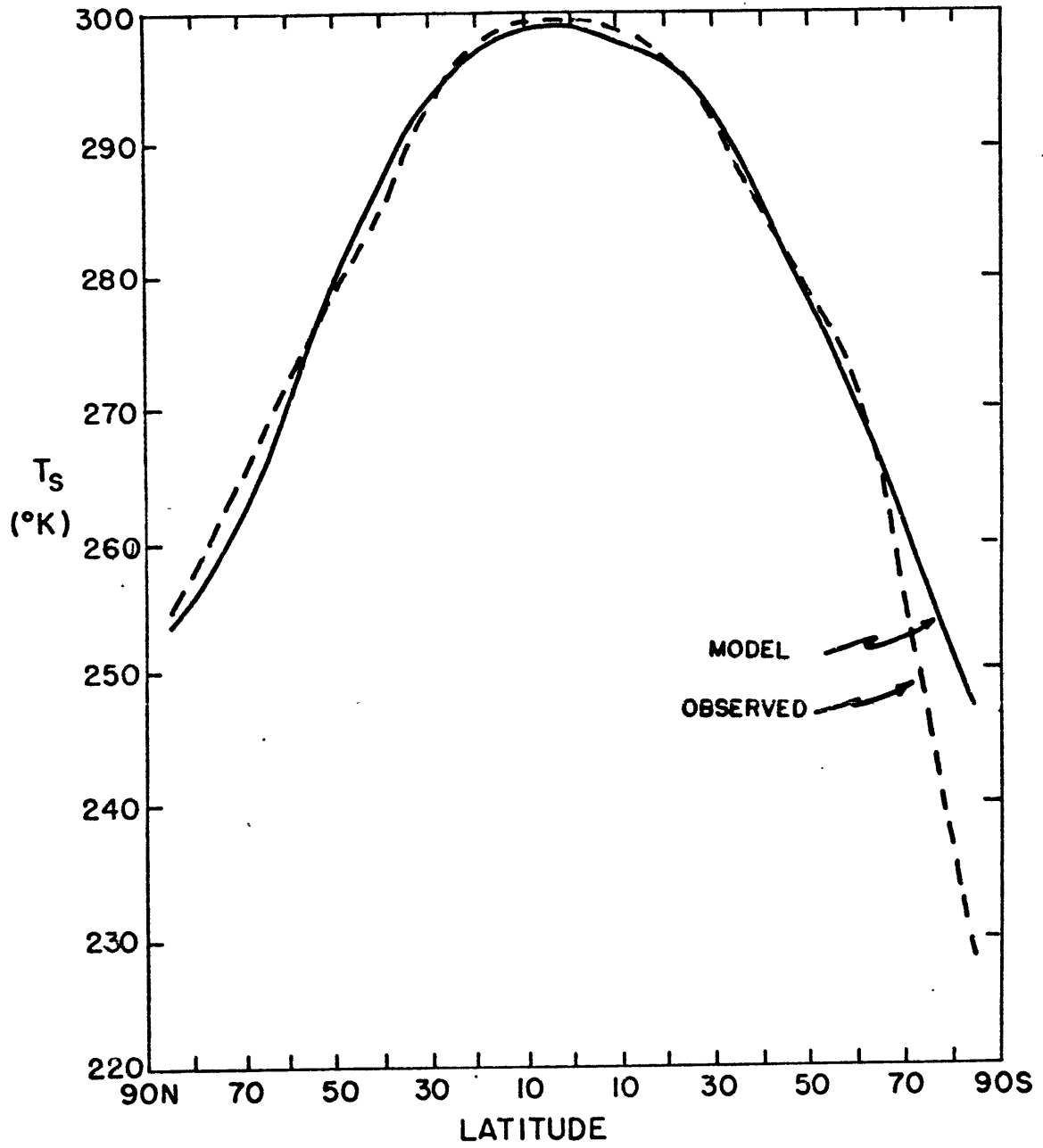


Figure 15. Annual average surface temperature. Data from S+G.

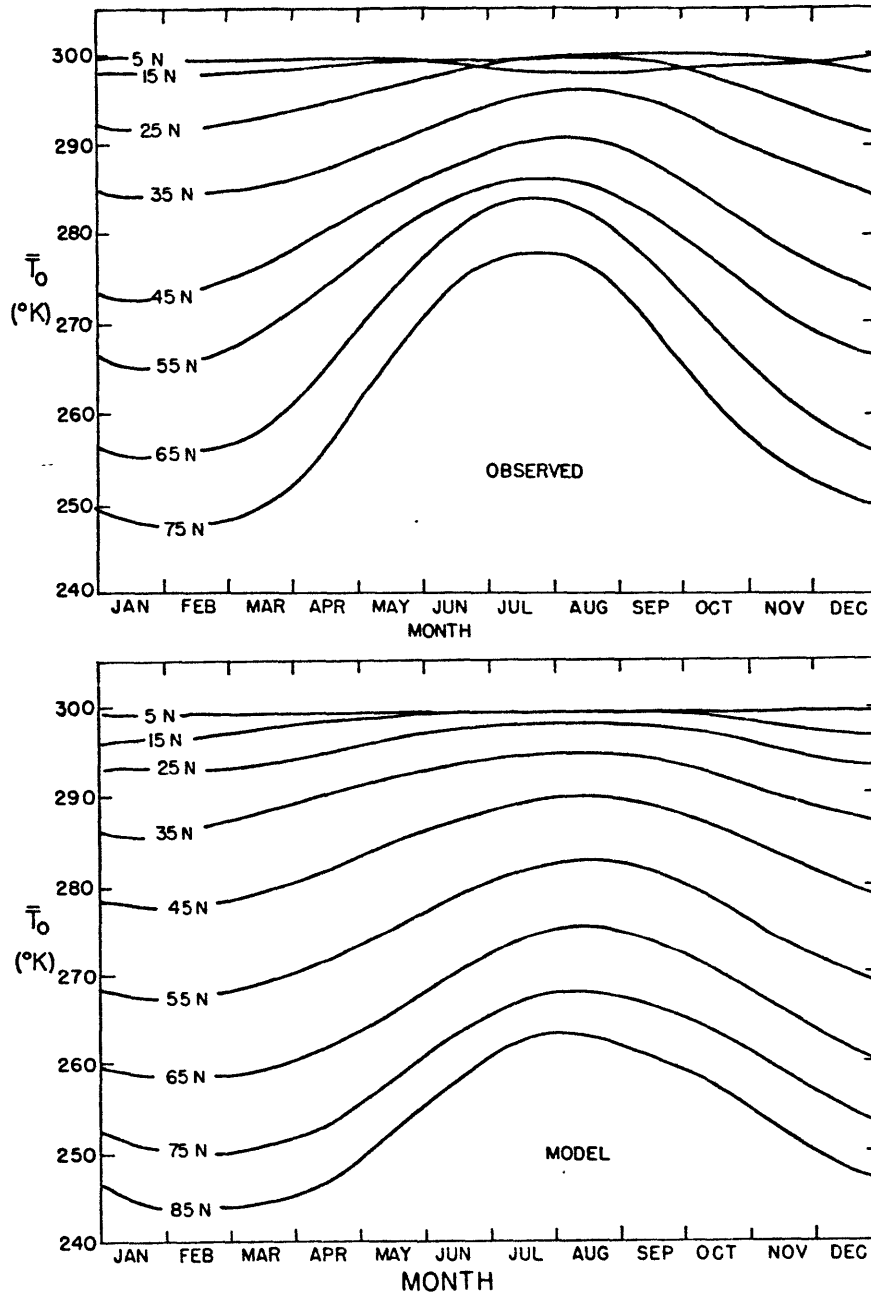


Figure 16. Northern Hemisphere seasonal  $\bar{T}_0$  cycle. Data from O+R.

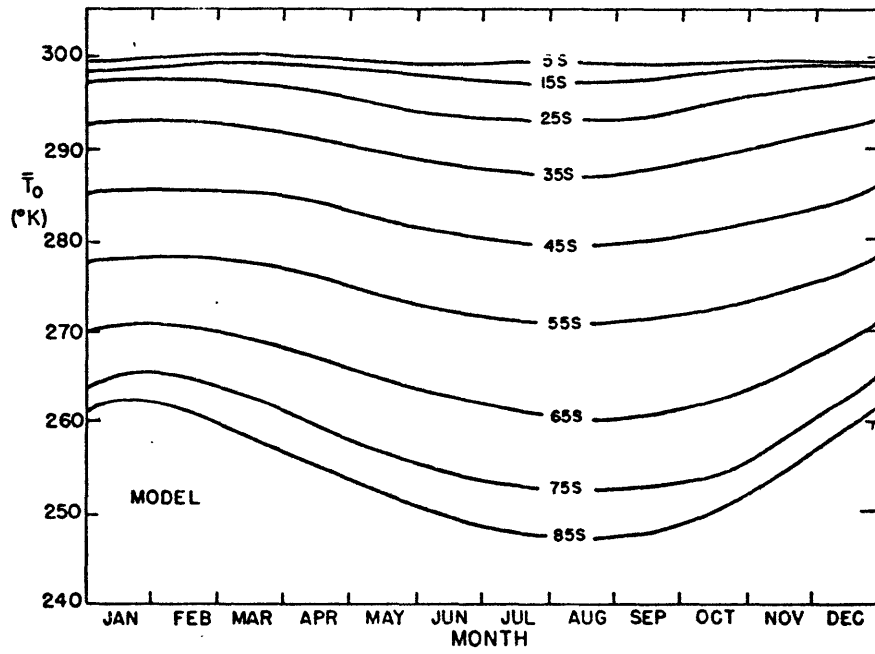


Figure 17. Southern Hemisphere seasonal  $\bar{T}_0$  cycle. Observations are not available.

Table 8. Amplitude of seasonal temperature cycle.

Latitude band	Model (1000 mb or surface)	S + G (surface) (°K)	O + R (1000 mb)	N (1000 mb) (surface S of 60°S)
80° - 90°N	19.6	34.6		31.8
70° - 80°N	17.9	29.1	31.1	34.3
60° - 70°N	16.5	32.3	27.8	31.6
50° - 60°N	15.0	25.6	20.4	27.7
40° - 50°N	12.2	21.0	17.6	19.7
30° - 40°N	8.9	15.3	13.0	11.9
20° - 30°N	5.9	9.5	7.9	8.1
10° - 20°N	3.0	3.5	2.1	4.4
0° - 10°N	1.1	1.2	0.8	1.6
0° - 10°S	1.5	1.7	2.3	1.8
10° - 20°S	2.8	3.1		3.1
20° - 30°S	4.6	6.2		4.7
30° - 40°S	5.8	5.9		6.5
40° - 50°S	6.8	4.3		5.9
50° - 60°S	8.3	4.6		4.9
60° - 70°S	11.0	12.8		6
70° - 80°S	13.7	17.8		12
80° - 90°S	15.6	27.2		12

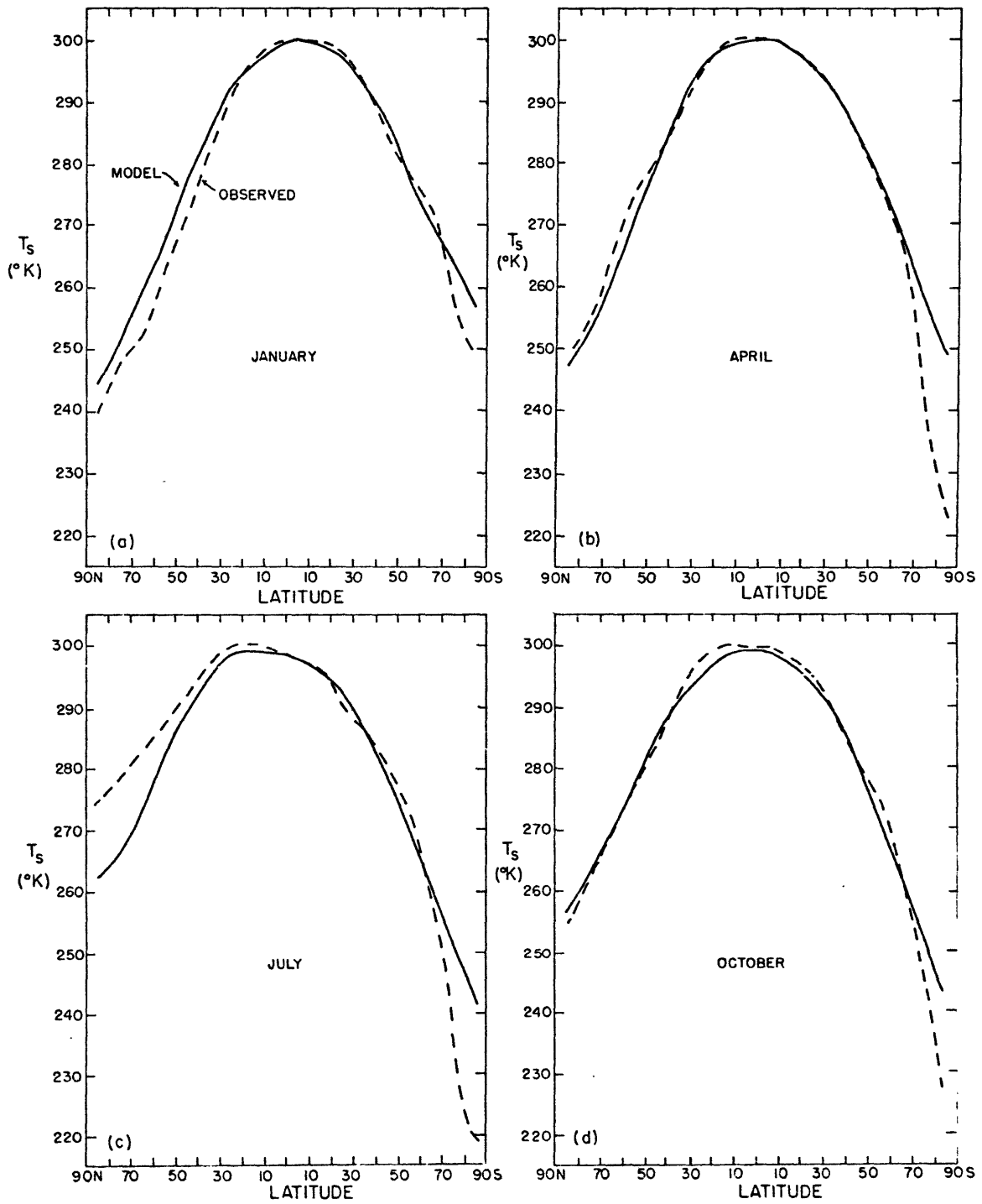


Figure 18. Surface temperature for four months. Data from S+G.

except at the SP. In January, the northern mid-latitudes and polar regions are too warm, and in July they are too cold. The SP is also too cold in these months and its seasonal cycle is too small.

In sections 5 and 6, the heat balance will be examined to try to explain these temperature discrepancies. But first some other simulated components are compared to data.

### 3. Sea ice

Figure 19 presents the seasonal ice and snow cycles. In the SH, the ice cycle is fairly well simulated. In the NH, the ice is calculated to be too far south, and the cycle to have too small an amplitude. Also the maximum extent is too late in the year.

### 4. Wind

The mean winds calculated by the model are shown with the data in Figures 20 and 21. Both the u and v components appear to be well simulated in magnitude, sign and seasonal change. The calculated u appears to be slightly too weak in the NH. It is also too weak in the SH, but since the data are only from the oceans, they would be expected to be stronger than the zonal average, which includes land.

### 5. Radiation

Figure 22 shows annual zonal averages of net radiation, absorbed solar radiation (QS) and emitted radiation (IR). The model calculations are close to the observations except at the poles where the net radiation is much too low due to too little QS, and in the subtropics where IR is slightly too low. Figures 23-27 show seasonal latitudinal

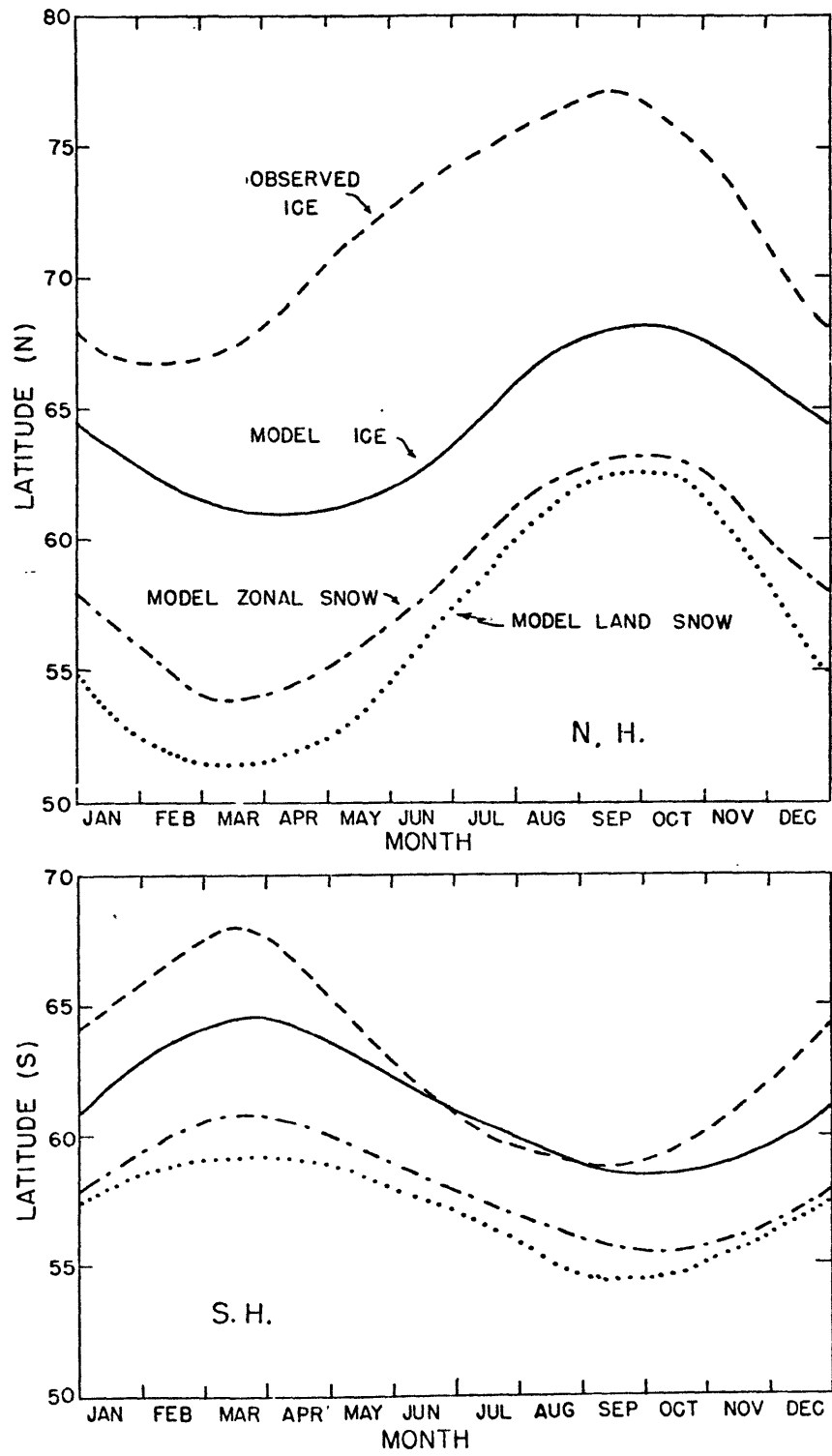


Figure 19. Ice and snow seasonal cycles. Data from A+M.

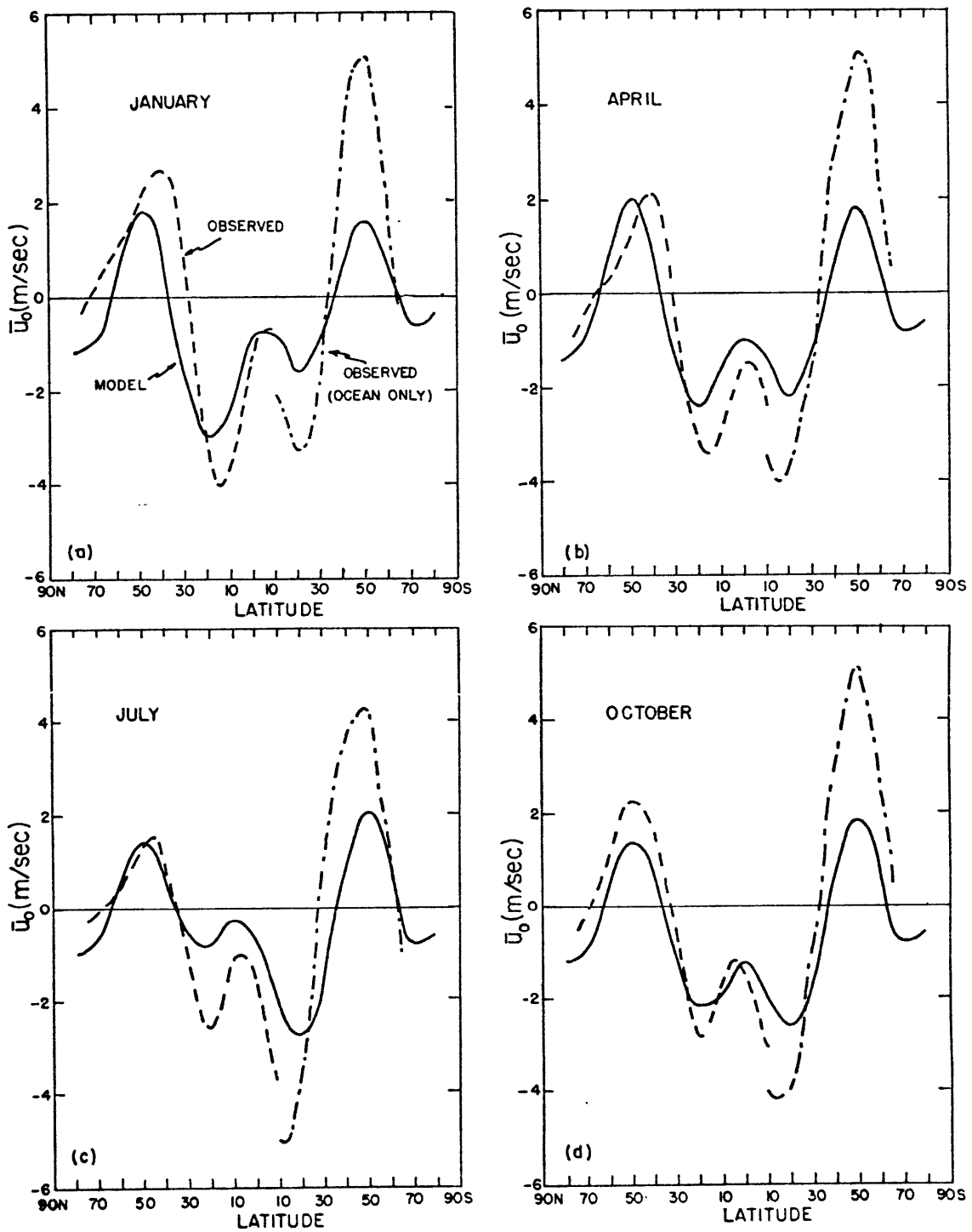


Figure 20. Surface east-west wind for four months. Data from O+R.



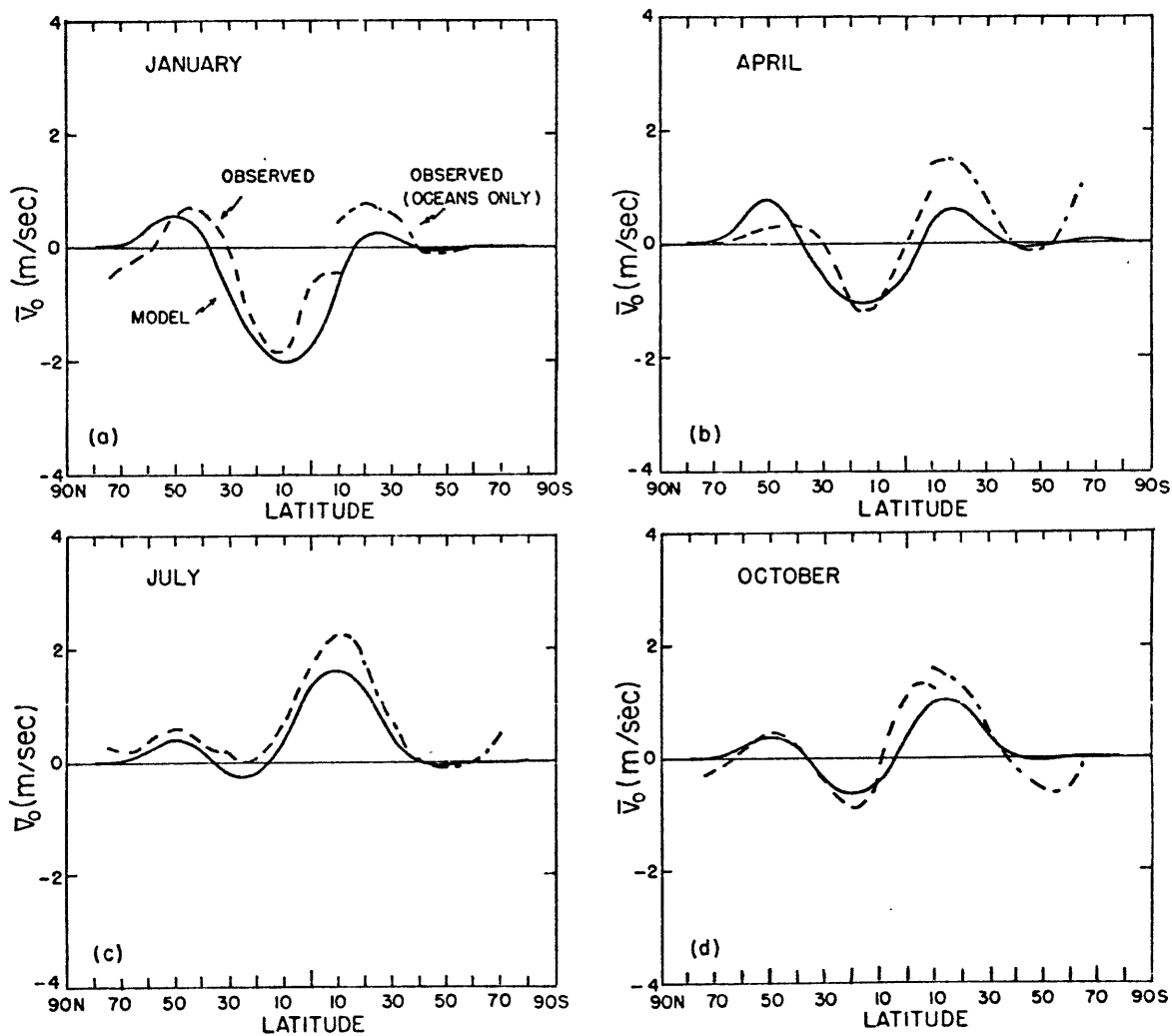


Figure 21. Surface north-south wind for four months. Data from O+R.

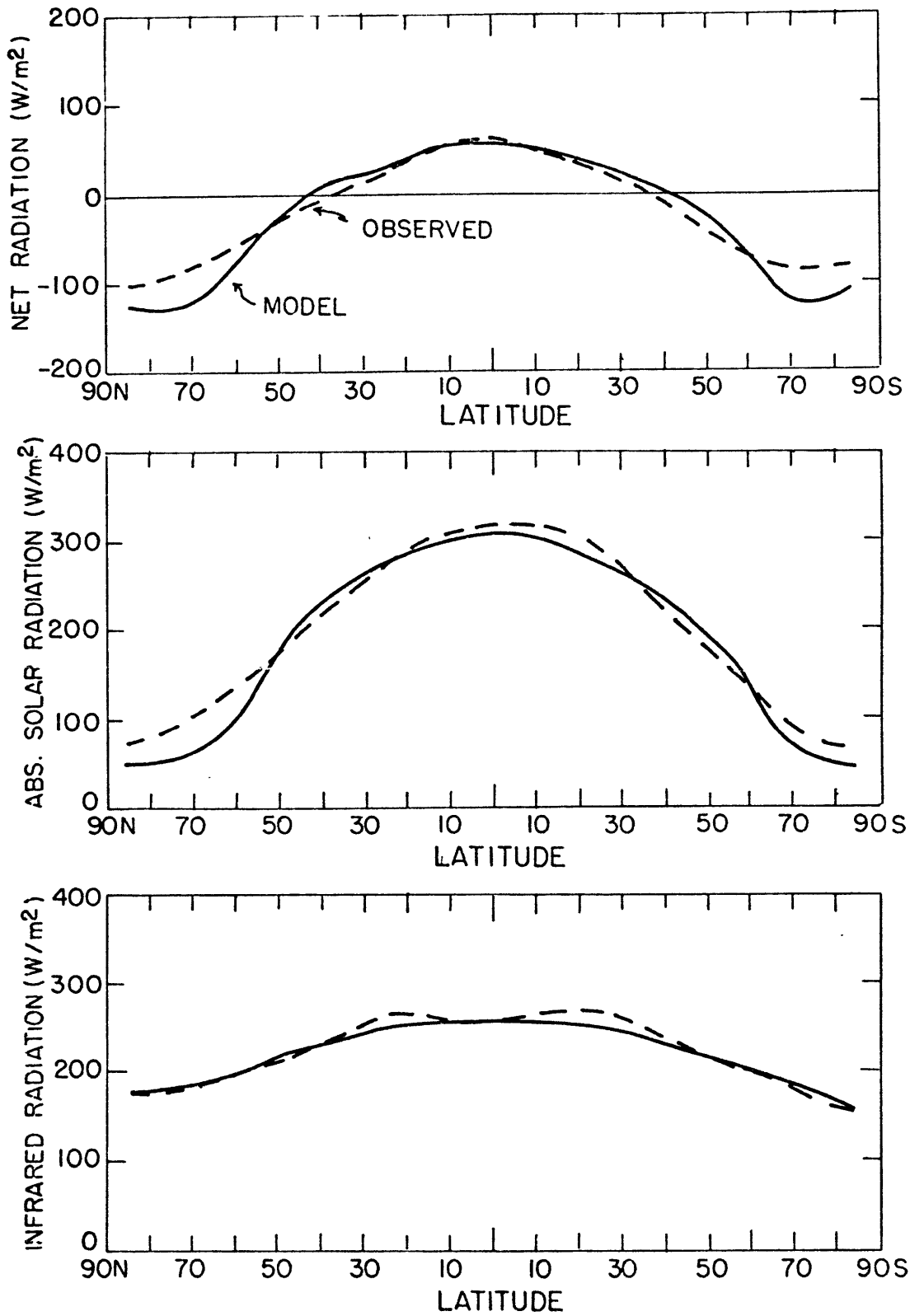


Figure 22. Annual average radiation. Data from E+V.

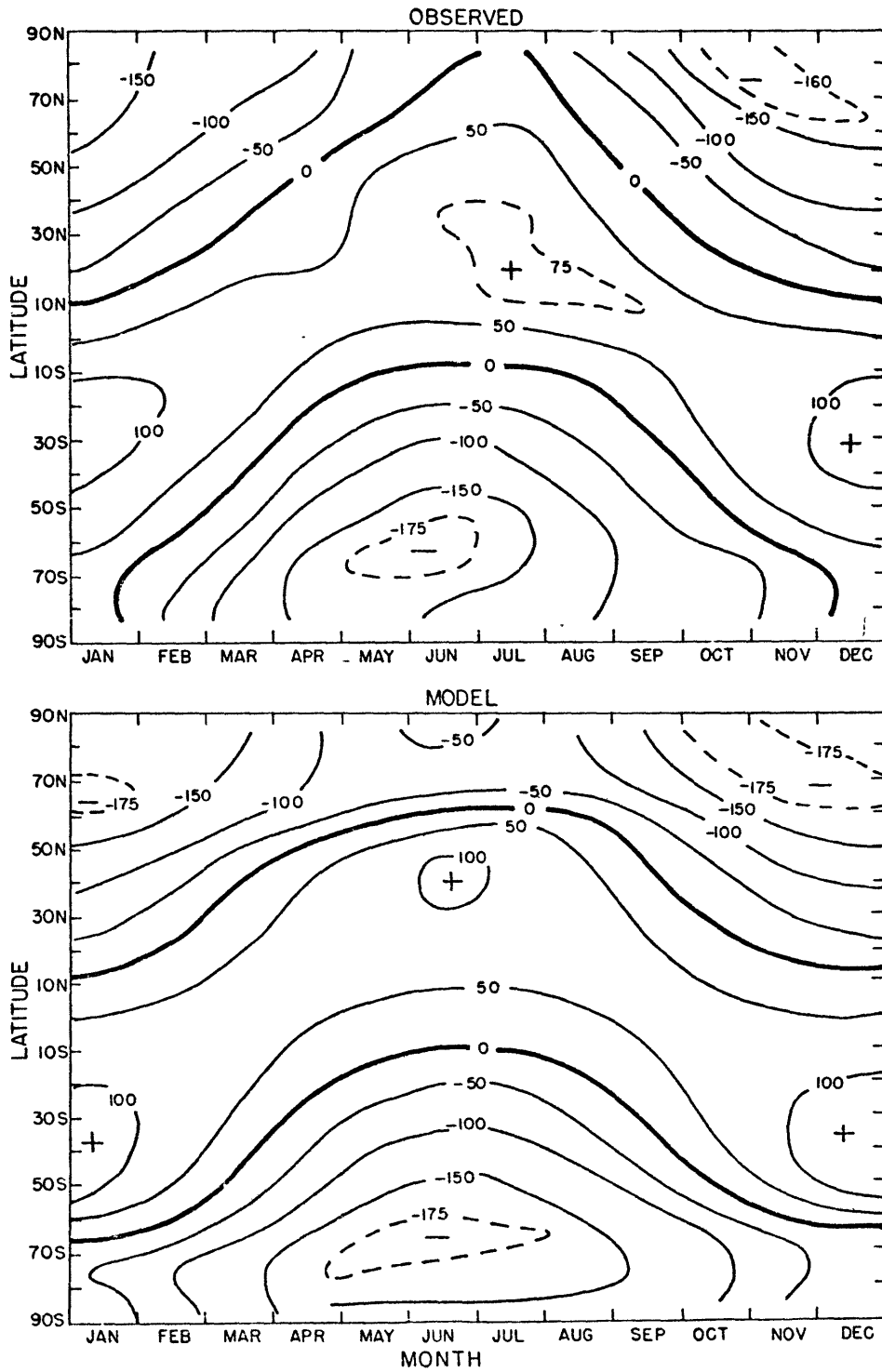


Figure 23. Net radiation field. Units are  $W/m^2$ . Data from E+V.

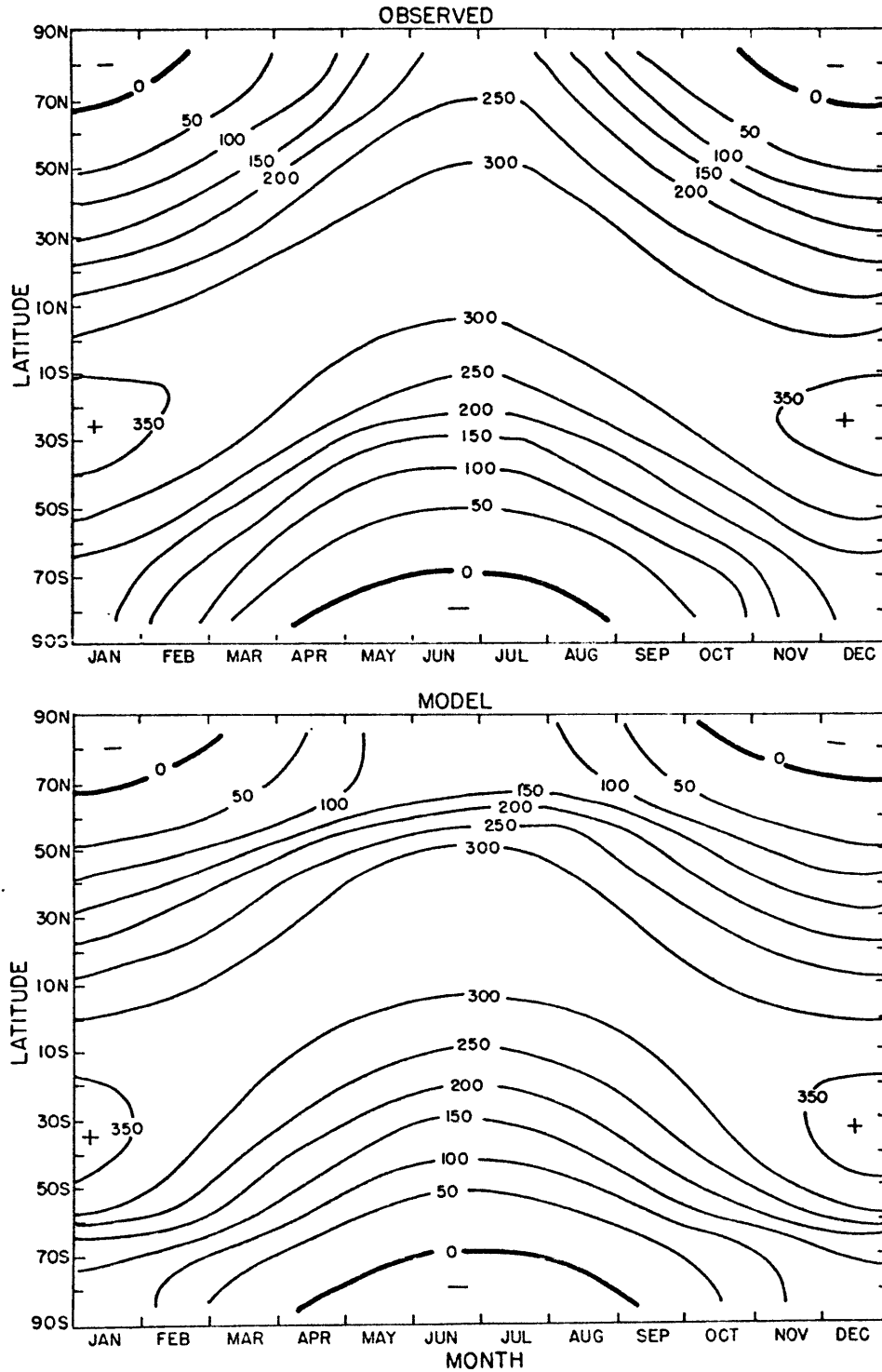


Figure 24. Absorbed solar radiation field. Units are  $W/m^2$ . Data from E+V.

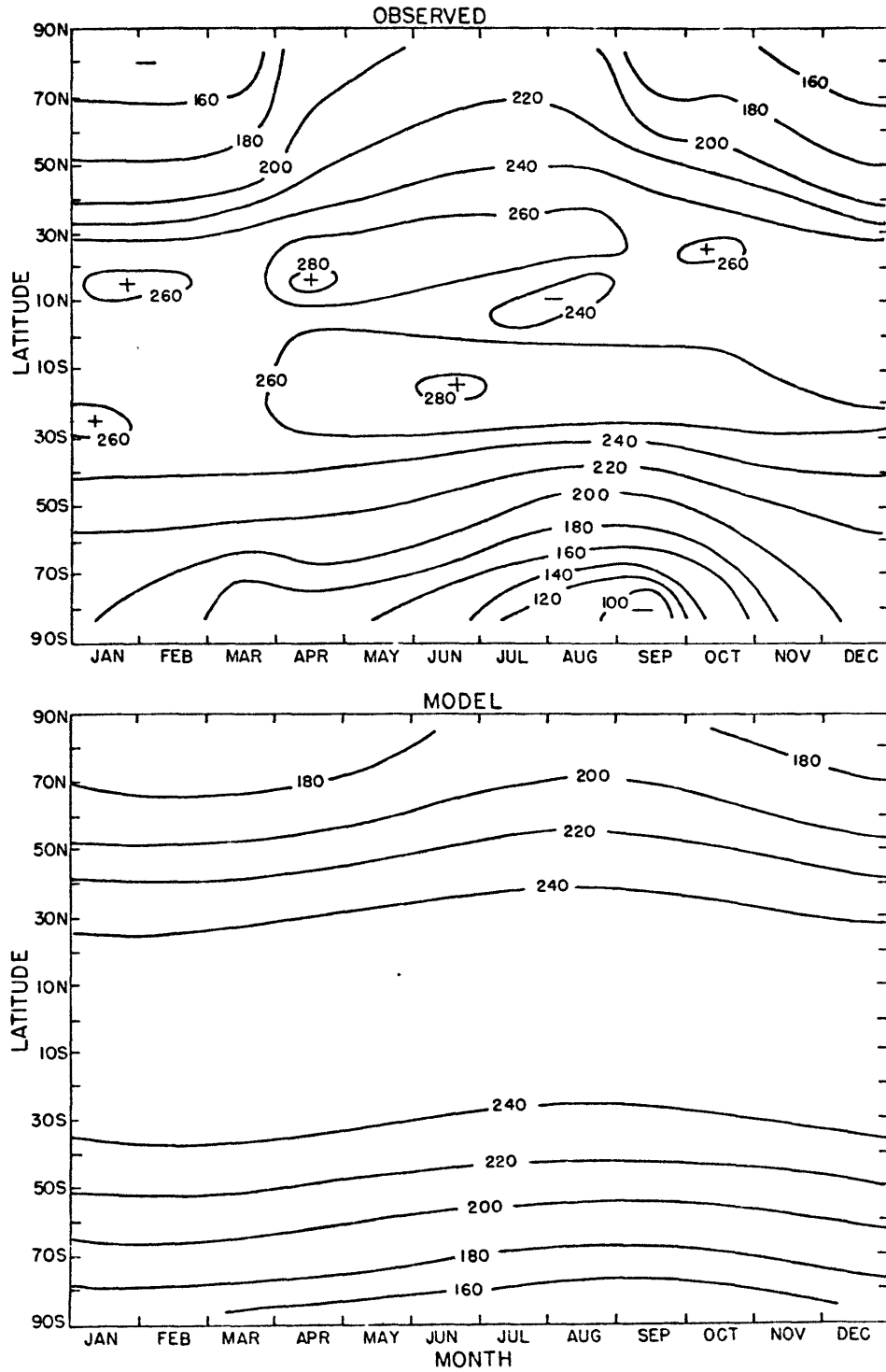


Figure 25. IR field. Units are  $W/m^2$ . Data from E+V.

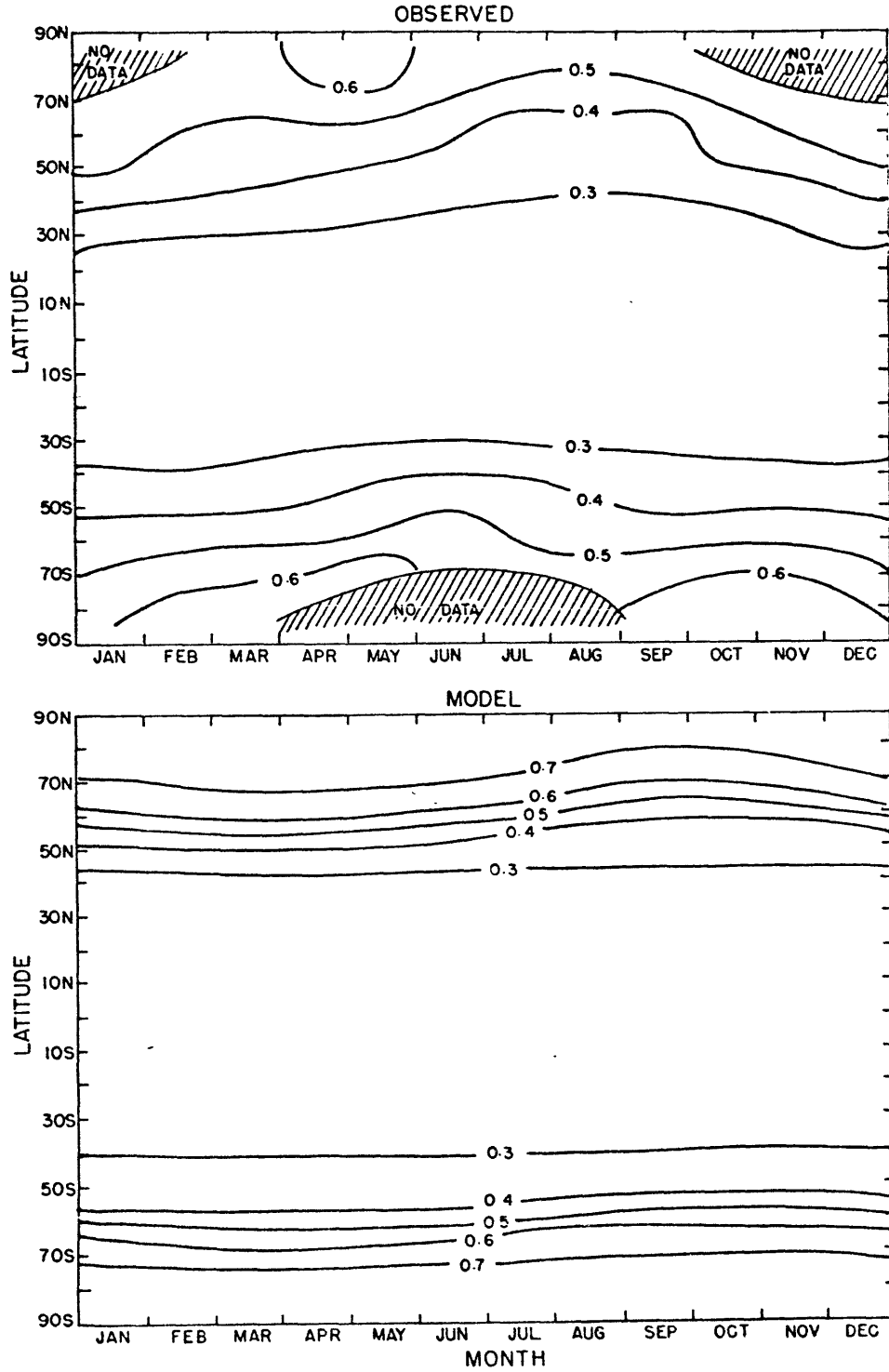


Figure 26. Total albedo field. Data from E+V.

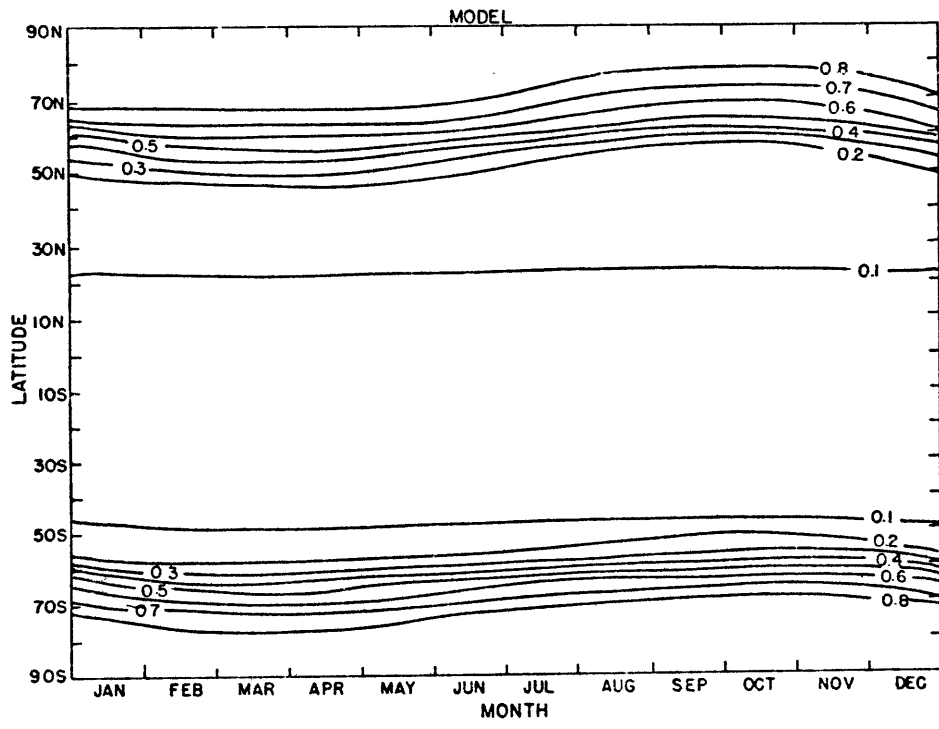


Figure 27. Surface albedo field. Observations are not available for all months.

analyses of net radiation, QS, IR, the total albedo and surface albedo. Latitudinal cross sections of these fields are also shown for four months in Figures 28-32.

Figures 23 and 28 show that the net radiation is calculated to be too low at the poles. At the SP it is correct in April and too low at other times. In the NH it is too low at 65°N and 75°N at all times, but especially in July, when the pole is also much too low. At other times and latitudes it appears to be correct. The inability of the model to calculate warm enough summer NH temperatures may then be explained by radiational considerations. The too warm NP winter temperatures and the SP year-round temperatures may not, however, and must be explained by inaccurate horizontal heat fluxes, inaccurate thermal inertias, or the inability to simulate the polar surface inversion. Heat fluxes will be discussed in the next section. The various components of the radiational balance will now be discussed, in order to explain the net radiation results.

QS, Figures 24 and 29, is slightly too low at both poles in spring and much too low in summer, especially at the NP. IR, Figures 25 and 30, is too high in the winter and too low in the summer at both poles. It is also slightly too low in the subtropics in both hemispheres during the whole year. In the summer, the too low net radiation at the poles is due to the larger effect of QS. In the winter the IR is too high at the poles, causing the net radiation to be too low.

Looking at the albedos helps explain the QS discrepancies. The total albedo, Figures 26 and 31, is too high at the poles in both hemispheres in the summer. It is too low in winter in the mid-latitudes.



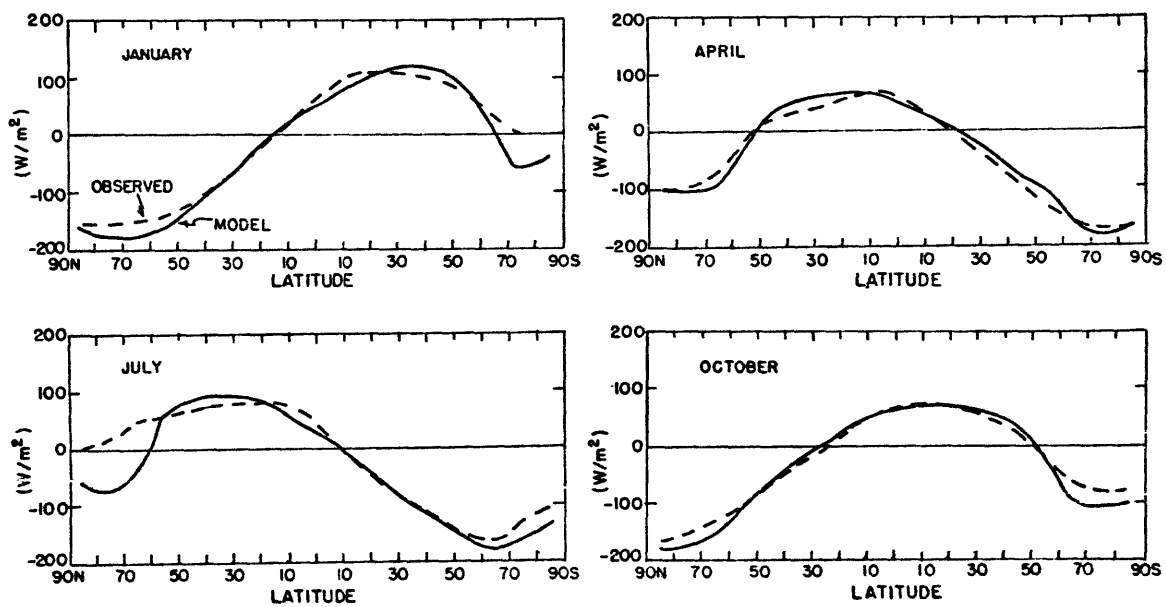


Figure 28. Net radiation for four months. Data from E+V.

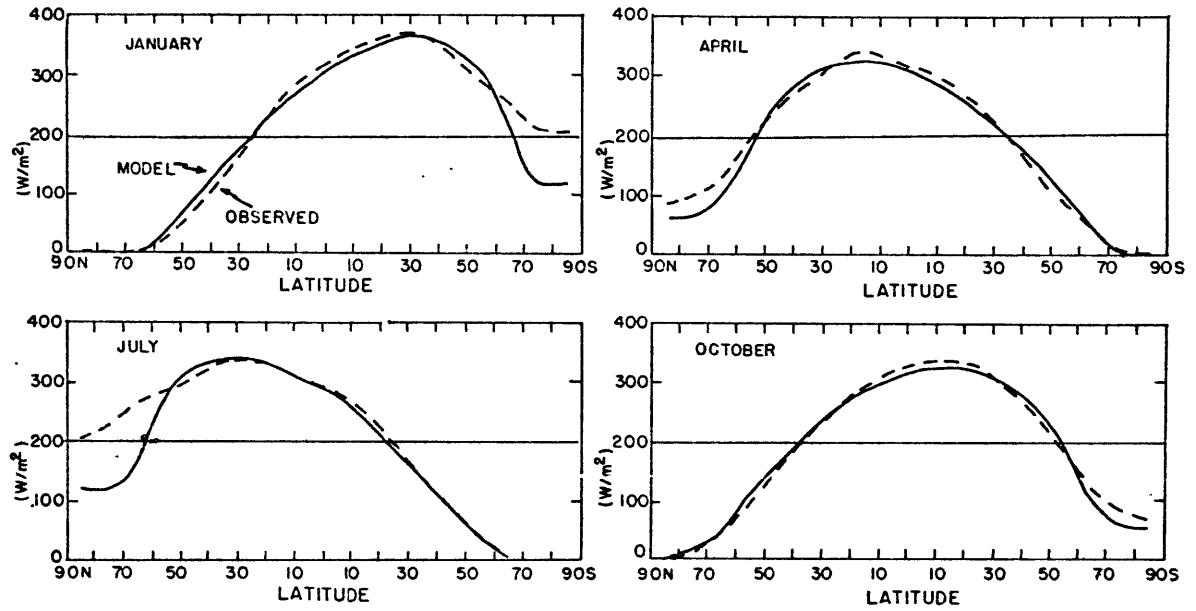


Figure 29. Absorbed solar radiation for four months. Data from E+V.

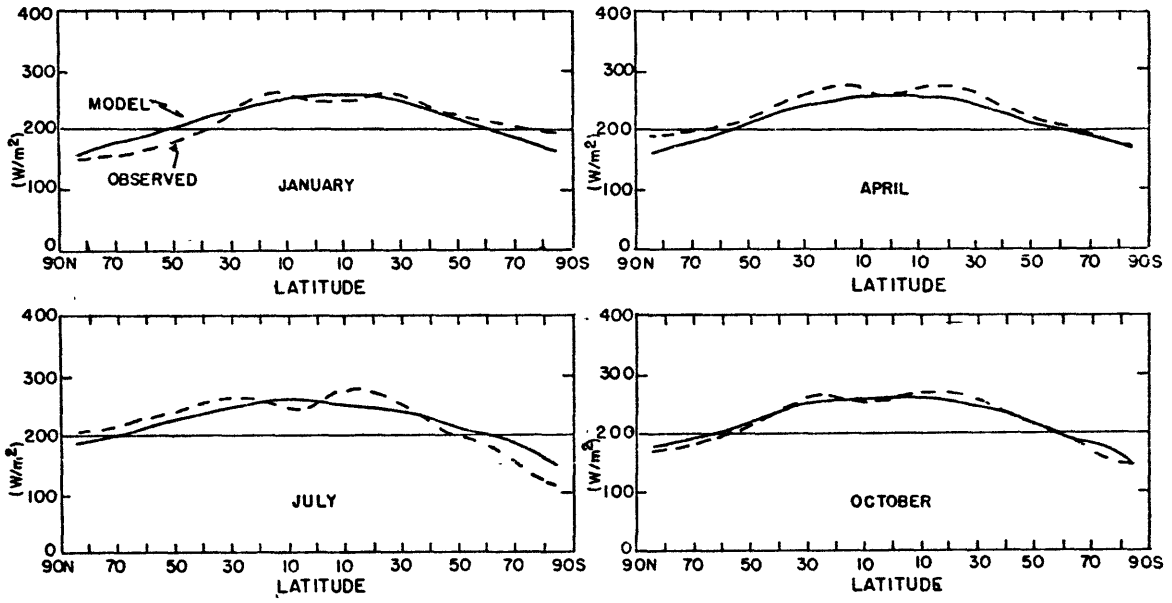


Figure 30. IR for four months. Data from E+V.

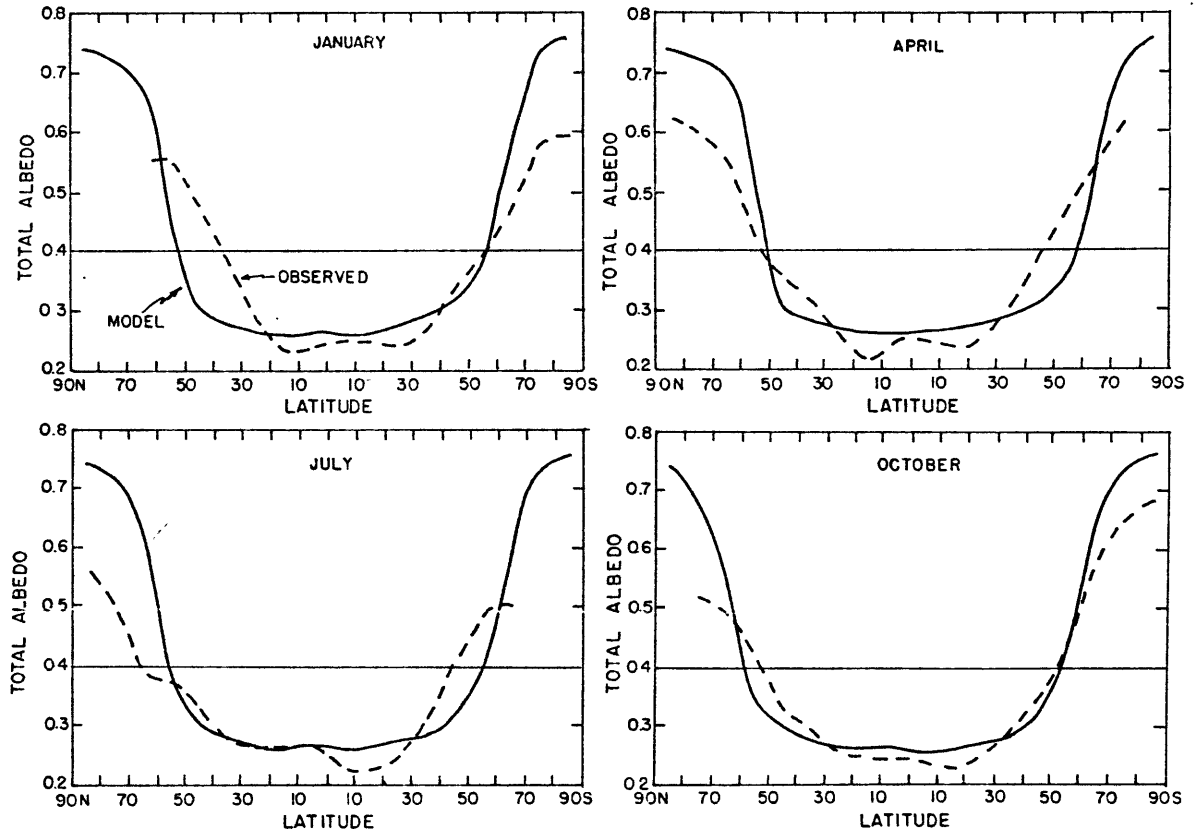


Figure 31. Total albedo for four months. Data from E+V.

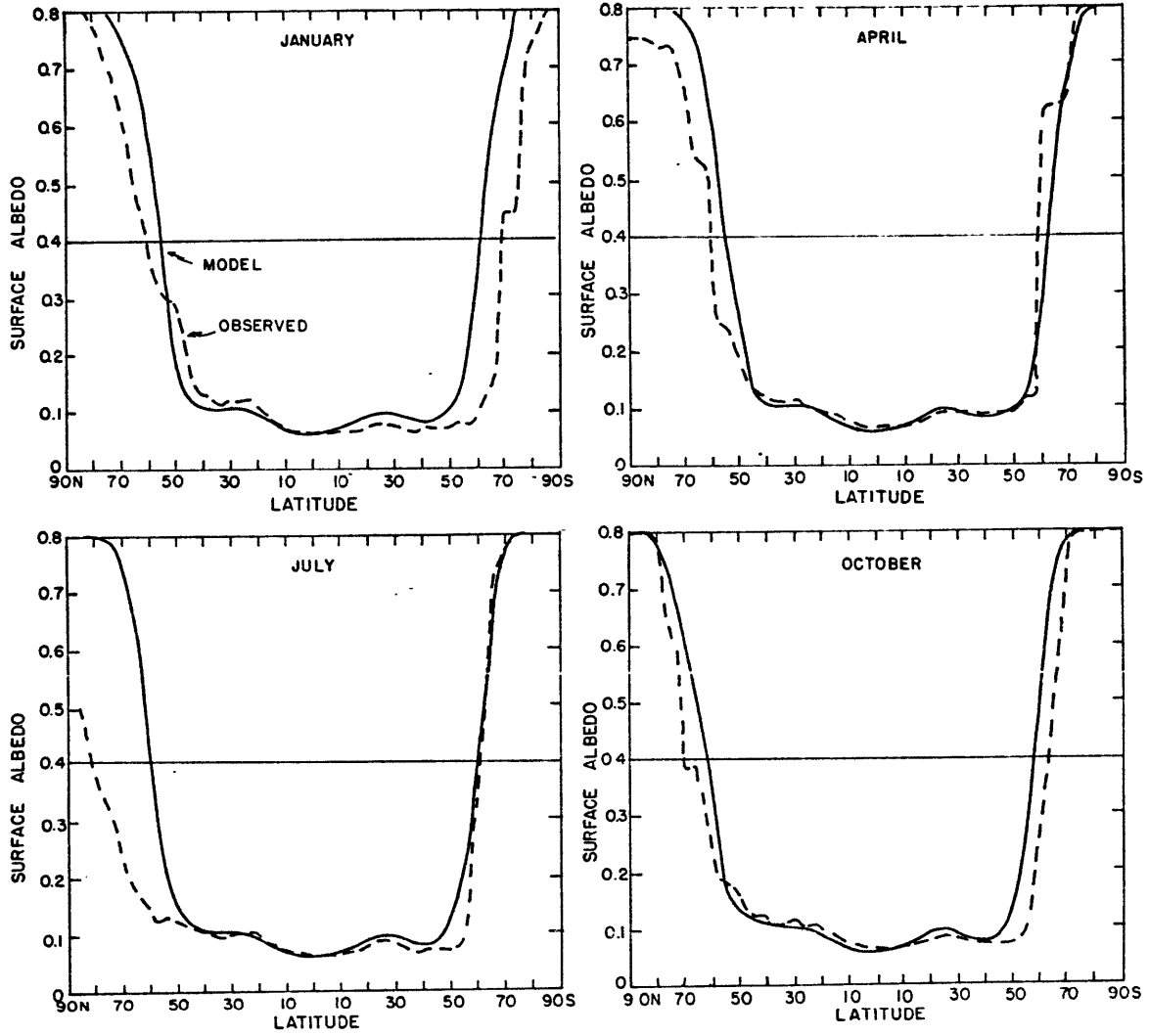


Figure 32. Surface albedo for four months. Data from S+G.

Part of this error is due to inaccurate surface albedo. The surface albedo, Figures 27 and 32, is much too high at the poles in the summer and slightly too high in the spring, with the largest discrepancies at the NP. At all other times and places it is correct. The ice and snow simulation of the model for the poles in the summer is therefore in error. Either the albedos or the calculated ice and snow areas are incorrect. The area effect would be larger in the NH, where ice and snow areas have a larger seasonal cycle. The data and the model may, however, be assuming the wrong albedo for snow. If a value of 0.75 were used instead of 0.80, the model would calculate total albedos at the poles to agree with the satellite observations.

An additional source of the total albedo error is the lack of a solar zenith angle effect in both the surface albedo and total albedo calculations in the model. Sea surfaces (Payne, 1972) and clouds (Cess, 1976) show large zenith angle effects on their surface albedos. Land, snow and ice also show effects, but smaller ones. The surface albedo zenith angle discrepancies do not show up in the data of Figure 32, but this data was based on distributions of different surface types and did not include zenith angle effects, except for the oceans, which are also included in the model. Lack of a seasonal cloud cycle in the model probably also contributes to the total albedo discrepancies. The thin atmosphere approximation in the total albedo calculation also excludes zenith angle effects, as pointed out by Coakley and Chylek (1975). The effects of the zenith angle errors on QS, which are approximately symmetric in their effects on total albedo, show up much more strongly in the summer hemisphere, where Q is the largest.

The IR emissions are closely related to the surface temperatures, but also to the clouds. Using annual zonal average cloudiness obscures the subtropical high regions, and causes less IR in these areas than observed. The polar discrepancies are due to the too small magnitude of the seasonal temperature cycle.

#### 6. Horizontal heat fluxes

Figure 33 shows the annual average north-south heat fluxes by the atmosphere and the ocean. Observations are available only for the NH. The total model heat flux is too large in the mid-latitudes. The atmospheric and oceanic fluxes are both too large. In the subtropics, the atmospheric flux is too large, while the oceanic flux is too small, balancing out. The oceanic flux appears to be quite poorly modeled.

This can also be seen in Figures 34-36, which give latitudinal seasonal analyses of the fluxes. The total flux is too small at all latitudes from October to December and too large at all other times. Since the real atmosphere has a larger N-S temperature gradient than the model in the fall and winter, and a smaller one in the spring and summer, this is understandable. A large southward flux in the tropics in the summer is not produced by the model. The calculated oceanic fluxes do not closely resemble the data. Large subtropical and tropical fluxes are not produced by the model.

The atmospheric fluxes are correct in November and too strong the rest of the year. A better picture of the atmospheric flux is shown in Figures 37-40, which show the various components of the flux for four different months. The eddy flux of sensible heat plus potential energy

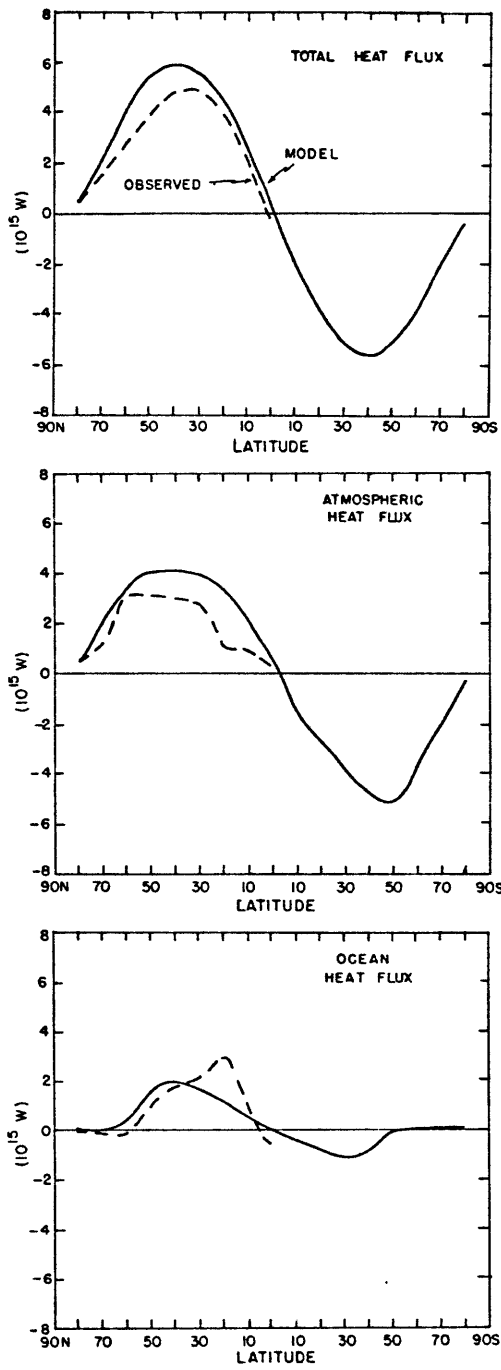


Figure 33. Annual average heat fluxes. Data from O+V.



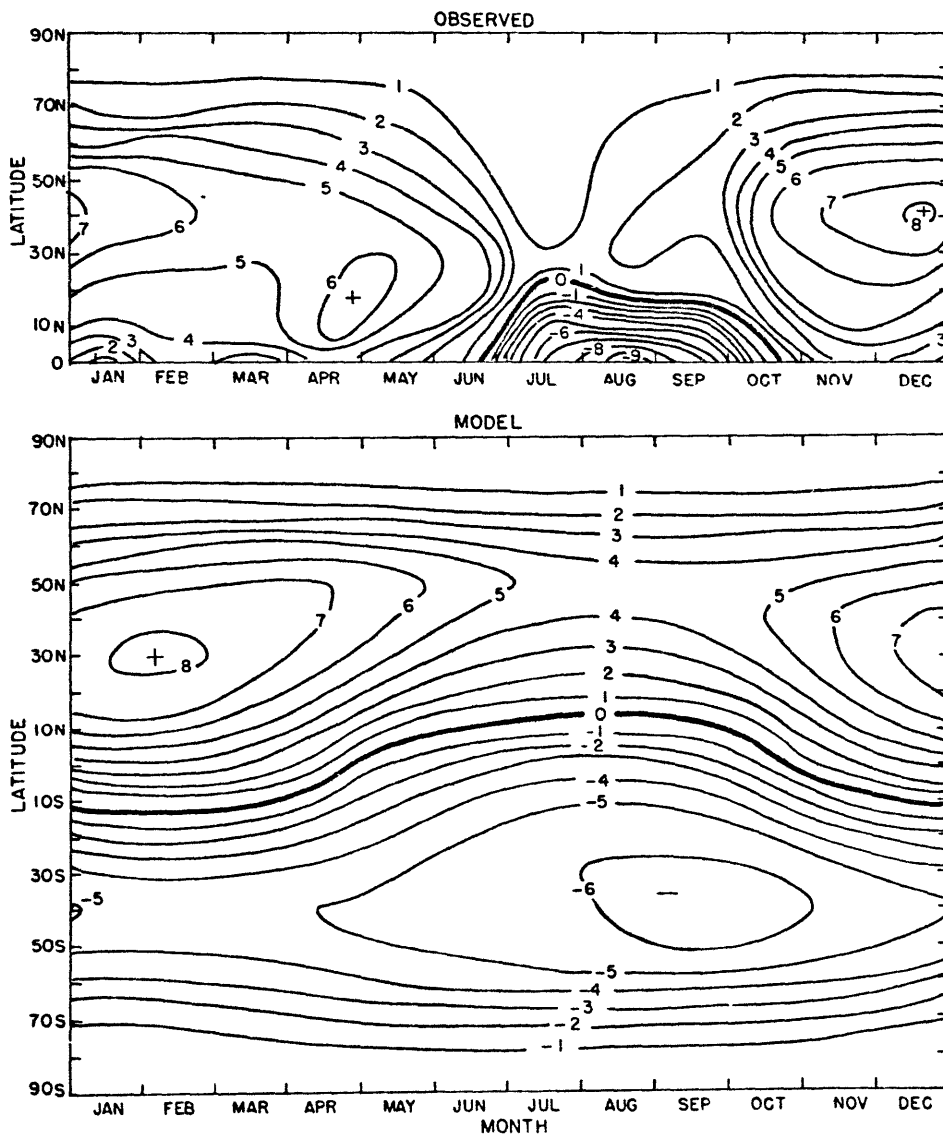


Figure 34. Total heat flux field. Units are  $10^{15}$  W. Data from O+V.

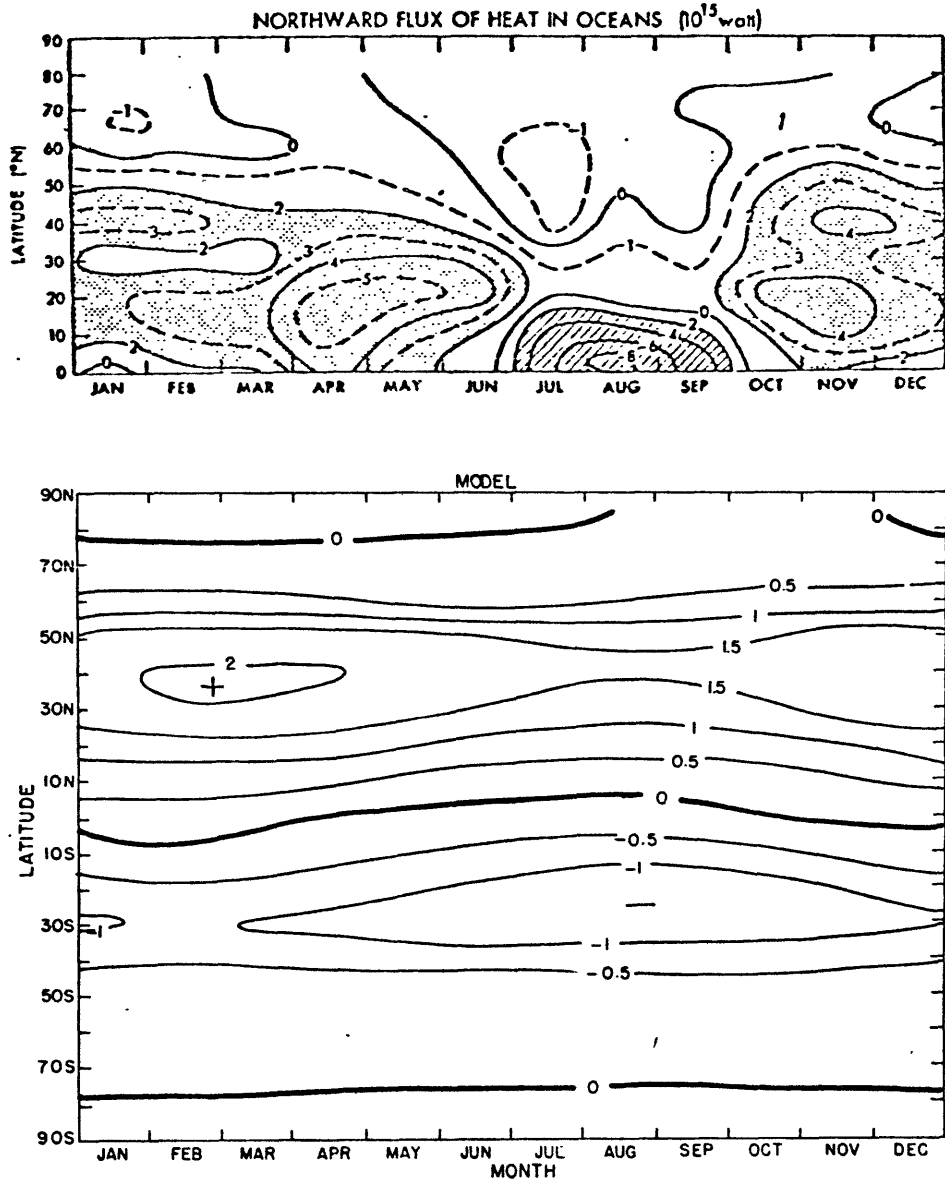


Figure 35. Ocean heat flux field. Units are  $10^{15}$  W. Upper figure from O+V.

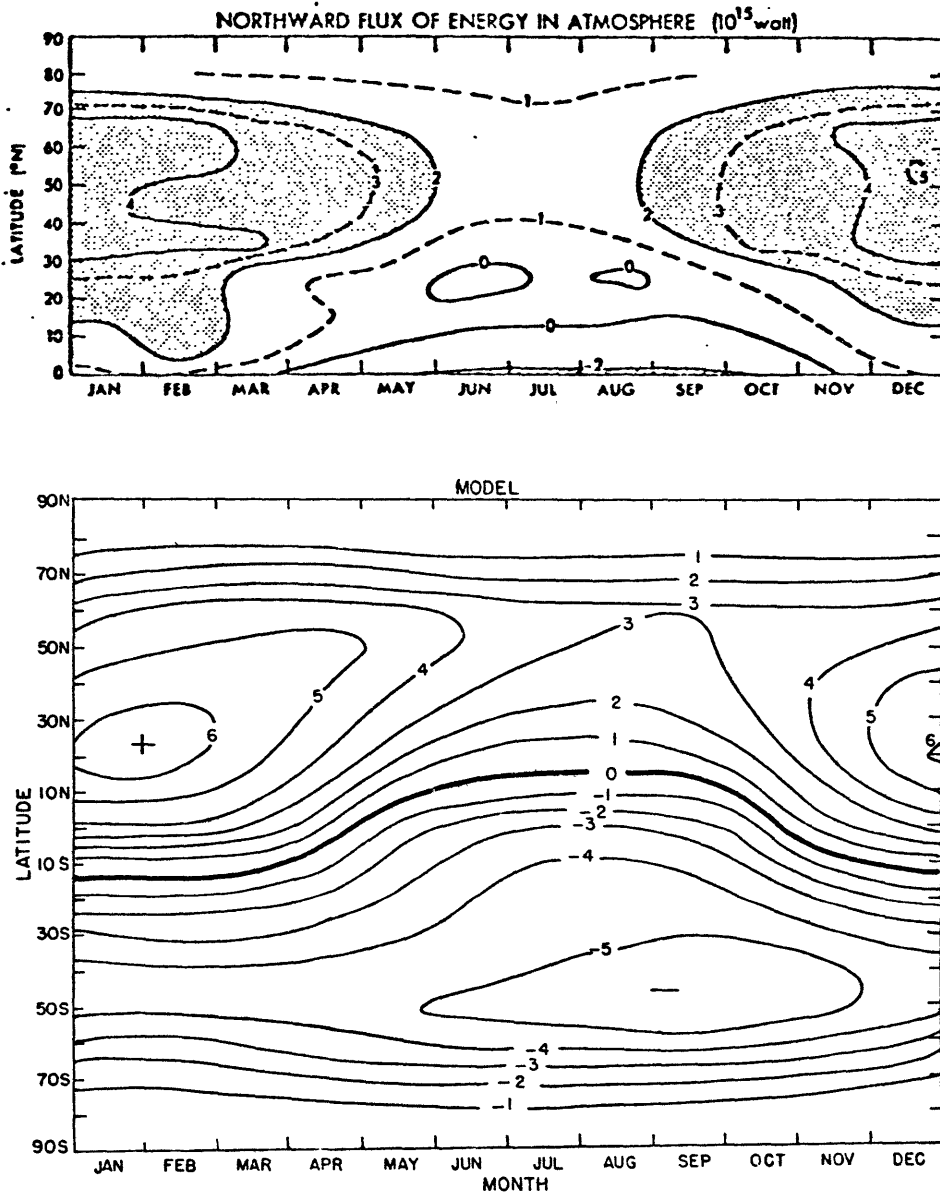


Figure 36. Atmospheric heat flux field. Units are  $10^{15}$  W. Upper figure from O+V.

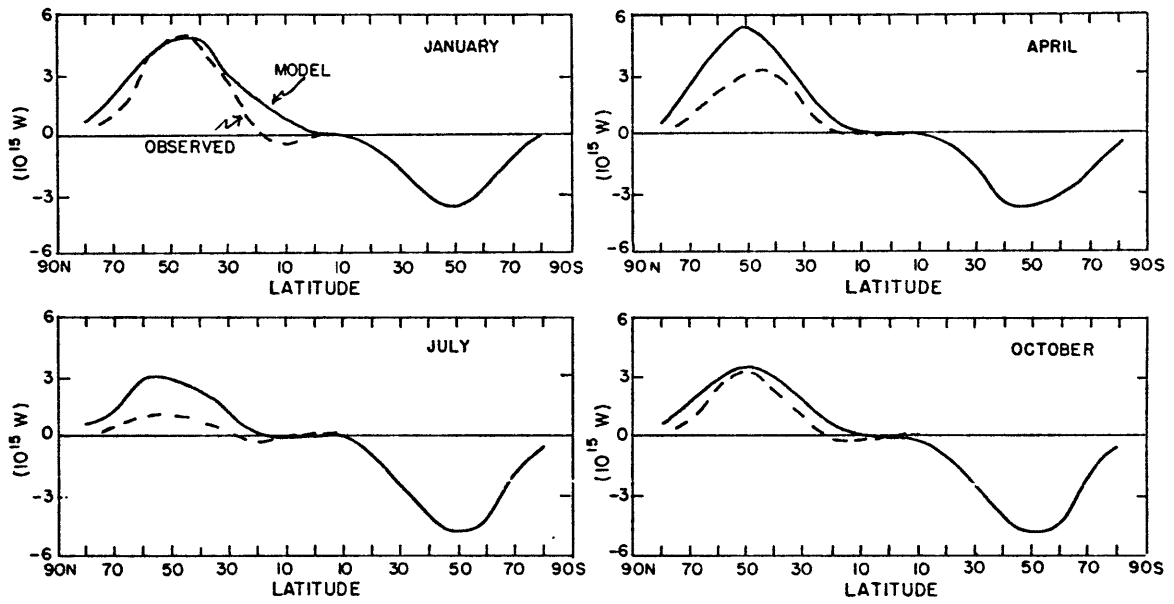


Figure 37. Atmospheric eddy flux of sensible heat plus potential energy for four months. Data from O+R.

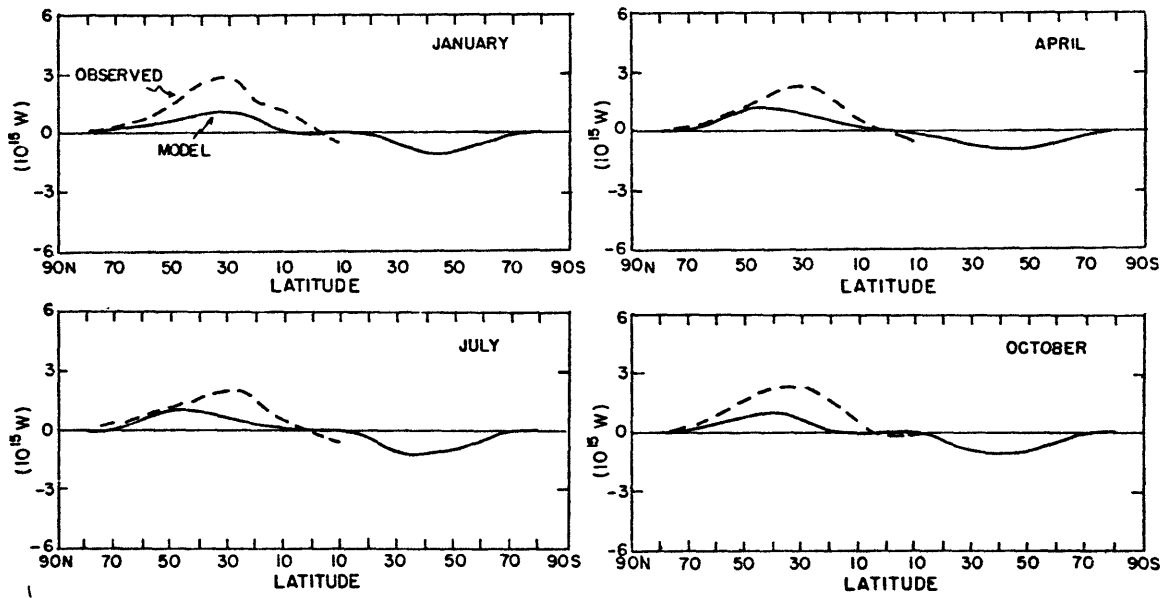


Figure 38. Atmospheric eddy flux of latent heat for four months. Data from O+R.

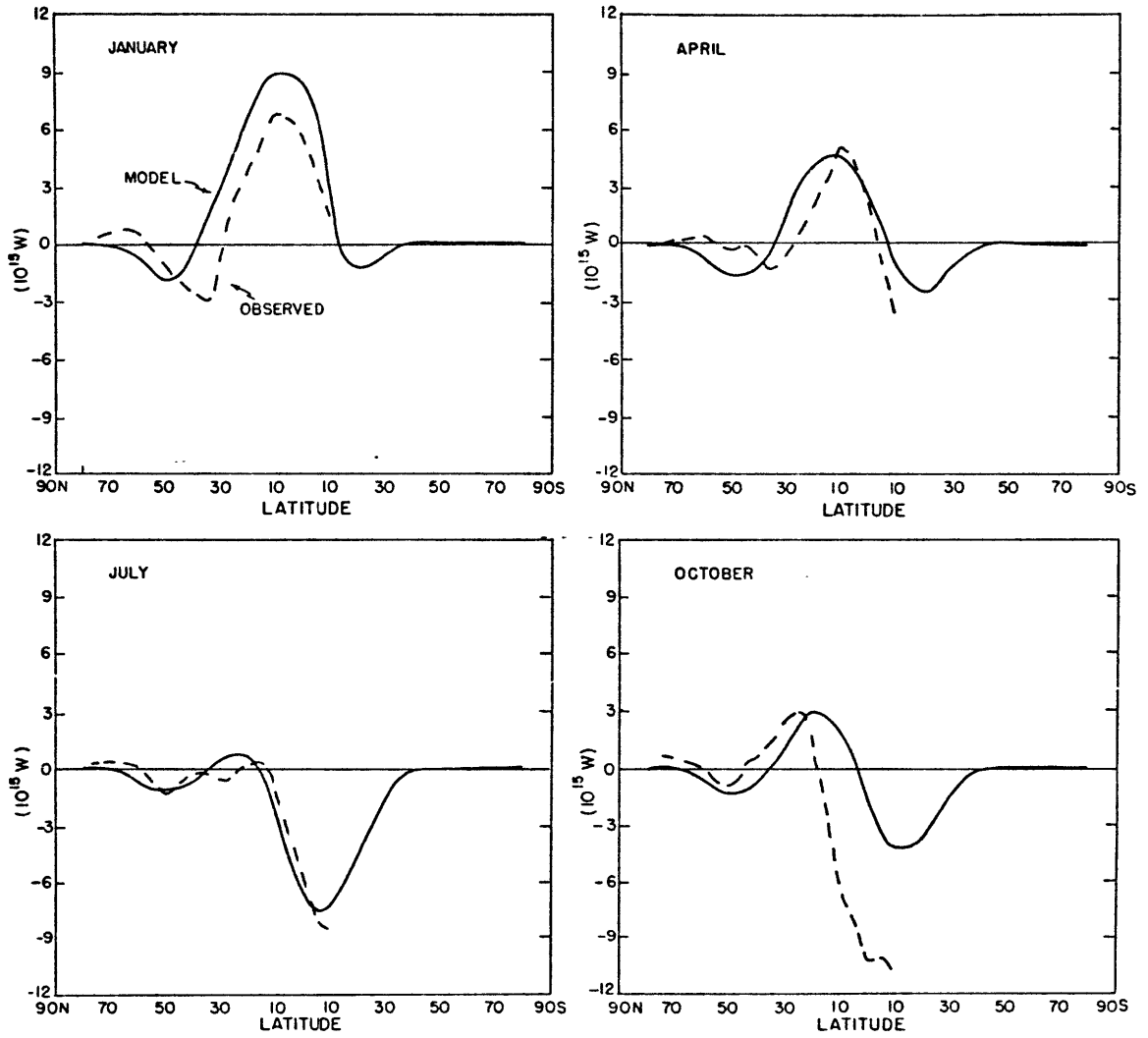


Figure 39. Atmospheric flux of sensible heat plus potential energy by the mean wind for four months. Data from O+R.

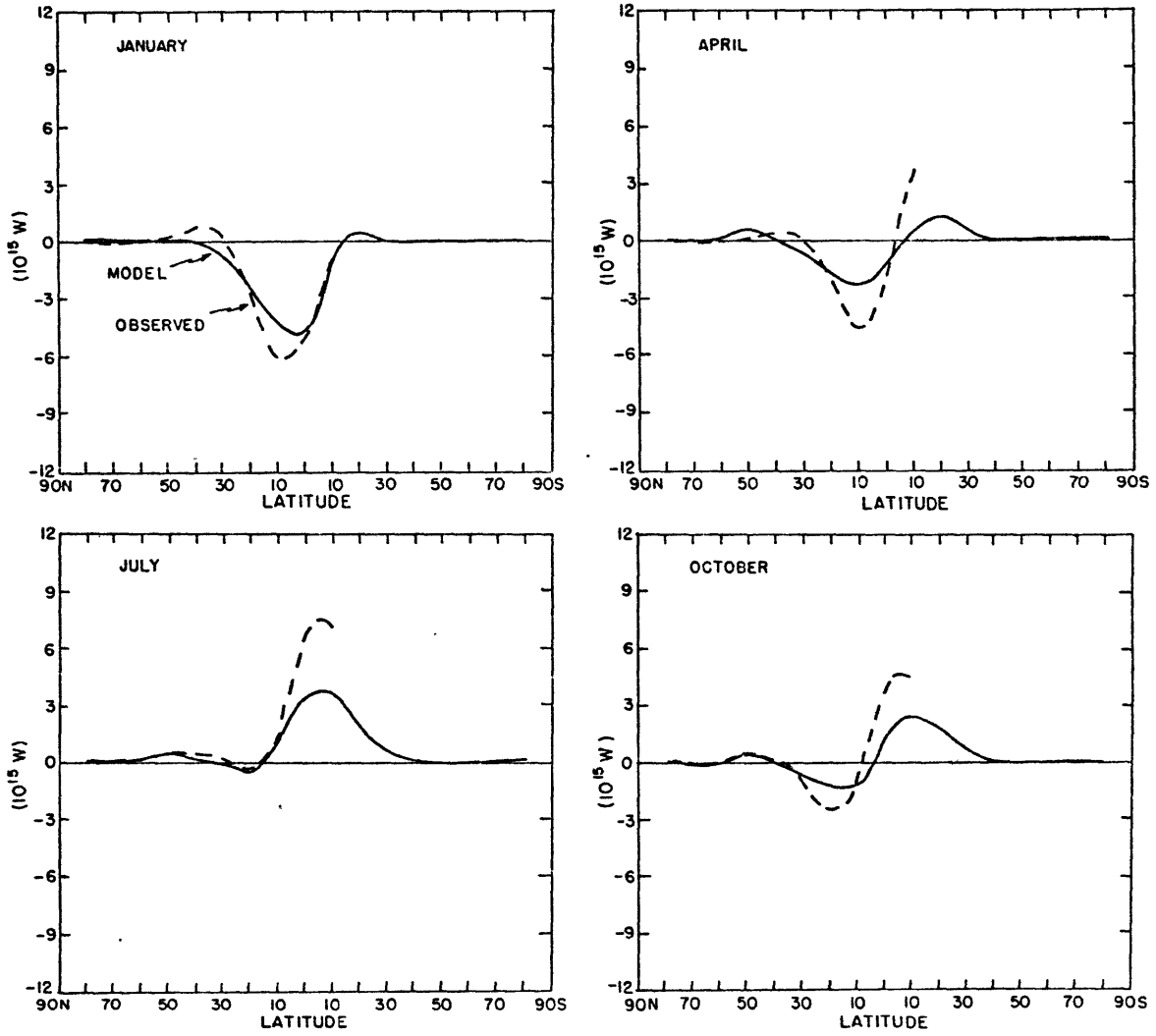


Figure 40. Atmospheric flux of latent heat by the mean wind for four months. Data from O+R.

is well-modeled in October and January, but too large in April and July. In all months, it is too large in the tropics, but this region is dominated by fluxes due to the mean winds. The eddy flux of latent heat is too small in the subtropics in all months, but correct elsewhere. The northward flux of sensible heat plus potential energy by the mean wind is too large in the tropics in January and October. In the same region, the flux of latent heat by the mean winds is slightly too small in magnitude.

All the atmospheric fluxes appear to be well-simulated in latitudinal distribution and seasonal cycle. Only the magnitudes appear to be slightly wrong.

#### 7. Summary

The model simulates the observed temperature fields quite well with the following exceptions:

1) The NP summer temperatures are too cold. The albedo is also too high resulting in too little absorbed solar radiation. This is the result of a faulty snow and ice model which gives too much sea ice, and either too much snow, or too high an albedo for the snow.

2) The SP is too warm year round. This is probably due to a calculated horizontal heat transport into the SP that is too large, combined with the inability of the model to simulate surface temperature inversions.

3) The NH and SP have seasonal temperature cycles that are too small. This may be due to a thermal inertia for the land that is too large, since the rest of the SH that is dominated by water has a proper



cycle. It may also be due to the incorrect seasonal cycle of some of the variables, due to either omission or faulty parameterization.

These include the albedo zenith angle effects mentioned previously, ocean mixed layer depth, snow and ice albedos, and possible biological effects. These will be discussed in more detail in section G.

The radiation fields are quite well simulated, but the omission of an albedo zenith angle dependence is noticeable. Also, as mentioned above, the NP summer albedo is too high. The polar albedos are too high, which may be due to incorrect assumptions of ice and snow albedos.

The horizontal flux fields are driven by the radiation fields, and behave as expected. The atmospheric flux components have magnitudes that are slightly wrong. The oceanic fluxes are quite different from the "observations", but the "observations" are derived as residuals from radiation observations which are not perfect, and so are open to question. Still, the model produces ocean fluxes with very little physical understanding of them. A better parameterization could be derived empirically from the data, but the physics are not well understood.

This model does at least as well at simulating the seasonal cycle as general circulation models do (Gates and Schlesinger, 1977 and Stone et al., 1977), and it calculates surface albedos and sea surface temperatures which are prescribed by the GCM's. It is certainly valid, then, to use this model to test theories of climate change, as it is the best model available for this purpose. The quantitative results will probably be in error, due to the model's inability to accurately reproduce the polar seasonal cycles, and hence the proper ice-albedo feedback, but the qualitative results will be a good indicator of the

relative validities of the different theories of climate change. Certainly the energy balance principle is well simulated by the model, and this is the important determining factor for climate change.

The question might be raised as to why the model does such a good job of reproducing the observed climate. Is it because the physical laws that produce the actual climate are well modeled, or is it because artificial parameters were adjusted to give results that look like the observations? By analyzing each component of the heat flux as was done in this section it is seen that all the individual components are well modeled, with certain shortcomings that were pointed out. Not only do they reproduce the correct annual average values of the flux, but they also reproduce the correct amplitude and phase of the seasonal cycles. Because each component of the heat flux is individually correctly modeled, the resulting temperatures are produced by the correct physical mechanisms. Certainly parameters are used to calculate the individual fluxes, but they are based on physical understanding as well as observations of the individual flux components, not of the resulting temperatures. Probably the most artificial parameter used is  $b$ , for the mean wind. This locks the circulation regime into the presently observed latitudinal distribution of high and low pressure belts, and although the parameterization reproduces the presently observed seasonal cycle quite well, it would not be expected to do so for a climate much different from the present one. The answer to the question, then, is that the model correctly simulates the present climate because the physical laws are well modeled. However, because of the parameterizations, it would not be expected to do a good job for

climates much different from the present one. For climate changes small compared to the seasonal cycle, such as during the last 100 years, the model should be valid, but solutions such as the ice covered earth should not be considered realistic with this model.

#### F. Parameter sensitivity

Because the model is highly parameterized, one would like to know how sensitive it is to different values of the parameters. One would also like to know how different parameterizations of certain processes affect the results. In particular, I wanted to see what effects the changes I made in Sellers' model had on the results. In this section the above questions are addressed. The determining factors for the model sensitivity to solar constant changes are also discussed.

##### 1. Changing the parameters by 1 %

In order to investigate the relative effect on the model output of changing the various parameters, I performed three experiments on fourteen parameters. The results are listed in Table 9. All the experiments were 100-year runs with the model. The model needs about 300 years in order to reach a perfectly balanced state after initial condition changes. However, more than 95 % of the resulting final change takes place in the first 100 years for almost all the parameters. In the first experiment, at each time step the value of the parameter was perturbed by a random amount. The random amount was a normally distributed random number with mean 0 and standard deviation equal to 1 % of the value of the parameter. The method of calculating the random numbers is described in Appendix D. All parameters were perturbed with

Table 9. Parameter sensitivity - results of 100 year runs.

<u>Parameters</u>		Perturbed with		+1%	-1%
<u>Name</u>	<u>Number</u>	SD = 1%			
		SD(T)	$\Delta T$	$\Delta T$	$\Delta T$
				(°C)	
Solar constant	1	0.0802	+0.141	+3.137	-4.536
IR cooling rate	1	0.0399	+0.013	-1.851	+1.250
Optical depth*	2	0.0137	+0.026	-0.557	+0.529
Cloud amount	18	0.0095	+0.022	-0.528	+0.502
Surface albedo	35	0.0071	+0.001	-0.267	+0.245
Eddy flux K	1	0.0037	-0.004	+0.160	-0.148
Relative humidity	35	0.0032	-0.004	+0.112	-0.102
Ice area	~5	0.0022	+0.001	-0.092	+0.094
Snow area on land	~5	0.0016	+0.007	-0.055	+0.068
Ozone emissivity†	2	0.0004	+0.001	+0.051	-0.051
Ocean flux $K_w$	17	0.0008	+0.001	+0.043	-0.034
CO <sub>2</sub> amount	1	0.0002	-0.001	+0.026	-0.026
Snow area on ice	~5	0.0003	+0.000	-0.011	+0.012
Wind constant b	17	0.0003	-0.000	-0.003	+0.003
None		0.00003	0.000		

\*  $\pm 0.01$  in actual value, not 1% of value;  $\tau(\text{clear}) = 0.3$ ,  $\tau(\text{cloudy}) = 5.0$ .

† A change of 1% in emissivity = A change of 6% in ozone amount.

the same set of random numbers. The resulting standard deviation of the global annual average temperature (T) and change of temperature from the beginning of the run to the end ( $\Delta T$ ) are listed in Table 9. This will be referred to as the perturbation (P) experiment. In the second experiment, the value of the parameters was increased by 1 % of its value at the beginning of the run and held at this value for the entire run. The temperature change ( $\Delta T$ ) is tabulated in the table. The third experiment was the same as the second one, but with the value of the parameter being lowered by 1 %. These will be referred to as the constant change (C) experiments. Some of the parameters have different values for different latitude bands (cloud amount, albedo and relative humidity), land and water (albedo), different latitude circles (ocean eddy flux constant and mean wind constant, b), different vertical layers (ozone emissivity), cloudy and clear (optical depth) and regions where the cover is between 0 and 1 (snow and ice area). In each of these cases, all the values of each parameter are changed by the same random number times 1 % of each value. In other words all the values of each parameter are changed by the same percentage.

The results are listed in Table 9 in descending order of sensitivity. The model is most sensitive to changes in the parameters which affect the total radiation, indicating that the radiative balance is more important in determining the climate than the horizontal heat fluxes. Accurate parameterization of the radiation is more crucial than that of the heat fluxes. The model is less sensitive to those parameters which affect only a portion of the radiation.

The model is most sensitive to changes in the solar constant. In fact, other runs show that a 1.3 % reduction in the solar constant will cause the model to go into an ice covered earth. The sensitivity to this one parameter is a means of comparing the model to other simple climate models. Budyko (1969) required a 1.6 % reduction in the solar constant, while Sellers (1969) required a 2.15 % reduction. Parameterizations of the infrared flux and surface albedo are the most important determining factors of the sensitivity. This subject is discussed in more detail at the end of the next section after the effects of different parameterizations are determined.

All the C changes are in the expected direction for the different parameters. For the four largest responses for C, the negative temperature response is larger than the positive temperature response. This is due to the larger ice-albedo feedback in this direction. For the same magnitude temperature change, a larger area of ice or snow is affected for a negative change since this is in the equatorward direction and due to the sphericity of the earth, the area of latitude bands increases. Also the total sunlight in this direction is larger and the same albedo change causes a larger net change of radiation.

In other experiments done with the model, whenever a parameter was changed and then returned to its original value, the model output always returned to the initial balanced state, indicating that the model is transitive. One exception to this was the ice-covered earth solution which occurred if the solar constant was reduced too much. The ice-free earth solution, as discussed by North (1975a, 1975b) among others, is another possible exception, but this has not been

investigated with the model.

## 2. Different parameterizations

These studies were undertaken with the aim of discovering how different parameterizations affect the model sensitivity. The changes made in the S, S' model are investigated, as well as the effects of eliminating the ice-albedo feedback and the seasonal cycle. The actual sensitivity of the real world is unknown. Model studies such as this one and observational studies such as Cess (1976) will eventually allow realistic estimates of the sensitivity to be made.

As shown in the previous section, the model is most sensitive to the solar constant. The sensitivity to this one parameter then provides a convenient way of comparing the different versions of the model. It also provides a way of comparing this model to other climate models. One measure of the sensitivity to the solar constant is the decrease required to produce an ice covered earth. As mentioned earlier, this model requires a 1.3 % decrease, while Budyko (1969) required a 1.6 % decrease and Sellers (1969) required a 2.15 % decrease. S never explicitly mentioned this value for his version of the model.

A better understanding of this sensitivity can be gained by performing an analysis similar to that of Cess (1976). The equation for a time average, spatial average heat balance of the globe is

$$IR = \frac{SC}{4} (1 - \alpha) \quad (69)$$

where IR is the infrared flux, SC is the solar constant, and  $\alpha$  is the planetary albedo. Differentiating with respect to surface temperature

( $T_S$ ) and rearranging terms one can derive the formula for the sensitivity parameter  $\beta$

$$\beta = SC_o \frac{\partial T_S}{\partial SC} = \frac{IR_o}{\frac{\partial IR}{\partial T_S} + \frac{SC}{4} \frac{\partial \alpha}{\partial T_S}} \quad (70)$$

$\beta$  divided by 100 is the number of degrees change in  $T_S$  for a 1 % change in SC. For a global annual average, the sensitivity is a function of the relative strengths of the negative infrared radiation and positive ice-albedo feedbacks. The horizontal fluxes only affect the sensitivity through the radiative-dynamical coupling feedback, that is only through their effects on the strengths of the radiation feedbacks. A discussion of the calculations for this section follows, after which  $\beta$  will be evaluated.

Ten different versions of the model were considered. The results are listed in Table 10. In each case, the IR cooling rate was adjusted so that the global annual mean T was 14.50°C in a balanced condition (seasonal cycles repeating exactly year after year). The solar constant was then either increased or decreased by 1 % and held at that constant value, and the model was run for 500 years to observe the effect on T. A linear regression of the IR flux ( $IR = A + BT_S$ ) was performed each month during the balanced run and the annual mean of the values so obtained is also listed in the table. The reduction of variance was over 99 %, indicating that the IR flux is very close to having a linear dependence on  $T_S$ . Budyko (1969) actually used a linear formula for IR in his model with the values  $A = 199 \text{ W/m}^2$  and  $B = 1.43 \text{ W/(m}^2 \text{ }^\circ\text{C)}$ . Values for these parameters can also be derived from the results of Manabe and



Table 10. Different parameterizations.

Parameterization differences	IR cooling rate  (°C/day)	SC↑1% SC↓1%		Linear regression of IR = A + BT <sub>S</sub> (T <sub>S</sub> in °C)	
		(500 year runs)		A	B
		ΔT	ΔT	(W/m <sup>2</sup> )	(W/m <sup>2</sup> °C)
		(°C)	(°C)		
None	1.50	+3.14	-4.65	207	1.81
CO <sub>2</sub> emissivity constant	1.50	+3.07	-4.44	206	1.82
No meltwater	1.50	+3.20	-4.58	206	1.81
Seasonal clouds	1.50	+3.07	-4.59	206	1.81
Seasonal sea albedo	1.51	+3.23	-4.89	207	1.81
12 time steps per year	1.49	+3.16	-4.59	206	1.81
Sellers' IR	1.59	+2.48	-3.57	204	2.01
Constant ice and snow at monthly values	1.50	+1.30	-1.30	207	1.81
Constant ice and snow at annual average values	1.51	+1.30	-1.30	207	1.81
No seasons	1.51	+3.91	-5.21	207	1.82

Wetherald's (1967) detailed radiation calculations. They give  $A = 218$  and  $B = 2.30$  in the same units.  $B$  corresponds to  $\frac{\partial IR}{\partial T_S}$  in equation (70).

The first six versions listed in the table, after the standard one, correspond to changes I made in  $S$ , as discussed in section D. I changed each one back to the way it was in  $S$  to see how much this changed the results. The first five made little difference. Making the  $CO_2$  emissivity constant took out the temperature feedback and made the model slightly less sensitive. Taking out the meltwater on ice slightly increased the ice albedos in summer and made the model slightly more sensitive for increased  $SC$ , and less for decreased  $SC$ . Putting in seasonal, as opposed to annual average, clouds made the model slightly less sensitive, and putting in seasonal sea albedos made the model slightly more sensitive. Using 12 time steps per year had little effect on the sensitivity, but made the amplitude of the seasonal cycles lower by about 10 % than for the 24-step run. The combined effects of these five changes are small.

Changing the IR calculations back to the way  $S$  did them, using clear temperatures to calculate IR in cloudy regions, required a cooling rate of  $1.59^\circ/\text{day}$ , close to that used by  $S$ , to balance  $T$  at  $14.5^\circ\text{C}$ . It also made the model much less sensitive.

Assuming no ice albedo feedback,  $\beta$  can be calculated from the balanced model.  $IR = 232 \text{ W/m}^2$  averaged over the globe and  $B = \frac{\partial IR}{\partial T_S} = 1.81 \text{ W/(m}^2 \text{ }^\circ\text{C)}$  giving  $\beta = 128^\circ\text{C}$ . This corresponds quite well to the results of the next two versions which held the ice and snow areas constant at their monthly and annual average values. Cess (1976) found, studying observed seasonal and latitudinal changes, that  $B$  should equal

$1.6 \text{ W}/(\text{m}^2 \text{ } ^\circ\text{C})$  and  $\beta$  should equal  $145^\circ\text{C}$ . My model comes closer to simulating these observed values than does S. Both models, however, give values within those calculated by Budyko (1969) and Manabe and Wetherald (1967).

The large sensitivity of my model as compared to the simpler Budyko model cannot be due to the IR formulations, as my IR model is less sensitive. The difference must be due to the ice-albedo feedback parameterization. The annual world average total albedo of the standard balanced model is 0.3138. After SC is raised by 1 % it is 0.3041 and after SC is lowered by 1 % it is 0.3315. Using these values and the temperature changes,  $\beta$  can be calculated from equation (70) including the ice-albedo feedback. For SC raised by 1 % it is  $305^\circ\text{C}$  and for SC lowered by 1 % it is  $440^\circ\text{C}$ . The model itself gives slightly higher sensitivity, indicating more complex interactions than in the simple theory. Cess (1976) suggests that  $\beta$  should be  $200\text{--}250^\circ\text{C}$  based on the numerical models of Wetherald and Manabe (1975) and a corrected version of Budyko (1969). However, my model, in the absence of the ice-albedo feedback, is less sensitive than these models, or Cess's observations. The large sensitivity of my model must therefore be due to its strong ice-albedo feedback. Once the surface albedo parameterization is corrected and zenith angle effects are included, to give the proper seasonal cycle and summertime albedo, this problem should be corrected.

The seasonal cycle could affect the sensitivity in two opposite ways, as compared to a model such as Budyko's with an annual average. In the summer the ice and snow line is farther north when the solar radiation is more intense, causing less albedo feedback than in an

annual average model. At the same time, the seasonal cycle, combined with the lower land thermal inertia, allows the snow line to advance much farther in the winter than it would in an annual average model, increasing the albedo feedback. The last version of the model listed in Table 10 is one with no seasonal cycle, using an annual average solar flux at each time step. Although the infrared sensitivity is the same, the no seasons version is more sensitive to SC changes. This must be due to the lower albedo feedback in the seasonal model. This further emphasizes the faulty albedo parameterization.

#### G. Suggestions for future model improvements

This model does a reasonably good job of simulating the seasonal cycles. Still, for future studies with it, some of the discrepancies between its climate and the real one should be corrected. This section will discuss ways in which this could be done, and also indicate the difficulties involved in trying to do this.

The radiative and oceanic horizontal fluxes appear to be most in error. The atmospheric fluxes appear to be off just in magnitude. Once the other fluxes are corrected, the feedback with the atmospheric fluxes may produce correct atmospheric fluxes. If not, then the atmospheric fluxes should be changed. Feedback may then require further radiative and oceanic parameterization changes. But the radiative and oceanic fluxes should be corrected first, as they appear most in error.

The first step in improving the radiative fluxes would be an improved ice and snow area model. It should be one that is energy consistent and not based solely on temperature. Perhaps a complete

hydrologic cycle, as in Sellers (1976), could be included, but he found sea ice areas in error. Perhaps the present model could be modified with different constants for the Northern and Southern Hemispheres, related to the relative ice and snow areas or with the permanent ice caps of Greenland and Antarctica differentiated from the transient seasonal ice and snow cover. The energy required for melting or freezing should be included in the energy balance equation. The summer NH snow extent is the most crucial feature in order to have the correct sensitivity. The model is now too sensitive because this snow extent is too large. Any small changes in it now affect a region with a very large solar input. The correct balance between correct albedo and correct snow extent, and their correct temperature response, must be included in any future parameterization. Unfortunately, data to use in developing such a parameterization is very poor at present.

The zenith angle effect should be included in surface albedos. Equation (53) could be used for the sea surface and other observational results could be used for the other surfaces. The zenith angle effect on total albedo should also be included. The model of Lacis and Hansen (1974) would be a large improvement, because it explicitly includes the zenith angle effect, and  $H_2O$  and  $O_3$  effects on the transmissivity. It requires, however, detailed assumptions about the vertical structure of the cloudiness. These could be made from observations, but they are very poor at present. Satellite observations in the future may allow this to be done, however. Using constant cloud observations would eliminate any cloud feedbacks with the radiation field, but Cess (1976) finds that cloud feedbacks are not important, based on present limited

observations. Sellers (1976) has proposed a relationship between fractional cloudiness and various other components of the hydrological cycle, which could be used if a complete hydrological cycle is included. The vertical cloud distribution would still have to be specified.

If cloudiness were better understood or predicted, improvements would be possible in the IR calculation. Staley and Jurica (1970) point out that their emissivities should not be used for thick layers, because they are so temperature dependent that they would not be representative. An IR model with more layers would solve this problem. Cess (1976) points out that whether a fixed cloud top height (as used in the present model) or a fixed cloud top temperature is used gives very different IR sensitivity to surface temperatures. Which way, or in what combination this occurs in nature has not been resolved, and this problem would have to be dealt with.

Other seasonal cycles should be included in the model. The observed change of the ocean mixed depth with season affects the ocean thermal inertia as well as the horizontal fluxes. Biological effects, such as the noticeable seasonal  $\text{CO}_2$  cycle in mid-latitudes and the effects on land albedo, may be important.

The ocean flux parameterization could probably be improved by removing the  $A_L$  dependence in equation (47) and raising the eddy coefficient. Present physical understanding of ocean circulation and heat transports does not permit a more detailed calculation.

Improving the parameterizations of the model, within the context of retaining its computer speed, presents complex problems. These include trying to simplify physical understanding, combined with limited

observations of the important variables. Hopefully, future theoretical and observational programs will allow this to be done. The model as presently constituted will be used to study different theories of climate change.

## Chapter IV. Results

The model described in Chapter III was used to test the following theories of climate change: solar forcing; volcanic dust; anthropogenic carbon dioxide, aerosols and heat; and internal causes. In this chapter the experiments done with the model are described and the results are reported.

### A. External causes

#### 1. Design of the experiments

For each of the five postulated external causes of climate change, the following procedure was used. The model was run for 380 years of simulated time starting with the year 1621. For anthropogenic forcing the experiments were instead run for 160 years starting in 1841, since no anthropogenic forcing occurred before then. The resulting temperature fields corresponding to the data of Mitchell (Figure 5) for five-year averages, and Budyko and Asakura (Figure 4) for annual and five-year averages were then compared to the actual data. The runs were 380 years long to allow the model to adjust to any imbalance imposed by the forcing, so that by the time the results were compared to the data, starting in 1840-1880 for the different data collections, there was no trend in the data caused by the initial conditions.

The model was forced by changing the external conditions in accordance with the various climate change theories. To test solar forcing, two runs were tried forcing the solar constant according to the



theory of Kondratyev and Nikolsky (K+N):

$$SC = 1.903 + 0.011 W^5 - 0.0006 W \text{ ly/min} \quad (71)$$

where SC is the solar constant and W is the Wolf sunspot number. In one run W was set at the annual average observed values each year, changing linearly from one year to the next at each time step. In the other run, W was set at the monthly average values for years after 1750, which is when these data are available.

Other possible simple relationships between SC and W were also tried, namely:

$$SC = A + B W \quad (72)$$

and 
$$SC = A + B W^5 \quad (73)$$

with  $A = 1.925 \text{ ly/min}$ ,  $B = 0.0003$  in (72) and  $B = 0.002$  in (73) in order to make  $SC \approx 1.94$  during the past century when the average W was  $\sim 50$ . Not knowing whether sunspots actually increase or decrease SC, a run was also tried with  $A = 1.955$  and  $B = -0.0003$  in (72). The magnitude of the W effect on SC was chosen so as to give a large enough signal in the T response to notice, but not so large as to make the model unstable. The linear relationship (72) was run for three different sets of W - monthly average, annual average, and with the sunspot cycle smoothed out (see Figure 7) according to Eddy's suggestion. Since the smoothed data set gave the only reasonable output, since the 11-year cycles produced by the other data are not observed, it was used for relationship (73) and for (72) with B negative.

The volcanic dust theory was tested in two runs, one using the data of Lamb (Table 2) and one using the data of Mitchell (Table 3). In both cases the volcanic dust was simulated by reducing the solar constant by an amount proportional to the dust veil index, calibrated by assuming the Agung dust (DVI = 160) produced a 0.5 % decrease in SC, following Schneider and Mass (1975). In both cases, the non-volcanic SC was set to 1.945 at the beginning of the run to make the average SC  $\approx$  1.94 and avoid any trend associated with imbalanced initial conditions.

Anthropogenic effects were simulated in three runs. Carbon dioxide was changed according to Broecker's data (Figure 10) in the first one. In the second one, aerosols were simulated by increasing the optical depth ( $\tau$  in equations (51) and (52)) by an amount proportional to the excess anthropogenic CO<sub>2</sub> with the distribution shown in Table 4. It was calibrated by assuming that in the most polluted grid area, the excess aerosol was equal to 20 % of the natural level in 1972. In the third run, heat was simulated with the same time dependence as carbon dioxide and aerosols, with the latitudinal distribution shown in Table 4, and calibrated by assuming the total anthropogenic heat input to be  $8 \times 10^{12}$  W in 1972.

The 12 runs described above are listed in Table 11.

The model results were plotted against the data for all nine of Mitchell's sets of five-year averaged temperatures, and annual and five-year averaged Budyko and Asakura temperature. It is not possible to present 11 graphs for each run, so representative ones are presented for some runs, and a complete set is presented for the best simulation.

Table 11. List of simulation runs, correlations with Budyko-Asakura data.

Run No.	Theory	Data	A	B	Correlation coefficients of results with Budyko-Asakura data	
					5 year average	1 year average
1	K + N	M			0.29	0.12
2	K + N	A			0.32	0.05
3	(72)	M	1.925	0.0003	0.18	0.10
4	"	A	"	"	0.17	0.10
5	"	S	"	"	0.18	0.07
6	(73)	"	"	0.002	0.20	0.08
7	(72)	"	1.955	-0.0003	-0.21	-0.10
8	Volcanoes	Lamb			0.88	0.75
9	"	Mitchell			0.92	0.77
10	Anthropogenic (1841-2000)	CO <sub>2</sub>			0.61	0.42
11	"	Aerosols			-0.63	-0.44
12	"	Heat			0.63	0.44

Table 12. Correlation coefficients of 5 year average results of simulation runs with Mitchell's data. W = winter, A = annual.

Run No.	0°-80°N		0°-60°N		0°-60°S		40°-70°N		30°N-30°S
	W	A	W	A	W	A	W	A	A
1	0.19	0.32	-0.06	0.21	0.05	0.09	-0.12	-0.21	0.22
2	0.22	0.35	-0.03	0.24	0.07	0.11	-0.11	-0.19	0.24
3	0.19	0.25	0.02	0.14	0.05	0.09	-0.08	-0.18	0.10
4	0.19	0.25	0.02	0.14	0.05	0.09	-0.09	-0.18	0.10
5	0.21	0.25	0.06	0.17	0.06	0.08	-0.08	-0.18	0.08
6	0.22	0.26	0.06	0.18	0.07	0.10	-0.06	-0.16	0.10
7	-0.26	-0.27	-0.11	-0.21	-0.09	-0.13	0.03	0.14	-0.12
8	0.95	0.89	0.95	0.89	0.81	0.86	0.82	0.76	0.82
9	0.94	0.90	0.86	0.88	0.77	0.80	0.72	0.67	0.77
10	0.84	0.66	0.82	0.78	0.61	0.71	0.82	0.76	0.67
11	-0.86	-0.67	-0.83	-0.80	-0.61	-0.71	-0.84	-0.78	-0.68
12	0.86	0.67	0.83	0.80	0.61	0.71	0.84	0.78	0.68

Correlation coefficients between the model output and the data were also calculated. These are shown in Tables 11 and 12 for all the runs. This method of comparison was used because it does not depend on the relative magnitudes of the model output and the data. Because the sensitivity of the model is questionable, as discussed in Chapter III, it would not be expected to give perfect quantitative responses to different climate forcings. Still, reasonable responses would be expected, since all the forcings used, except equations (72) and (73), are based on the observed magnitudes of the forcings.

## 2. Solar forcing

None of the solar forcing runs produced results resembling the observational data. The correlation coefficients for all the data sets were low. There was little difference in the results between using monthly or annually averaged sunspot data (see Tables 11 and 12 and Figure 41). The thermal inertia of the model was high enough to integrate the variable monthly forcing. Using smoothed data also made no difference in the resulting correlations with the observations, but gave different looking temperature series. The monthly and annually averaged runs gave results with very evident sunspot cycles, which were missing from the observed data. Run 6, using formula (73), gave results almost identical to the other runs. Run 7, with a negative effect of sunspots on the solar constant, also gave very low correlations with the observed data. Solar forcing alone, therefore, cannot explain the past observed climate change.

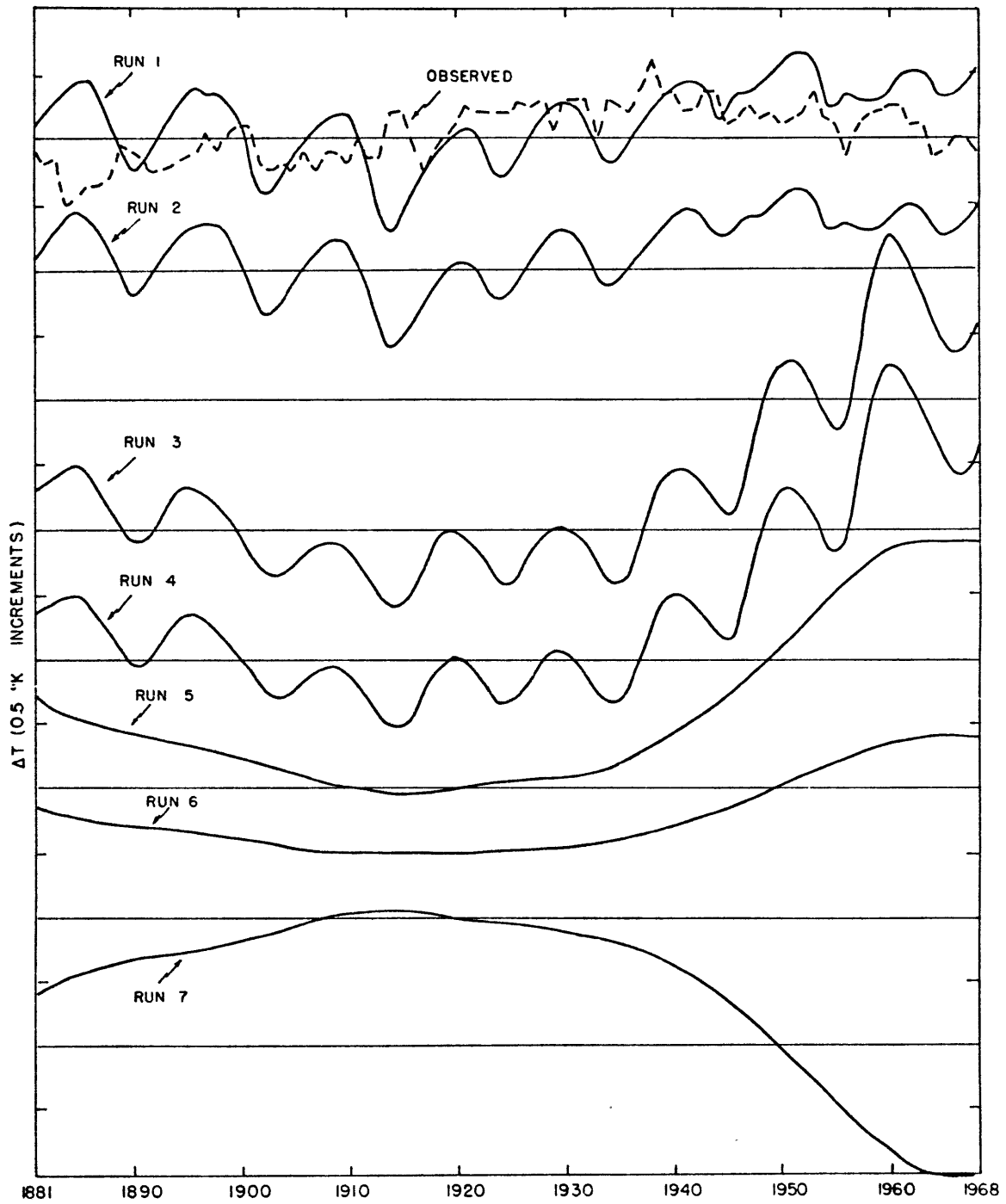


Figure 41. Results of solar forcing runs (1-7) compared to Budyko-Asakura annual average data for 1881-1968.

### 3. Volcanic dust

Both volcanic dust runs produced results resembling the observations. Figure 42 compares the 0°-80°N annual data of Mitchell with both results and Figure 43 presents all the other data fields compared to the results of run 9, forced by Mitchell's volcanic data. Although the Mitchell run produced slightly lower correlations than the Lamb run (run 8), the results include the temperature drop after the 1940's, forced by volcanoes that Lamb did not include.

The best results are those for the entire Northern Hemisphere - Budyko and Asakura, and Mitchell 0°-80°N. This is understandable, since the volcanic dust data was NH average data. Forcing with the correct latitudinal dependence would probably give equally good results for all the fields. The worst results are for 40°-70°N which presumably is the best of the data records, with the longest record and the highest station density. The worst agreement is for the period before 1880, where the model results have the temperature increasing sharply and the data has the temperature relatively constant. I think this is because the data is in error. There are very few stations used for this portion of the data and Mitchell admits that they may not be enough to be representative (personal communication). Furthermore, two other available records (Figures 3b and 3c) show a rising temperature during this period, closely resembling the model results, and not Mitchell's data. Without this discrepancy, the 40°-70°N results would be as good as the others.

The difference between the winter and annual temperature records observed by Mitchell were not reproduced by the model. For the NH, the

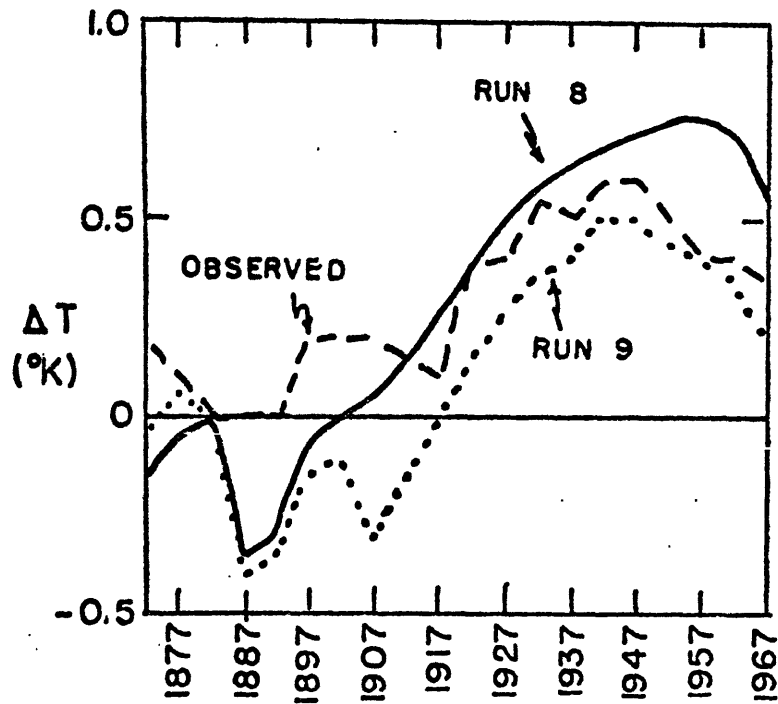


Figure 42. Results of volcanic dust simulation runs (8-9) compared to Mitchell-Reitan 0°-80°N annual five-year average data for 1870-1969.



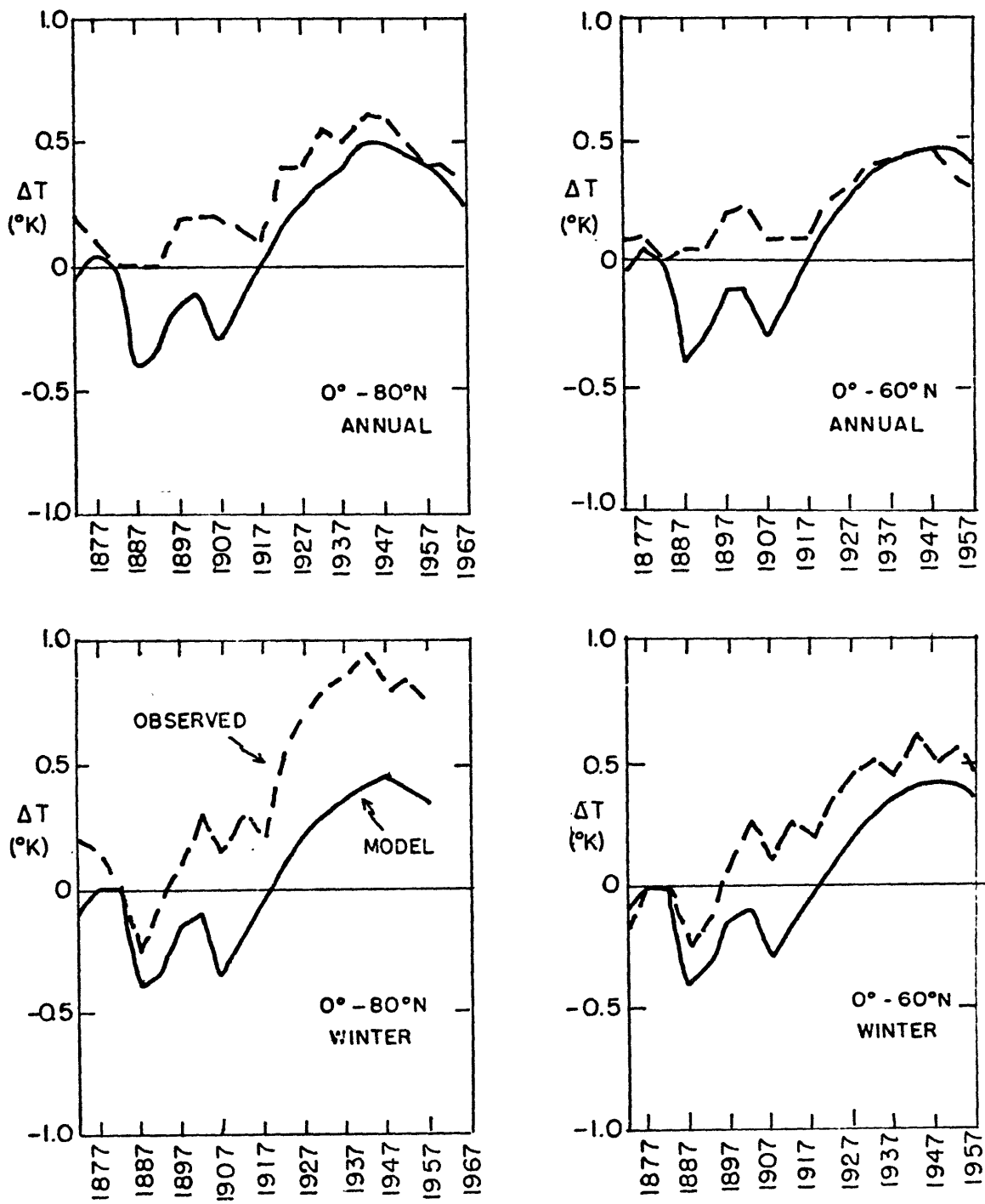


Figure 43. Results of Mitchell volcanic dust simulation run (9) compared with observations of Mitchell-Reitan for five year periods and Budyko-Asakura for one and five year periods.

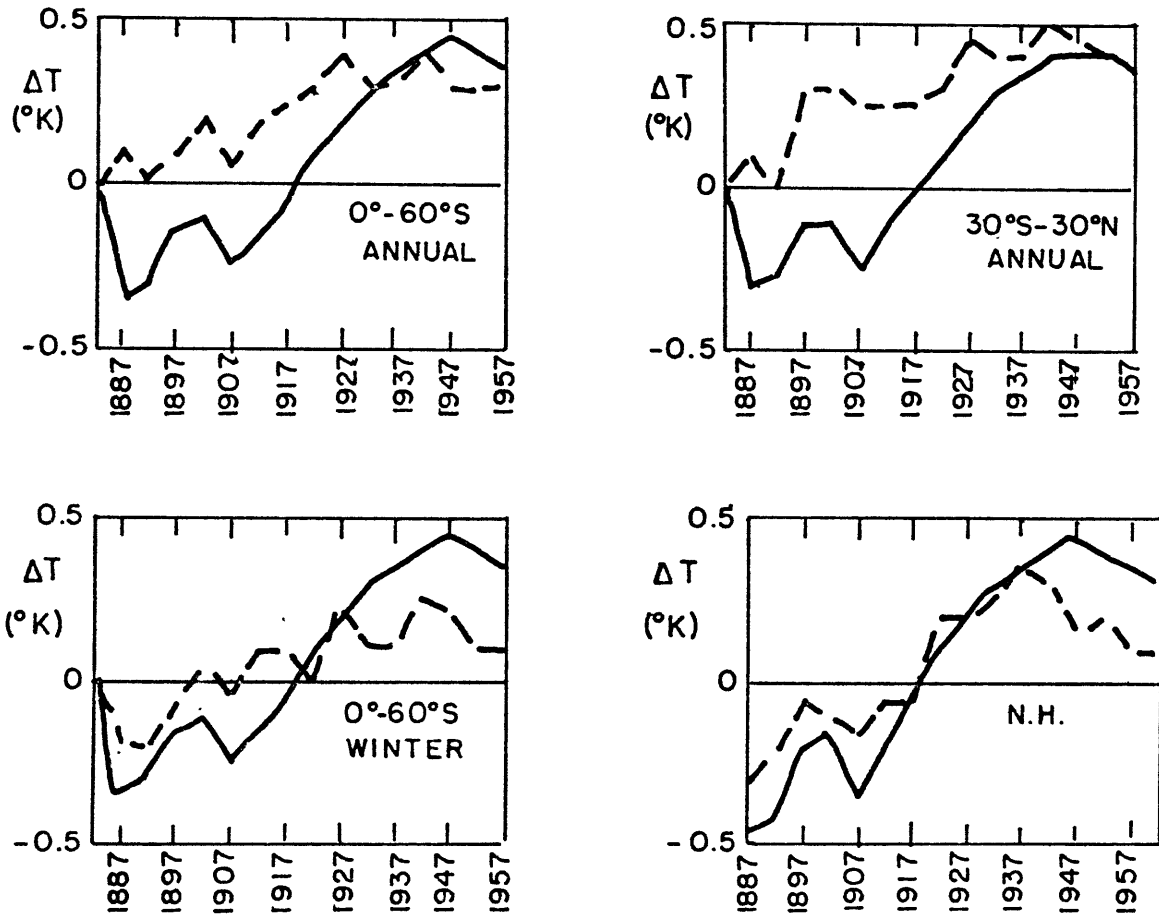


Figure 43. (continued)

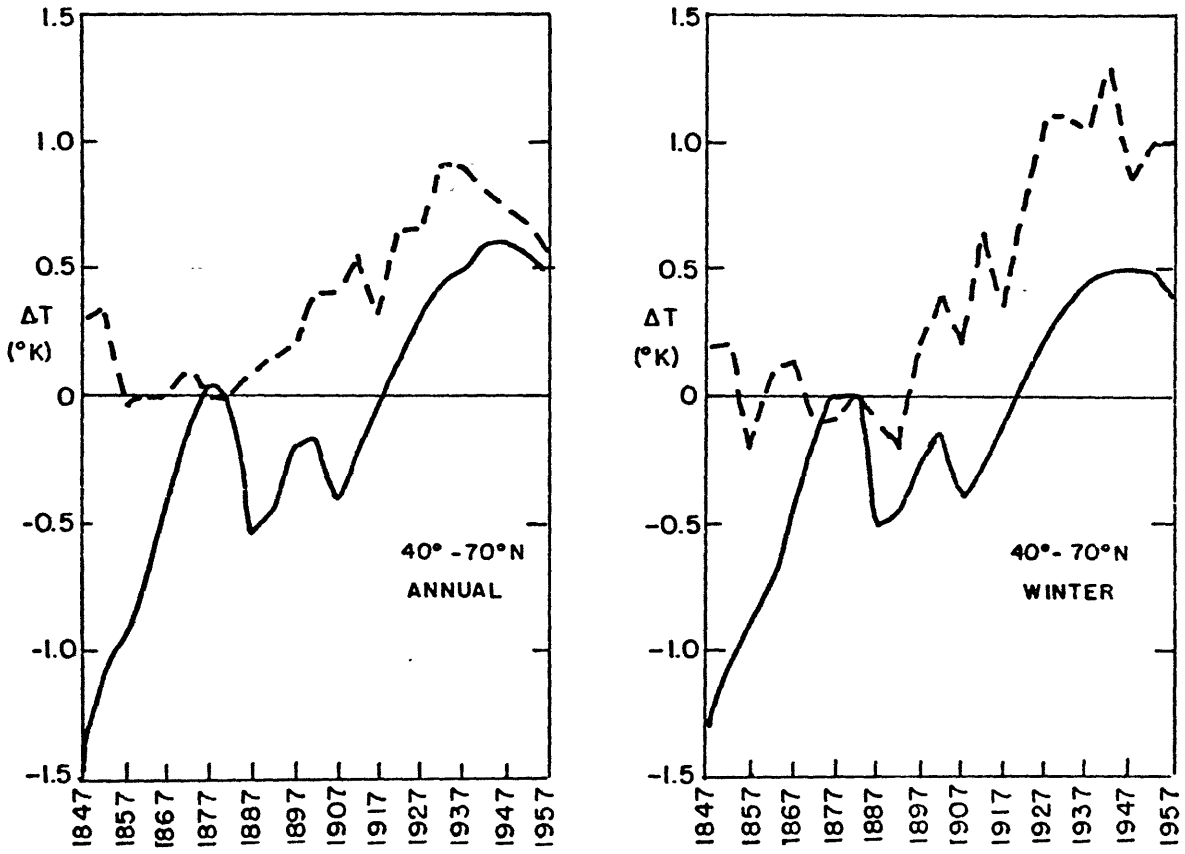


Figure 43. (continued)

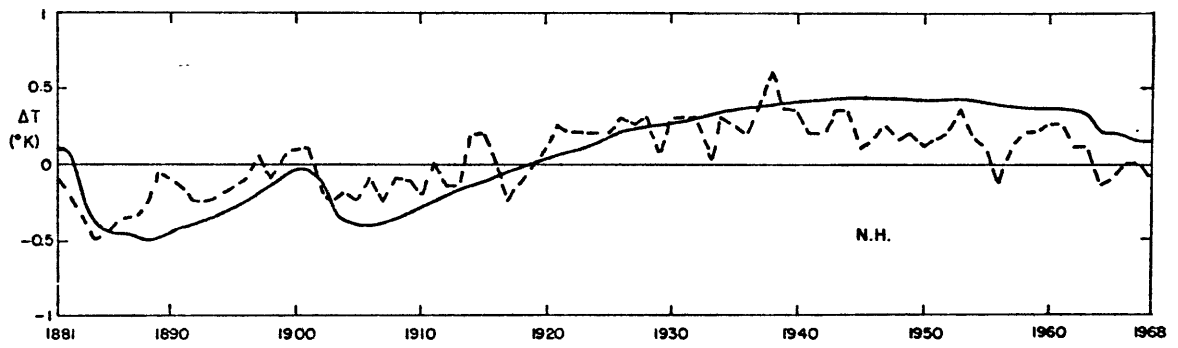


Figure 43. (continued)

model results more closely resembled the winter records rather than the annual ones. This failure of the model can probably be explained by its inaccurate albedo simulation which resulted in a faulty seasonal cycle. Once this flaw is corrected, the model will hopefully reproduce the seasonally differentiated climate response found by Mitchell.

The magnitude of the model response quite closely resembles the observations, except in the tropics and the Southern Hemisphere, but the volcanic data were not adjusted for these regions. In Figure 43, of the annually averaged results, two other inaccuracies can be seen. The magnitude of the temperature drop after the 1940's peak is slightly too low, while the rise before the 1940's is slightly too high. This could be due to inaccuracies in the model sensitivity or in the volcanic data or to other forcings. It can also be seen that the model results are much less noisy than the data.

Volcanic dust, therefore, seems to have been an important cause of climate change during the past 100 years. The general shape of the observations is very well simulated, but not the details. This is due to several causes. First, there are inaccuracies in the model, the past temperature record and in the volcanic data. The most serious of these is that the volcanic data is averaged for the entire NH, and Cadle et al. (1976) have shown that volcanic dust in the stratosphere is confined to smaller latitudinal regions (see Figures 8 and 9). Better, latitude-dependent volcanic forcing would probably produce equally good agreement in all latitude bands. Second, the observational data is much noisier than the model output. This noise can be simulated as due to the natural variability of the system and is discussed in section B.

of this chapter. Also, anthropogenic effects may have been important. These are discussed in the next section.

#### 4. Anthropogenic effects

Three runs were made testing anthropogenic effects of CO<sub>2</sub>, aerosols and heat. The 0°-80°N results are shown in Figure 44. The correlation coefficients with the observations are shown in Tables 11 and 12, and the resulting temperature changes are shown in Table 13 for three different years.

Both CO<sub>2</sub> and heat produced warming, with the CO<sub>2</sub> effect being almost an order of magnitude larger than the heat effect. Aerosols produced cooling, but the magnitude, and even the sign of this effect, are open to much question due to our incomplete knowledge of the physical and chemical processes involved, as discussed in Chapter II.

CO<sub>2</sub> produced a slightly larger effect in the NH than in the SH, due to the larger percentage of land in the NH. This results in less thermal inertia and a larger snow-albedo feedback, both contributing to the larger sensitivity. Both aerosols and heat produced an even larger hemispheric difference, due to the additional fact that their forcing is much stronger in the NH. The response in the region 40°-70°N is even larger than the NH response. This is because this region has a high percentage of land and it is near the pole, which is more sensitive to climatic change than the hemispheric average. This geographic distribution of response is discussed in section C. It is also in agreement with Mitchell's data, which shows a larger climatic change in this region than in the whole NH.

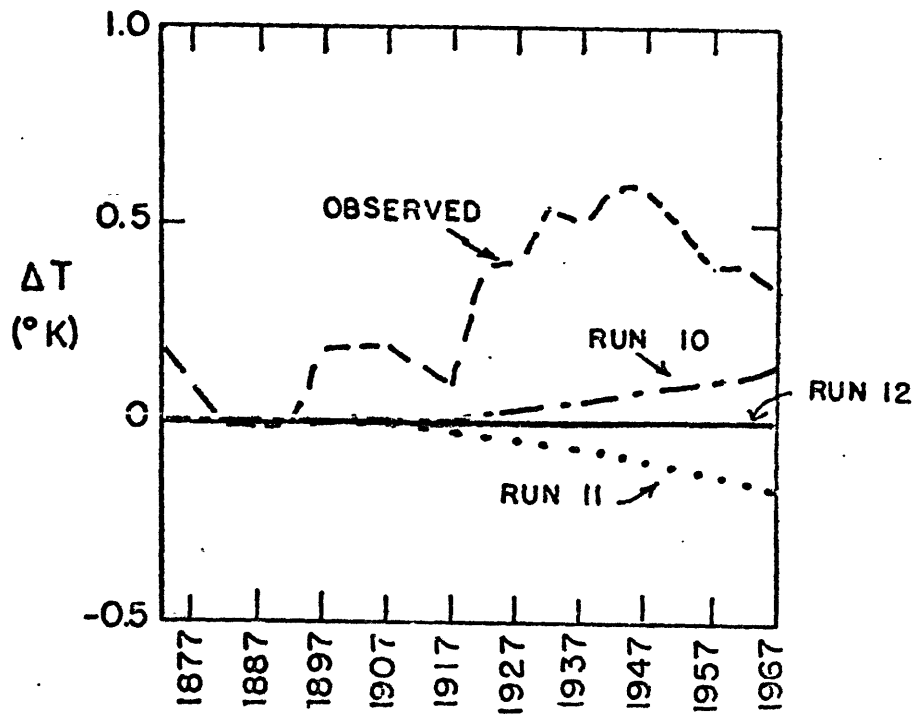


Figure 44. Results of anthropogenic forcing simulation runs (10-12) compared to  $0^{\circ}$ - $80^{\circ}N$  annual Mitchell-Reitan five-year average data for 1870-1969.

Table 13. Results of anthropogenic simulation runs. Annual average temperature change from 1880 values.

	WORLD	NH	SH	40°-70°N
	$\Delta T$ (°C)			
<u>1960</u>				
CO <sub>2</sub>	+0.119	+0.130	+0.110	+0.173
AEROSOLS	-0.112	-0.137	-0.085	-0.186
HEAT	+0.014	+0.019	+0.010	+0.026
<u>1980</u>				
CO <sub>2</sub>	+0.221	+0.238	+0.205	+0.312
AEROSOLS	-0.207	-0.256	-0.157	-0.345
HEAT	+0.026	+0.035	+0.019	+0.050
<u>2000</u>				
CO <sub>2</sub>	+0.423	+0.442	+0.404	+0.572
AEROSOLS	-0.408	-0.507	-0.309	-0.687
HEAT	+0.055	+0.072	+0.037	+0.106



One could sum the anthropogenic effects for each region, which would show almost no effect in the NH and warming in the SH. Drawing conclusions from this exercise would not be meaningful, however, due to our lack of understanding of the aerosol effect.

All the effects almost double every 20 years. They are not of sufficient magnitude to have much effect on the observational records, which end about 1960, but will have a very measurable effect in the near future.

The relative magnitudes of the effects may change in the future due to changing human pollution policies. Restrictions on particulate pollution, and anticipated measures against sulfate aerosols will lessen the effects of industrial aerosols. Increased dependence on nuclear energy would increase the ratio of heat to CO<sub>2</sub> effect, while an increased dependence on coal would not.

It can be seen in Tables 11 and 12 that the anthropogenic runs produce large positive and negative correlations with the observations that might be interpreted as significant. In fact the aerosol and heat runs produce identical values with opposite signs due to the almost identical latitudinal and temporal distribution of their forcings, but opposite effects. The reason for the high correlations is that the observations have an upward linear trend, and the smooth rising or falling temperatures produced by the anthropogenic forcings produce high correlations. Because the magnitudes of the effects are small, and may cancel, it cannot be concluded that these high correlations show that man has produced climate change.

Anthropogenic effects, therefore, have had a small effect up to the present on climate change, but will be important in the near future. The total effect is not known due to our inadequate understanding of the effect of aerosols. The model shows a net anthropogenic warming effect in the SH, with no effect in the NH, but a slight change in the assumptions about the aerosols could produce large warming or cooling effects.

B. Internal causes

1. Design of the experiments

The model in the balanced state exactly reproduces the seasonal cycle of all the variables year after year and produces a constant annual average temperature. In order to simulate the natural variability observed in the atmosphere, random perturbations of the eddy flux of sensible heat are introduced in the model. The resulting temperature record is then compared to observations, to see whether the resulting variations are of a magnitude that could be interpreted as climate change.

Without perturbations, the eddy sensible heat flux can be expressed as

$$\overline{v'T'} = -K \frac{\partial T}{\partial y} \quad (73)$$

where

$$K = \overline{\overline{c' \left| \frac{\partial T}{\partial y} \right|}}$$

The double bar indicating a 1-2-1 smoothing. With perturbations, the flux is expressed as

$$\overline{v'T'} = -K \frac{\partial T}{\partial y} + R \quad (74)$$

where  $R' = \hat{B}_\ell \left( \frac{\partial T}{\partial y} \right)^2$

$\ell$  = latitude index

$$\hat{B}_\ell = \sqrt{70} (B_{\ell-2} + 4B_{\ell-1} + 6B_\ell + 4B_{\ell+1} + B_{\ell+2})$$

Each B is a random normally distributed number with mean 0 and standard deviation equal to a given percentage of C'. For these experiments 0.4 C' was chosen because it gave the largest magnitude for the standard deviation of the atmospheric eddy heat flux without numerical instability for a first-order Markov process. The procedure for calculating the random numbers is described in Appendix D. The 1-4-6-4-1 smoothing applied to  $\hat{B}$  simulates the observed latitudinal extent of baroclinic eddies. The  $\sqrt{70}$  factor keeps the expected value of the standard deviation of  $\hat{B}$  the same as that of B. Making the perturbations proportional to the temperature gradient squared makes them strongest in the mid-latitudes, and in the winter, both in agreement with the observations of Oort and VonderHaar (1976). For a zero-order Markov process,  $R = R'$ . For a first-order Markov process,  $R_N = \hat{\alpha} R_{N-1} + R'$ , where N refers to the time step. Since the model time step is about 15 days, and McGuirk and Reiter (1976) found flux oscillations with periods of about 24 days, they were simulated as a first-order Markov process. The constant  $\hat{\alpha}$  was chosen to be 0.5. Runs using a zero-order Markov process and the same set of random perturbations gave almost the same temperature perturbations, but with a smaller magnitude.

## 2. Results

Three 100-year runs were made as described in the previous section, with three different sets of random numbers, starting from balanced initial conditions. In these runs, the eddy perturbations were simulated as a first-order Markov process, with the standard deviation of  $B = 0.4 C'$  and  $\hat{\alpha} = 0.5$ . Each of these runs was then extended for another 100 years. These additional runs may be looked at as independent 100 year runs, or extensions of the initial runs. Three other runs were done, using the same set of random numbers as one of the first 100-year runs, to test the sensitivity to parameterizations. In one of these, the perturbations were treated as a zero-order Markov process. In another, the standard deviation of  $B$  was set equal to  $0.2 C'$ . In the final one, Sellers' IR scheme was used, to see the response of a system with a different sensitivity. These runs are summarized in Table 14, and the resulting world, NH and SH temperature records are shown in Figures 45-48.

For each run, the standard deviation of the annual average atmospheric energy flux was calculated for comparison to the data of VonderHaar and Oort (1973), shown in Table 5. They found an average standard deviation of 9.9 % for the portion of the globe that was covered by their data. They originally attributed all of this variation to observational error, but now think that most of it is due to actual atmospheric variability (Oort, personal communication). The computed standard deviations are shown in Table 14. The average standard deviation of the six similar runs is about 7.7 %. This is within the observation limit of Oort, but may be off by 2 or 3 %.

Table 14. Results of 100 year atmospheric eddy perturbation runs.

Run No.	1	2	3	4	5	6	7	8	9
N <sub>o</sub>	19	1088955923	3	-1184365053	11	-47704565	19	19	19
Note:		Starting from end of #1		Starting from end of #3		Starting from end of #5	Sellers' IR	Zero order Markov	SD of flux = 0.2 C'
<u>Standard deviation of:</u>									
Atmospheric energy flux (% of total)	7.35	7.73	8.08	8.28	6.86	7.99	7.37	3.73	3.53
WORLD T	0.152	0.260	0.228	0.207	0.171	0.191	0.137	0.074	0.074
WORLD T*	0.152	0.252	0.153	0.203	0.168	0.191	0.137	0.072	0.071
NH T	0.271	0.424	0.336	0.352	0.384	0.361	0.249	0.125	0.120
NH T*	0.261	0.423	0.273	0.350	0.379	0.361	0.235	0.124	0.119
SH T	0.200	0.292	0.264	0.245	0.186	0.179	0.174	0.100	0.108
SH T*	0.178	0.272	0.222	0.211	0.185	0.174	0.160	0.087	0.089
(°K)									

\* with linear trend removed

N<sub>o</sub> is initial number for random number generator.

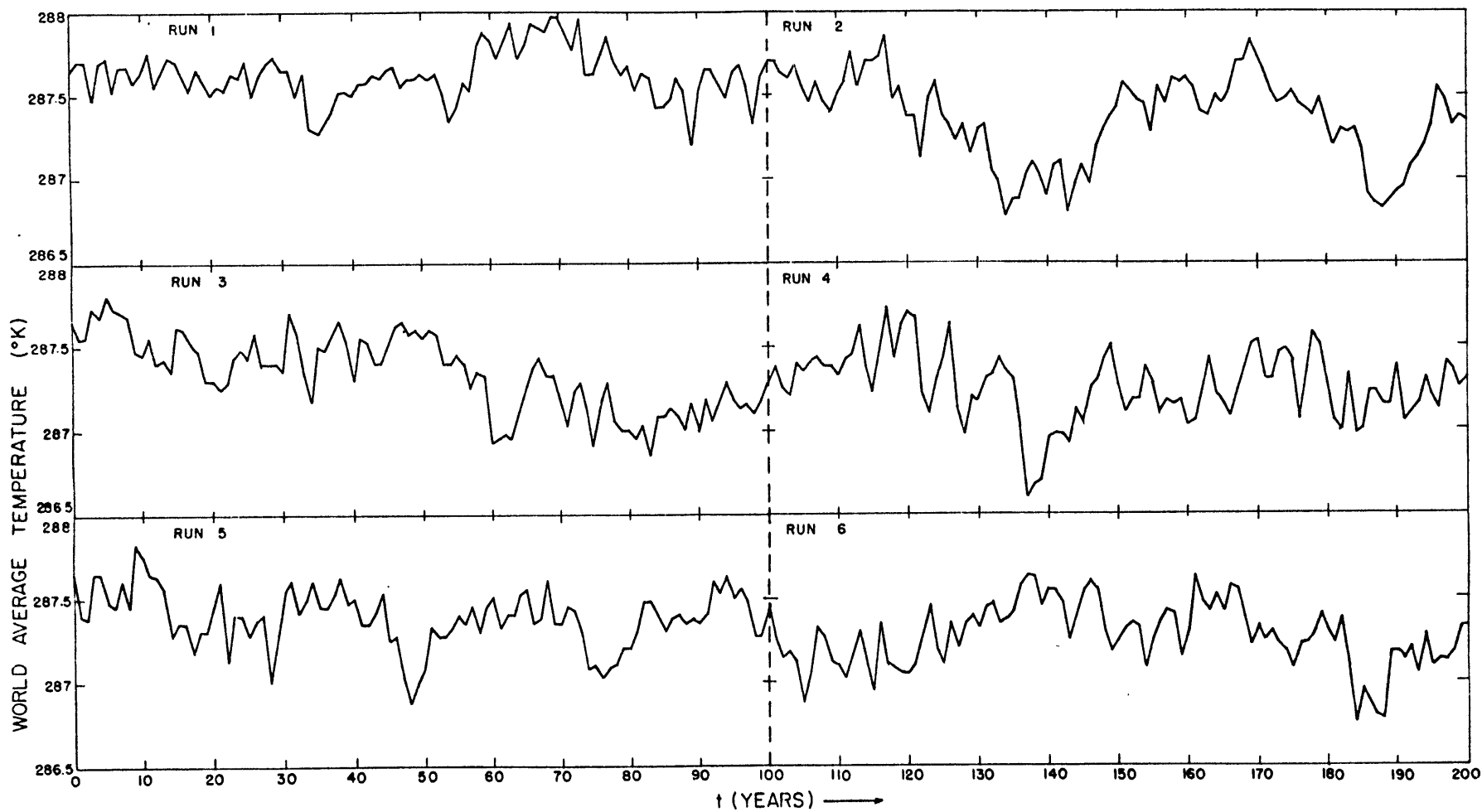


Figure 45. World average temperature from internal forcing runs (1-6).

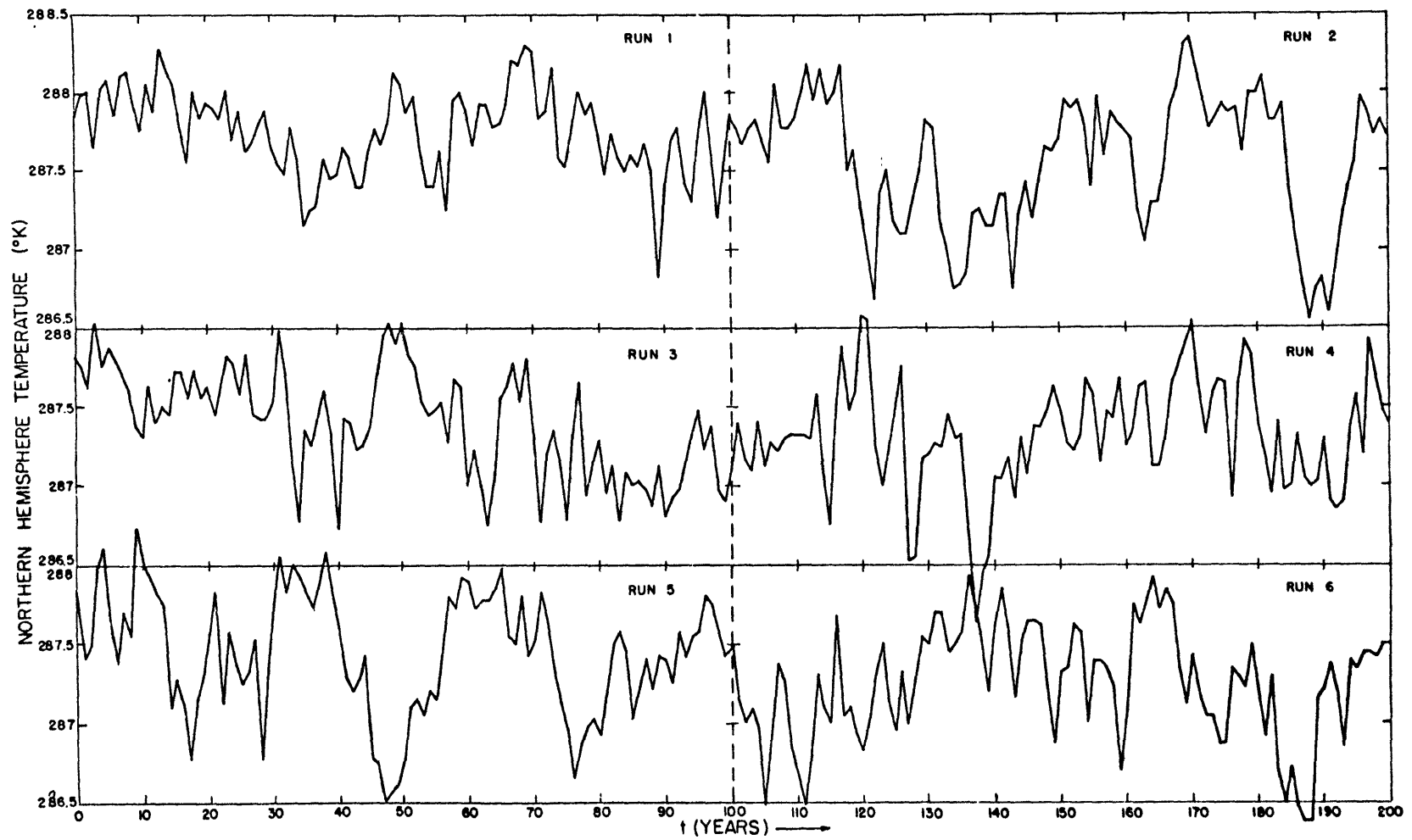


Figure 46. Northern Hemisphere temperature from internal forcing runs (1-6).

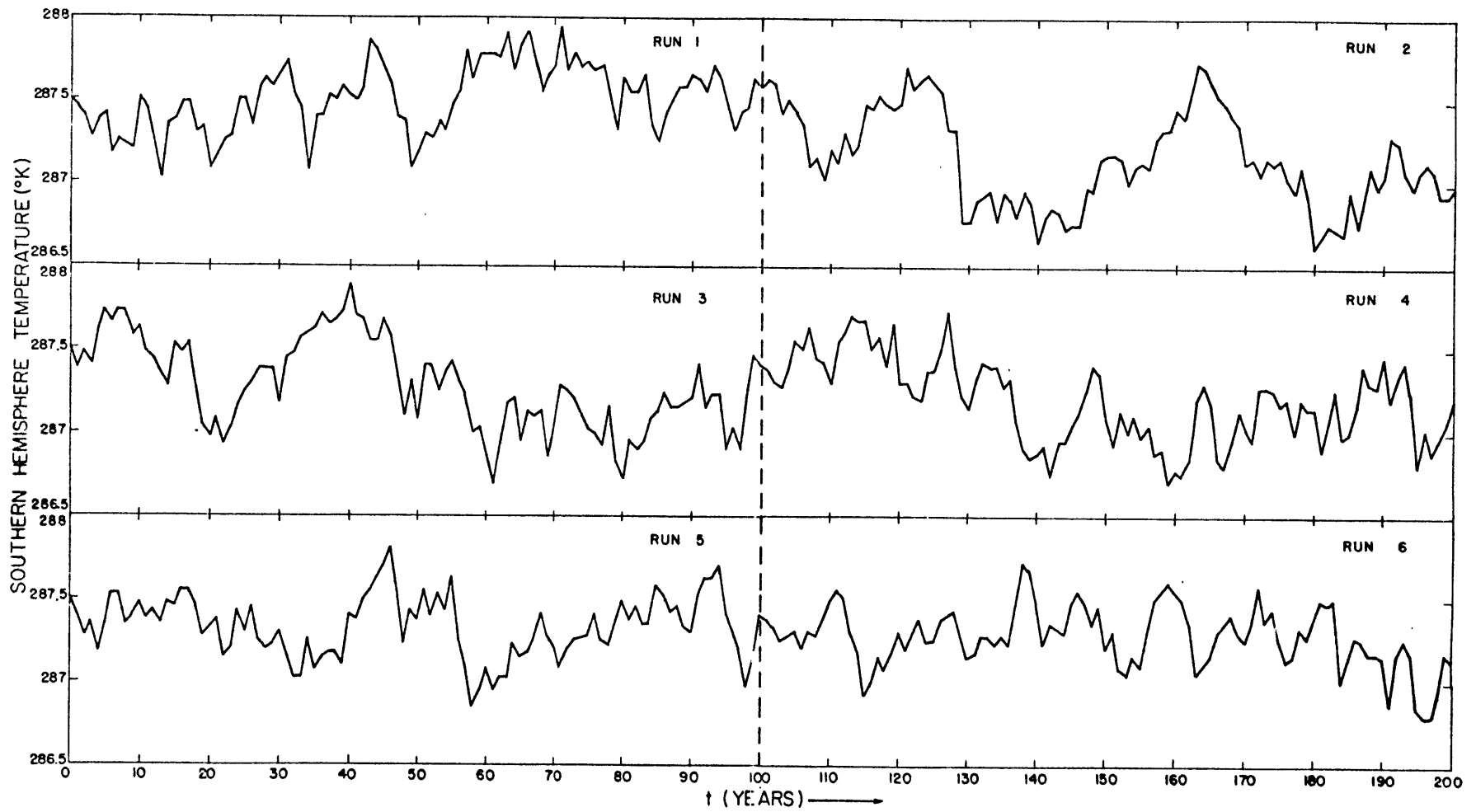


Figure 47. Southern Hemisphere temperature from internal forcing runs (1-6).



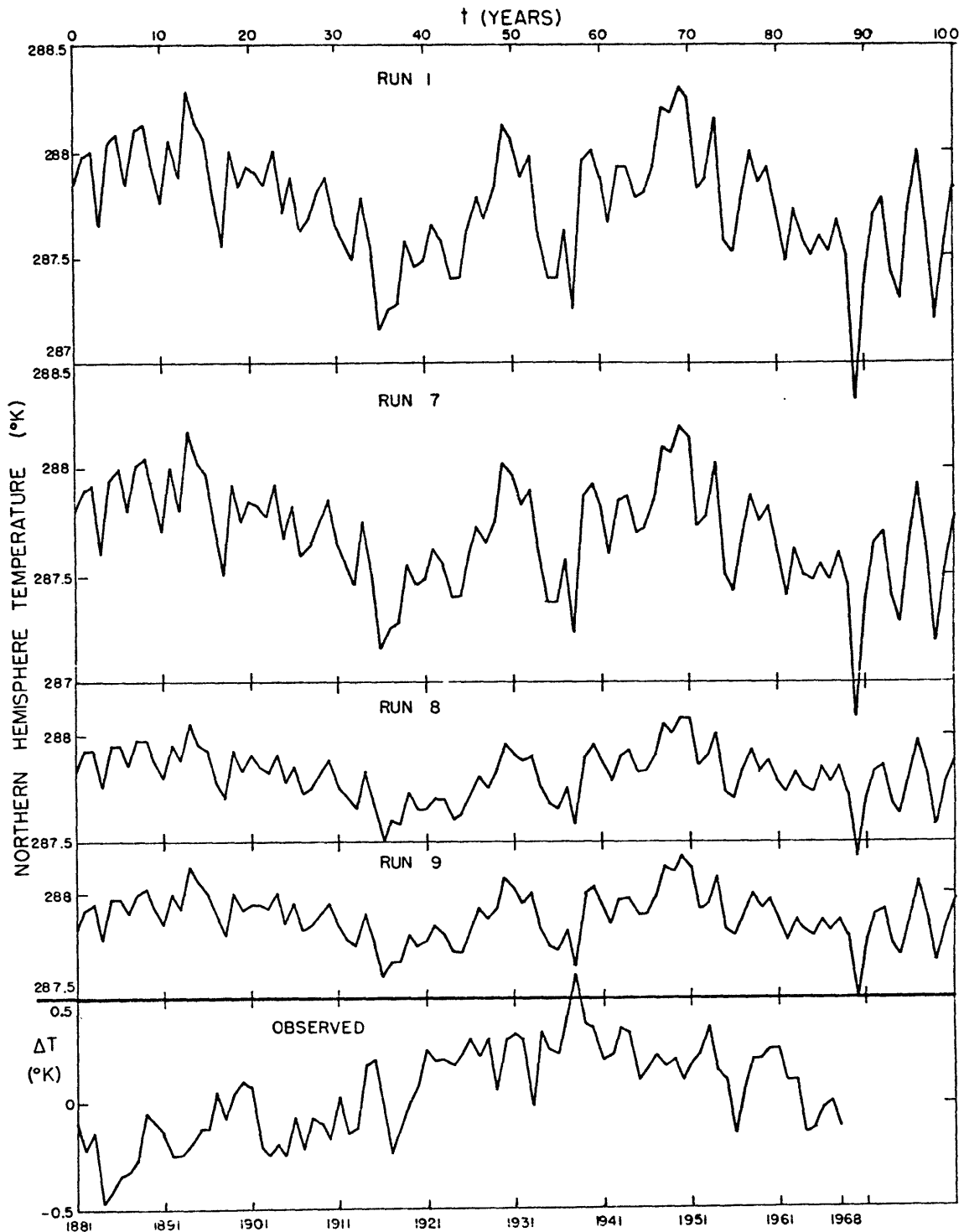


Figure 48. Northern Hemisphere temperature from internal forcing runs (1,7-9) compared to Budyko-Asakura data.

For each run, the standard deviations of the resulting annual average world, NH and SH temperature fields were also calculated and are shown in Table 14. Because some of the fields had a linear trend which added to the standard deviation, this linear trend was subtracted out, and the standard deviations were recalculated. They are also shown in Table 14. These results are compared to the standard deviation of the Budyko-Asakura NH temperature record, which is  $0.22^{\circ}\text{K}$  for the raw data, and  $0.18^{\circ}\text{K}$  with the linear trend removed.

The six similar runs produced NH standard deviations larger than observations, with a mean of about  $0.35^{\circ}\text{K}$ . The zero-order Markov run and the run with half the standard deviation of the forcing both produced standard deviations of the atmospheric energy flux and the temperature that were about half those of the standard run. The run using Sellers' IR scheme had virtually the same flux deviation, but the standard deviation of the temperature was about 10 % lower.

These results are not incompatible with the conclusion that the variability of the annual mean temperature can be explained by the forcing due to random unstable atmospheric eddies. If the strength of the forcing were lowered to a standard deviation of the flux of about 4.4 %, then this model would give NH temperature standard deviations equal to the observations. This value of the flux deviation is within the observations of Oort, although maybe too low. Changes in the model might, however, lower the sensitivity and allow a higher flux deviation to produce the same temperature deviation. As shown in Chapter III, the model itself may be too sensitive. The run with Sellers' IR shows that if the model were less sensitive, the same flux deviation would produce

a lower temperature deviation.

The temperature graphs from these runs show that not only is "noise" about a mean produced by the random eddy perturbations but also large excursions of the temperature. Even if the temperature response is scaled down so that the standard deviations are the same as the observations, NH temperature excursions of  $0.5^{\circ}\text{K}$  occur in one year. The temperature may remain relatively constant for up to ten years and then shift to a value  $0.5^{\circ}\text{K}$  different and stay at that value for several years. Rapid shifts year after year also occur. Long-term trends are also produced. In fact, with no external forcing, internal variations of the observed magnitude produce NH temperature fluctuations as large as those observed for the past 100 years!

### C. Geographical sensitivity

Certain regions of the globe are more sensitive to climate change than others, both in observations and in the model results. This is due mainly to thermal inertia differences for different surface composition, namely that the oceans have a much larger thermal inertia than land or ice. Snow has virtually the same thermal inertia as land or ice and so the snow-albedo feedback does not affect the sensitivity through thermal inertia. However, the radiative effects of this feedback act to make regions where it is occurring more sensitive than other regions. To summarize, land and ice regions are more sensitive than ocean due to their lower thermal inertia. The additional effects of snow-albedo feedback make regions with a large portion of land even more sensitive. This feedback has a much smaller effect on ice because of the smaller

albedo difference between ice and snow.

The above mechanisms work to make the NH more sensitive than the SH, and this was found to be the case in all the simulation experiments, both external and internal. These mechanisms also work to make the polar regions more sensitive than the tropics. Table 15 shows the latitudinal distribution of the temperature response from lowering the solar constant by 1 %, after 500 years. The response is typical of all the other experiments, and shows the polar regions approximately twice as sensitive as the tropics. This response can also be seen in Mitchell's data, Figure 5.

Table 15. Latitudinal distribution of temperature response to lowering SC by 1%, after 500 years.

Latitude band	$\overline{\Delta T_o}$ (°K)
80° - 90°N	-6.72
70° - 80°N	-6.87
60° - 70°N	-6.99
50° - 60°N	-6.56
40° - 50°N	-5.36
30° - 40°N	-4.49
20° - 30°N	-4.02
10° - 20°N	-3.82
0° - 10°N	-3.77
0° - 10°S	-3.77
10° - 20°S	-3.75
20° - 30°S	-3.86
30° - 40°S	-4.24
40° - 50°S	-4.84
50° - 60°S	-5.80
60° - 70°S	-6.12
70° - 80°S	-6.05
80° - 90°S	-5.80

## Chapter V. Conclusions

The following conclusions, some of which have been proposed before, are supported as a result of the work in this thesis:

The climate system is very complex, involving interactions on many different time and space scales. It is a multi-disciplinary subject, requiring the study and understanding of:

- thermodynamics, including water in all its three phases and transformations between the phases
- radiation, including solar and terrestrial, and all the atmospheric interactions with both types at all levels due to gases, aerosols and clouds
- dynamics of the atmosphere, including the stratosphere and the general circulation and its variability
- dynamics of the ocean, including variation of the depth of the mixed layer, eddy fluxes, deep currents and salinity effects
- predictability and statistics
- ice dynamics, including glaciology
- aerosol chemistry
- solar physics
- volcanology
- orbital mechanics
- continental drift

There are many sources of error in the observational record of the past 100 years. The magnitude of the errors is unknown.

The model used in this thesis does a good job of simulating the seasonal cycle, with a few exceptions. After a few of the parameterizations are improved, this type of highly parameterized simple climate model will be of great use in studying the climate. In particular, the ice and snow model, zenith angle albedo effects and the ocean flux should be improved before more studies are done.

An accurate record of sunspots exists back to 1750 and can be extended fairly accurately back to 1610. The magnitude and time variation of the solar flux, and its relationship to sunspots, are unknown. Ozone may provide a mechanism through which the ultraviolet radiation, which is related to the sunspot cycle, may influence the total radiation reaching the surface. The magnitude of this effect is unknown. Model experiments do not support this theory, however.

Volcanic dust is probably an important cause of climate change, blocking solar radiation and causing cooling. Effects are limited in latitudinal and temporal extent. Unfortunately an adequate chronology of latitudinal extent of stratospheric dust loading does not exist, but it may be possible to construct one for the past 100 years. Model results show that a large part of the past observed variations are explained by this theory.

Anthropogenic carbon dioxide heats the atmosphere, but the magnitude of the effect is not well known. Model results show that the effect is small now, but may become larger in the near future.

Anthropogenic heat has a much smaller effect than carbon dioxide, according to the model. If there is a rapid shift to nuclear power, this relationship will change.

The effect of anthropogenic aerosols is not clear due to inadequate understanding of their physical and chemical interactions with the rest of the system. Further study of their chemical composition and distribution, and then their radiative properties, will, in conjunction with detailed radiation models, allow their effect to be much better understood soon. Model results, which must be considered speculative, show a cooling effect of amplitude equivalent to carbon dioxide heating. Anti-pollution measures will lessen this effect in the future.

The natural variability of the atmosphere, through short-term variations in the dynamical fluxes, and possibly also in the radiative transmittance of the atmosphere, produces long-term variations in the climate which cannot be predicted. The magnitudes of both the short-term variability, and the long-term effects are not well known, but model results show that the climate change produced may be larger than all but the volcanic dust effect on 100-year time scales, and that, in combination with volcanic dust, may explain the climate change of the past 100 years.

Globally forced climate change is amplified at the poles, especially in the Northern Hemisphere. The Northern Hemisphere is more sensitive than the Southern, and land areas are more sensitive than oceans.



Appendix A. Derivation of geopotential height equation (21)

Assume a hydrostatic atmosphere:

$$\frac{\partial p}{\partial z} = -\rho g$$

Introduce the gas law:

$$\frac{\partial p}{\partial z} = -\frac{\rho g}{R_d T}$$

Assume horizontal uniformity:

$$dz = -\frac{R_d}{g} \frac{\bar{T}}{p} dp$$

Introduce equation (13) and integrate from the surface to a given geopotential height  $\bar{h}$  at pressure  $p$ :

$$\int_0^{\bar{h}} dz = -\frac{R_d}{g} \int_{p_0}^p \left( \bar{T}_0 - p_0 \frac{\partial \bar{T}}{\partial p} \right) \frac{1}{p} + \frac{\partial \bar{T}}{\partial p} dp$$

$$\bar{h} = \frac{R_d}{g} \left[ \left( \bar{T}_0 - p_0 \frac{\partial \bar{T}}{\partial p} \right) \ln \frac{p_0}{p} + \frac{\partial \bar{T}}{\partial p} (p_0 - p) \right]$$

which is equation (21).

Appendix B. Derivations of a coefficients, equations (24)-(34)

For  $a_G$ , start with equation (3):

$$G_s = \frac{1}{g} \int_0^{P_0} \frac{\partial \bar{s}}{\partial x} dp = \frac{1}{g} a_{Gs} \frac{\partial \bar{s}_0}{\partial x} P_0$$

Let  $\bar{s} = \overline{c_p T}$ , and introduce (13):

$$\int_0^{P_0} \frac{\partial}{\partial x} \bar{T} dp = \int_0^{P_0} \frac{\partial}{\partial x} \left( \bar{T}_0 - (P_0 - p) \frac{\partial \bar{T}}{\partial p} \right) dp$$

$$\left( \frac{\partial}{\partial x} P_0 \frac{\partial \bar{T}}{\partial p} = 0 \right)$$

$$= P_0 \frac{\partial \bar{T}_0}{\partial x} \Rightarrow a_{GH} = 1 \quad (24)$$

Let  $\bar{s} = \overline{gh}$ , and introduce (21):

$$\int_0^{P_0} \frac{\partial}{\partial x} \bar{h} dp = \int_0^{P_0} \frac{\partial}{\partial x} \left( \frac{R_d}{g} \left[ \left( \bar{T}_0 - P_0 \frac{\partial \bar{T}}{\partial p} \right) \ln \frac{P_0}{p} + \frac{\partial \bar{T}}{\partial x} (P_0 - p) \right] \right) dp$$

$$\left( \frac{\partial}{\partial x} P_0 \frac{\partial \bar{T}}{\partial p} = 0, \quad \bar{h}_0 = R_d \bar{T}_0 / g \right)$$

$$= \frac{R_d}{g} \frac{\partial \bar{T}_0}{\partial x} P_0 \Rightarrow a_{GP} = 1 \quad (25)$$

Let  $\bar{s} = \overline{Lq}$ , and introduce (16):

$$\int_0^{p_0} \frac{\partial}{\partial x} \bar{q} \, dp = \frac{\partial}{\partial x} \bar{q}_0 \int_0^{p_0} \left(\frac{p}{p_0}\right)^{a_1} dp$$

$$= \frac{1}{a_1 + 1} \frac{\partial \bar{q}_0}{\partial x} p_0 \Rightarrow a_{GV} = \frac{1}{a_1 + 1} \quad (26)$$

For  $a_x$ , start with equation (4):

$$\Delta_x S = \frac{1}{g} \int_0^{p_0} \bar{\mu} \frac{\partial \bar{s}}{\partial x} \, dp = \frac{1}{g} a_{xs} \bar{\mu}_0 \frac{\partial \bar{s}_0}{\partial x} p_0 A_L'$$

Let  $\bar{s} = \bar{Lq}$ , and introduce (14) and (16):

$$\int_0^{p_0} \bar{\mu} \frac{\partial \bar{q}}{\partial x} \, dp = \int_0^{p_0} \left( \bar{\mu}_0 + (p - p_0) \frac{\partial \bar{\mu}}{\partial p} \right) \frac{\partial}{\partial x} \left( \bar{q}_0 \left(\frac{p}{p_0}\right)^{a_1} \right) dp$$

$$= \left( \bar{\mu}_0 - p_0 \frac{\partial \bar{\mu}}{\partial p} \right) \frac{\partial}{\partial x} \left( \frac{\bar{q}_0}{p_0^{a_1}} \int_0^{p_0} p^{a_1} \, dp \right)$$

$$+ \frac{\partial \bar{\mu}}{\partial p} \frac{\partial}{\partial x} \left( \frac{\bar{q}_0}{p_0^{a_1}} \int_0^{p_0} p^{a_1 + 1} \, dp \right)$$

$$= \left( \bar{\mu}_0 - p_0 \frac{\partial \bar{\mu}}{\partial p} \right) \frac{\partial}{\partial x} \left( \frac{\bar{q}_0 p_0}{1 + a_1} \right) + \frac{\partial \bar{\mu}}{\partial p} \frac{\partial}{\partial x} \left( \frac{\bar{q}_0 p_0^2}{2 + a_1} \right)$$

$$= \frac{1}{1 + a_1} \left( 1 - \frac{1}{2 + a_1} \frac{p_0}{\bar{\mu}_0} \frac{\partial \bar{\mu}}{\partial p} \right) \bar{\mu}_0 \frac{\partial \bar{q}_0}{\partial x} p_0$$

$$\Rightarrow a_{xv} = \frac{1}{1 + a_1} \left( 1 - \frac{1}{2 + a_1} \frac{p_0}{\bar{\mu}_0} \frac{\partial \bar{\mu}}{\partial p} \right) \quad (27)$$

Let  $\bar{s} = \frac{c}{p} T$ , and introduce (14), (22) and (23):

$$\begin{aligned}
 \int_0^{p_0} \bar{\mu} \frac{\partial \bar{T}}{\partial x} dp &= \int_{p_0/2}^{p_0} (\bar{\mu}_0 + (p-p_0) \frac{\partial \bar{\mu}}{\partial p}) \left( \frac{1}{p_0} (2p-p_0) \frac{\partial \bar{T}_0}{\partial x} \right) dp \\
 &= \frac{\partial \bar{T}_0}{\partial x} \int_{p_0/2}^{p_0} (\bar{\mu}_0 - p \frac{\partial \bar{\mu}}{\partial p}) \left( \frac{2p}{p_0} - 1 \right) + \frac{\partial \bar{\mu}}{\partial p} \left( \frac{2p^2}{p_0} - p \right) dp \\
 &= \frac{\partial \bar{T}_0}{\partial x} \left[ (\bar{\mu}_0 - p \frac{\partial \bar{\mu}}{\partial p}) \frac{p_0}{4} + \frac{\partial \bar{\mu}}{\partial p} \frac{5p^2}{24} \right] \\
 &= \frac{1}{4} \left( 1 - \frac{1}{6} \frac{p_0}{\bar{\mu}_0} \frac{\partial \bar{\mu}}{\partial p} \right) \bar{\mu}_0 \frac{\partial \bar{T}_0}{\partial x} p_0 \\
 \Rightarrow a_{xH} &= \frac{1}{4} \left( 1 - \frac{1}{6} \frac{p_0}{\bar{\mu}_0} \frac{\partial \bar{\mu}}{\partial p} \right) \quad (28)
 \end{aligned}$$

Let  $\bar{s} = \bar{gh}$ , and introduce (14) and (21):

$$\begin{aligned}
 \int_0^{p_0} \bar{\mu} \frac{\partial \bar{h}}{\partial x} dp &= \int_0^{p_0} (\bar{\mu}_0 + (p-p_0) \frac{\partial \bar{\mu}}{\partial p}) \frac{\partial}{\partial x} \frac{R_d}{g} \\
 &\quad \left[ (\bar{T}_0 - p_0 \frac{\partial \bar{T}}{\partial p}) \ln \frac{p_0}{p} + \frac{\partial \bar{T}}{\partial p} (p_0 - p) \right] dp
 \end{aligned}$$

(from (22) and (23):

$$\begin{aligned}
 \frac{\partial}{\partial x} \frac{\partial \bar{T}}{\partial p} &= \frac{\partial}{\partial p} \frac{\partial \bar{T}}{\partial x} = \frac{2}{p_0} \frac{\partial \bar{T}_0}{\partial x} & p \geq p_0/2 \\
 &= 0 & p < p_0/2
 \end{aligned}$$

$$\begin{aligned}
 &= \frac{R_d}{g} \int_{p_{1/2}}^{p_0} \left( \bar{\mu}_0 + (p-p_0) \frac{\partial \bar{\mu}}{\partial p} \right) \frac{\partial \bar{T}_0}{\partial x} \left( -\ln \frac{p}{p_0} + 2 \left( 1 - \frac{p}{p_0} \right) \right) dp \\
 &= \frac{R_d}{g} \int_{p_{1/2}}^{p_0} \left( \bar{\mu}_0 - p_0 \frac{\partial \bar{\mu}}{\partial p} \right) \left( 2 - \frac{2p}{p_0} - \ln \frac{p}{p_0} \right) + \frac{\partial \bar{\mu}}{\partial p} \left( 2p - \frac{2p^2}{p_0} - p \ln \frac{p}{p_0} \right) dp \\
 &= \frac{R_d}{g} \frac{\partial \bar{T}_0}{\partial x} \left[ \left( \bar{\mu}_0 - p_0 \frac{\partial \bar{\mu}}{\partial p} \right) \left( \frac{1}{4} - \frac{1}{2} \ln \frac{1}{2} - \frac{1}{2} \right) + p_0 \frac{\partial \bar{\mu}}{\partial p} \left( \frac{1}{6} - \frac{1}{8} \ln \frac{1}{2} - \frac{3}{16} \right) \right] \\
 &= 0.0966 \left( 1 - 0.319 \frac{p_0}{\bar{\mu}_0} \frac{\partial \bar{\mu}}{\partial p} \right) \frac{R_d}{g} \bar{\mu}_0 \frac{\partial \bar{T}_0}{\partial x} p_0 \\
 \Rightarrow \quad a_{xp} &= 0.0966 \left( 1 - 0.319 \frac{p_0}{\bar{\mu}_0} \frac{\partial \bar{\mu}}{\partial p} \right) \quad (29)
 \end{aligned}$$

For  $a_m$ , start with equation (6):

$$M_s = \frac{1}{g} \int_0^{p_0} \bar{v} \bar{s} dp = \frac{1}{g} a_{ms} \bar{v}_0 \bar{s}_0 p_0$$

Let  $\bar{s} = \frac{c_p \bar{T}}{p}$ , and introduce (13) and (15):

$$\begin{aligned}
 \int_0^{p_0} \bar{v} \bar{T} dp &= \int_0^{p_0} \bar{v}_0 \left( \frac{2p-p_0}{p_0} \right) \left( \bar{T}_0 - (p_0-p) \frac{\partial \bar{T}}{\partial p} \right) dp \\
 &= \bar{v}_0 \left[ \bar{T}_0 \int_0^{p_0} \left( 2 \frac{p}{p_0} - 1 \right) dp + \frac{\partial \bar{T}}{\partial p} \int_0^{p_0} \left( -2p + 2 \frac{p^2}{p_0} + p_0 - p \right) dp \right] \\
 &= \frac{1}{6} \frac{p_0}{\bar{T}_0} \frac{\partial \bar{T}}{\partial p} \bar{v}_0 \bar{T}_0 p_0 \quad \Rightarrow \quad a_{mH} = \frac{1}{6} \frac{p_0}{\bar{T}_0} \frac{\partial \bar{T}}{\partial p} \quad (30)
 \end{aligned}$$

Let  $\bar{s} = \bar{L}q$ , and introduce (15) and (16):

$$\begin{aligned} \int_0^{P_0} \bar{v} \bar{q} \, dP &= \int_0^{P_0} \bar{v}_0 \left( \frac{2P - P_0}{P_0} \right) \bar{q}_0 \left( \frac{P}{P_0} \right)^{a_1} \, dP \\ &= \bar{v}_0 \bar{q}_0 \int_0^{P_0} \frac{(2P - P_0) P^{a_1}}{P_0^{a_1+1}} \, dP \\ &= \frac{a_1}{(1+a_1)(2+a_1)} \bar{v}_0 \bar{q}_0 P_0 \Rightarrow a_{mV} = \frac{a_1}{(1+a_1)(2+a_1)} \quad (31) \end{aligned}$$

Let  $\bar{s} = \bar{g}h$ , and introduce (15) and (21):

$$\begin{aligned} \int_0^{P_0} \bar{v} \bar{h} \, dP &= \int_0^{P_0} \bar{v}_0 \left( \frac{2P - P_0}{P_0} \right) \frac{R_d}{g} \left[ \left( \bar{T}_0 - P_0 \frac{\partial \bar{T}}{\partial P} \right) \ln \frac{P_0}{P} + \frac{\partial \bar{T}}{\partial P} (P_0 - P) \right] \, dP \\ &= \frac{R_d}{g} \bar{v}_0 \left[ \left( \bar{T}_0 - P_0 \frac{\partial \bar{T}}{\partial P} \right) \int_0^{P_0} \left( \frac{2P - P_0}{P_0} \right) \ln \frac{P_0}{P} \, dP + \frac{\partial \bar{T}}{\partial P} \int_0^{P_0} \left( \frac{2P - P_0}{P_0} \right) (P_0 - P) \, dP \right] \\ &= \frac{R_d}{g} \bar{v}_0 \left[ \left( \bar{T}_0 - P_0 \frac{\partial \bar{T}}{\partial P} \right) \left( -\frac{P_0}{2} \right) + \frac{\partial \bar{T}}{\partial P} \left( -\frac{P_0^2}{6} \right) \right] \\ &= \left( -\frac{1}{2} + \frac{1}{3} \frac{P_0}{\bar{T}_0} \frac{\partial \bar{T}}{\partial P} \right) \bar{v}_0 \frac{R_d \bar{T}_0}{g} P_0 \Rightarrow a_{mH} = 2 a_{mV} - 0.5 \quad (32) \end{aligned}$$

For  $a_E$ , start with equation (7):

$$E_s = -\frac{1}{g} \int_0^{P_0} K_s \frac{\partial \bar{s}}{\partial y} \, dP = -\frac{1}{g} a_{Es} K_s \frac{\partial \bar{s}}{\partial y} P_0$$

Let  $\bar{s} = \frac{c_p T}{p}$ , and introduce (13):

$$\int_0^{p_0} \frac{\partial \bar{T}}{\partial y} dp = \int_0^{p_0} \frac{\partial}{\partial y} \left( \bar{T}_0 - (p_0 - p) \frac{\partial \bar{T}}{\partial p} \right) dp$$

$$\left( \frac{\partial}{\partial y} \left( \frac{\partial \bar{T}}{\partial p} \right) = 0 \right)$$

$$= \frac{\partial \bar{T}_0}{\partial y} p_0 \quad \Rightarrow \quad a_{EH} = 1.0 \quad (33)$$

Let  $\bar{s} = \bar{L}q$ , and introduce (16):

$$\int_0^{p_0} \frac{\partial \bar{q}}{\partial y} dp = \int_0^{p_0} \frac{\partial}{\partial y} \left( \bar{q}_0 \left( \frac{p}{p_0} \right)^{a_1} \right) dp$$

$$= \frac{1}{1+a_1} \frac{\partial \bar{q}_0}{\partial y} p_0 \quad \Rightarrow \quad a_{EV} = \frac{1}{1+a_1} \quad (34)$$

Appendix C. IR model

This appendix describes how the fourth powers of the layer temperatures,  $\bar{T}_{A1}$  and  $\bar{T}_{A2}$ , are calculated. They are calculated separately for no cloud and cloudy conditions and used in equations (59) and (60) to determine the IR flux from each grid area.

The known quantities are the surface temperature,  $\bar{T}_s$ , surface emissivity,  $\epsilon_0$ , layer emissivities,  $\epsilon_1$  and  $\epsilon_2$ , and a specified cooling rate,  $H$ . The model consists of two layers, 1 and 2, as shown in Figures 49 and 50 for no cloud and cloudy conditions. The appropriate heat flux equation for each layer is

$$\frac{\partial T}{\partial t} = - \frac{1}{\rho c_p} \frac{\partial F}{\partial z} \quad (C1)$$

Make the hydrostatic assumption:

$$\frac{\partial p}{\partial z} = - \rho g$$

so that (C1) becomes

$$\frac{\partial T}{\partial t} = \frac{g}{c_p} \frac{\partial F}{\partial p}$$

This can be written in finite difference form



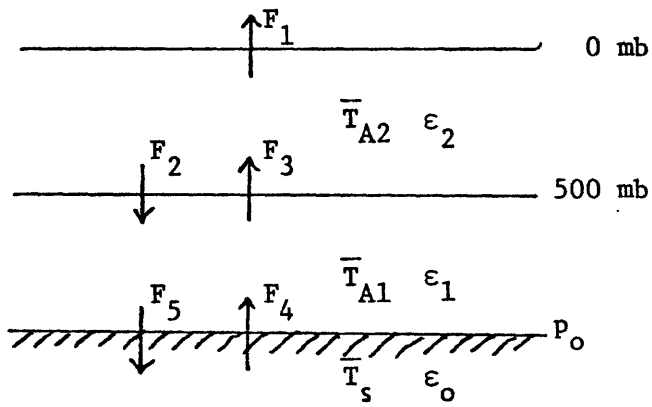


Figure 49. IR model with no clouds.

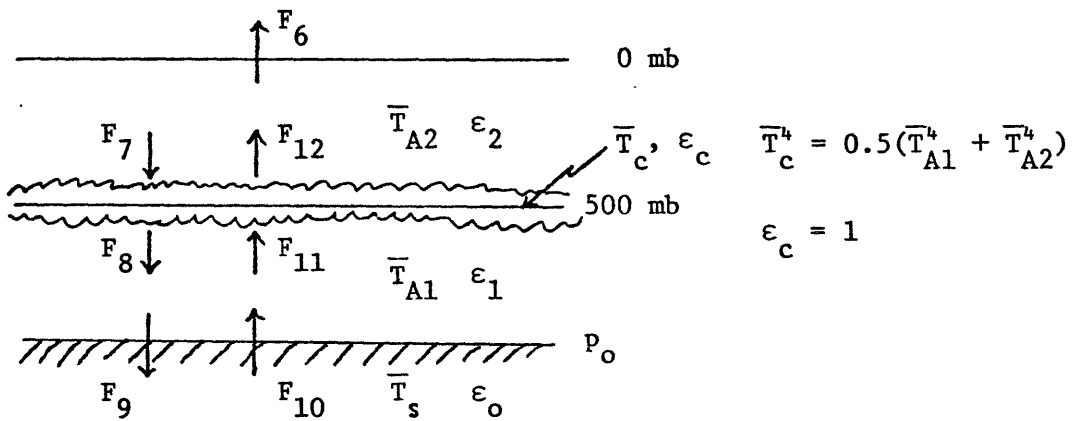


Figure 50. IR model with clouds.

$$\frac{\partial T}{\partial t} = \frac{g}{c_p} \frac{F_{\text{BOT}} - F_{\text{TOP}}}{p_{\text{BOT}} - p_{\text{TOP}}}$$

Given is:  $\frac{\partial T}{\partial t}_i = \epsilon_i H_i = I_i$ , so that

$$I_i = \frac{g}{c_p} \frac{F_{\text{BOT}} - F_{\text{TOP}}}{p_{\text{BOT}} - p_{\text{TOP}}} \quad (\text{C2})$$

for each layer  $i$ .

1. No cloud (NC) case

The vertical fluxes for the no cloud case are shown in Figure 49.

They are introduced into (C2) for each layer, so that

$$I_2 = \frac{g}{c_p} \frac{F_3 - F_2 - F_1}{500 \text{ mb}} \quad (\text{C3})$$

$$I_1 = \frac{g}{c_p} \frac{F_4 - F_5 - F_3 + F_2}{p_0 - 500 \text{ mb}} \quad (\text{C4})$$

where

$$F_2 = \sigma \epsilon_2 \overline{T_{A2}}^4$$

$$F_5 = \sigma \epsilon_1 \overline{T_{A1}}^4 + (1 - \epsilon_1) F_2$$

$$F_4 = \sigma \epsilon_0 \overline{T}_S^4 + (1 - \epsilon_0) F_5$$

$$F_3 = \sigma \epsilon_1 \overline{T}_{A1}^4 + (1 - \epsilon_1) F_4$$

$$F_1 = \sigma \epsilon_2 \overline{T}_{A2}^4 + (1 - \epsilon_2) F_3$$

(C3) and (C4) are then 2 equations with 2 unknowns and are solved simultaneously for  $\overline{T}_{A1NC}^4$  and  $\overline{T}_{A2NC}^4$ .

## 2. Cloudy (C) case

The vertical fluxes for the cloudy case are shown in Figure 50.

They are introduced into (C2) for each layer, so that:

$$I_2 = \frac{g}{c_p} \frac{F_{12} - F_7 - F_6}{500 \text{ mb}} \quad (C5)$$

$$I_1 = \frac{g}{c_p} \frac{F_{10} - F_9 - F_{11} + F_8}{p_0 - 500 \text{ mb}} \quad (C6)$$

where

$$F_8 = F_{12} = \sigma \cdot 0.5 (\overline{T}_{A1}^4 + \overline{T}_{A2}^4)$$

$$F_9 = \sigma \epsilon_1 \overline{T}_{A1}^4 + (1 - \epsilon_1) F_8$$

$$F_{10} = \sigma \epsilon_0 \overline{T}_S^4 + (1 - \epsilon_0) F_9$$

$$F_{11} = \sigma \epsilon_1 \overline{T}_{A1}^4 + (1 - \epsilon_1) F_{10}$$

$$F_7 = \sigma \epsilon_2 \overline{T}_{A2}^4$$

$$F_6 = \sigma \epsilon_2 \overline{T}_{A2}^4 + (1 - \epsilon_2) F_{12}$$

(C5) and (C6) are then 2 equations with 2 unknowns and are solved simultaneously for  $\overline{T}_{A1C}^4$  and  $\overline{T}_{A2C}^4$ .

Appendix D. Random number generator

Pseudo-random numbers with a normal distribution, mean 0 and standard deviation 1 are generated by the following simple procedure. An initial integer  $N_0$  is chosen. All the following random integers are determined by  $N_i = 125 N_{i-1}$ . Since the IBM computer has 32 bit words, and overflow does not produce an error, this procedure generates numbers with a uniform distribution from  $-2^{31}$  to  $+2^{31}$ . They are then divided by  $2^{31}$  to give  $N'_i$ , with a uniform distribution from -1 to 1, and a standard deviation of  $\sqrt{1/3}$ . A random number with approximately a normal distribution with mean 0 and standard deviation 1,  $N''$ , is then formed by

$$N'' = \frac{1}{2} \sum_{i=1}^{12} N'_i$$

so that

$$N'' = \frac{1}{2^{32}} \sum_{i=1}^{12} N_i$$

Each time this is repeated,  $N_0$  is chosen as  $N_{12}$  from the previous calculation.

$N''$  is multiplied by the chosen standard deviation of the parameter to which it is to be added to make it the appropriate magnitude.

REFERENCES

- Abbott, C. G., 1963: Solar variation and weather. Smithsonian Misc. Coll., 146, No. 3, 67 pp.
- Abbott, C. G., 1966: An account of the Astrophysical Observatory of the Smithsonian Institution, 1904-1953. Smithsonian Misc. Coll., 148, No. 7, 16 pp.
- Alexander, Richard C. and Robert L. Mobley, 1976: Monthly average sea-surface temperatures and ice-pack limits on a 1° global grid. Mon. Wea. Rev., 104, 143-148.
- Angell, J. K. and J. Korshover, 1975: Estimate of the global change in tropospheric temperature between 1958 and 1973. Mon. Wea. Rev., 103, 1007-1012.
- Angell, J. K. and J. Korshover, 1977: Estimate of the global change in temperature, surface-100 mb, between 1958 and 1975. To be published.
- Angione, Ronald J., Edward J. Medeiros and Robert G. Roosen, 1976: Stratospheric ozone as seen from the Chappuis band. Nature, 261, 289-290.
- Barrett, Earl W., 1971: Depletion of short-wave irradiance at the ground by particles suspended in the atmosphere. Solar Energy, 13, 323-337.
- Begelman, Mitchell C. and Martin J. Rees, 1976: Can cosmic clouds cause climatic catastrophes? Nature, 261, 298-299.
- Berger, Andre L., 1971: Investigation of anomalies of minimum and maximum temperature for winter and summer at Omaha, Nebraska, S.M. thesis, Mass. Inst. Tech., 105 pp.
- Borzenkova, I. I., K. Ya. Vinnikov, L. D. Spirina and D. I. Stekhnovskiy, 1976: Change in air temperature in the Northern Hemisphere during the period 1881-1975. Meteorology and Hydrology, No. 7, 34-45. (27-35 in Russian)
- Bray, J. R., 1974: Volcanism and glaciation during the past 40 millenia. Nature, 252, 679-680.
- Bray, J. R., 1976: Volcanic triggering of glaciation. Nature, 260, 414-415.
- Broecker, Wallace S., 1975: Climatic change: are we on the brink of a pronounced global warming? Science, 188, 460-463.

- Bryson, Reid A. and Gerald J. Dittberner, 1976: A non-equilibrium model of hemispheric mean surface temperature. J. Atm. Sci., 33, 2094-2106.
- Bryson, Reid A. and Wayne M. Wendland, 1970: Climatic effects of atmospheric pollution. Global Effects of Environmental Pollution, S. Fred Singer, ed., 130-138.
- Budyko, M. I., 1969: The effect of solar radiation variations on the climate of the earth. Tellus, 21, 611-619.
- Budyko, M. I. and I. L. Karol, 1975: Man's impact on the global climate. Proc. WMO/IAMAP Symposium on Long-Term Climatic Fluctuations, Norwich, 465-471.
- Budyko, M. I. and K. Ya. Vinnikov, 1976: Global warming. Meteorology and Hydrology, No. 7, 19-33. (16-26 in Russian)
- Cadle, R. D. and G. W. Grams, 1975: Stratospheric aerosol particles and their optical properties. Rev. Geophysics and Space Physics, 13, 475-501.
- Cadle, R. D., C. S. Kiang, and J.-F. Louis, 1976: The global scale dispersion of the eruption clouds from major volcanic eruptions. J. Geophysical Res., 81, 3125-3132.
- Calder, Nigel, 1974: Arithmetic of the ice ages. Nature, 252, 216-218.
- Cess, Robert D., 1974: Radiative transfer due to atmospheric water vapor: global considerations of the earth's energy balance. J. Quant. Spectrosc. Radiat. Transfer, 14, 861-871.
- Cess, Robert D., 1975: Global climate change: an investigation of atmospheric feedback mechanisms. Tellus, 27, 193-198.
- Cess, Robert D., 1976: Climatic change: an appraisal of atmospheric feedback mechanisms employing zonal climatology. J. Atm. Sci., 33, 1831-1843.
- Chappel, J., 1974: Relationship between sea levels, <sup>18</sup>O variations and orbital perturbations, during the past 250,000 years. Nature, 252, 199-202.
- Charney, J. G., 1975: Dynamics of deserts and drought in the Sahel. Quart. J. Roy. Met. Soc., 101, 193-202.
- Charney, J., P. H. Stone and W. J. Quirk, 1975: Drought in the Sahara: a biogeophysical feedback mechanism. Science, 187, 434-435.

- Chernigovskiy, N. T., 1966: Radiational properties of the central Arctic ice coat. Soviet Data on The Arctic Heat Budget and its Climatic Influence, Part F, Rand Memorandum RM-5003-PR, 151-173.
- Chervin, Robert M., Warren M. Washington, and Stephen H. Schneider, 1976: Testing the statistical significance of the response of the NCAR general circulation model to North Pacific ocean surface temperature anomalies. J. Atm. Sci., 33, 413-423.
- Chylek, Petr and James A. Coakley, Jr., 1974: Aerosols and climate. Science, 183, 75-77.
- CLIMAP Project Members, 1976: The surface of the ice-age earth. Science, 191, 1131-1137.
- Coakley, James A. and Petr Chylek, 1975: The two-stream approximation in radiative transfer: including the angle of incident radiation. J. Atm. Sci., 32, 409-418.
- Coakley, J. A., Jr. and G. W. Grams, 1976: Relative influence of visible and infrared optical properties of a stratospheric aerosol layer on global climate. J. App. Met., 15, 679-691.
- Cohen, Theodore J. and Paul R. Lintz, 1974: Long term periodicities in the sunspot cycle. Nature, 250, 398-400.
- Cohen, Theodore J. and Erton I. Sweetser, 1975: The 'spectra' of the solar cycle and of data for Atlantic tropical cyclones. Nature, 256, 295-296.
- Currie, Robert G., 1974: Solar cycle signal in surface air temperature. J. Geophysical Res., 79, 5657-5660.
- Damon, Paul E. and Steven M. Kunen, 1976: Global cooling? Science, 193, 447-453.
- Dickinson, Robert E., 1974: Climatic effects of stratospheric chemistry. Can. J. Chem., 52, 1616-1624.
- Dickinson, Robert E., 1975: Solar variability and the lower atmosphere. Bull. Am. Met. Soc., 56, 1240-1248.
- Dyer, A. J., 1974: The effect of volcanic eruptions on global turbidity, and an attempt to detect long-term trends due to man. Quart. J. Roy. Met. Soc., 100, 563-571.
- Eddy, John A., 1976: The Maunder Minimum. Science, 192, 1189-1202.
- Ellis, James S. and Thomas H. VonderHaar, 1976: Zonal average earth radiation budget measurements from satellites for climate studies. Atm. Sci. Paper No. 240, Colorado State Univ., 57 pp.



- Fiocco, Giorgio, Gerald Grams and Alberto Mugosi, 1976: Energy exchange and temperature of aerosols in the earth's atmosphere (0-60 km). J. Atm. Sci., 33, 2415-2424.
- Foukal, P. V., P. E. Mack and J. E. Vernazza, 1977: The effect of sunspots and faculae on the solar constant. To be submitted to The Astrophysical J.
- GARP, 1974: Report of the International Study Conference on the Physical Basis of Climate and Climate Modeling, 29 July-9, August, 1974.
- Gates, W. Lawrence, 1976a: The numerical simulation of ice-age climate with a global general circulation model. J. Atm. Sci., 33, 1844-1873.
- Gates, W. L., 1976b: Modeling the ice-age climate. Science, 191, 1138-1144.
- Gates, W. Lawrence and Yale Mintz, 1974: Understanding Climatic Change: A Program for Action. Report of the Panel on Climatic Variation to the U.S. Committee for GARP. Nat. Academy of Sci., Wash., D.C., 317 pp.
- Gates, W. Lawrence and Michael E. Schlesinger, 1977: Numerical simulation of the January and July global climate with a two-level atmospheric model. J. Atm. Sci., 34, 36-76.
- Gordon, A. H. and N. C. Wells, 1976: Changes in temperature from month to month for central England for a quintile distribution. J. App. Met., 15, 928-932.
- Gribbin, John, 1973: Planetary alignments, solar activity and climatic change. Nature, 246, 453-454.
- Gribbin, John, 1975a: Man against nature in the climatic stakes. Nature, 258, 195-196.
- Gribbin, John, 1975b: Aerosol and climate: hotter or colder? Nature, 253, 162.
- Gribbin, John, 1976: Mason develops Milankovitch theory. Nature, 260, 396.
- Gribbin, John R. and Stephen H. Plagemann, 1974: The Jupiter Effect, Walker and Co., New York, 136 pp.
- Hays, J. D., John Imbrie and N. J. Shackelton, 1976: Variations in the earth's orbit: pacemaker of the ice ages. Science, 194, 1121-1132.
- Herman, Benjamin M. and Samuel R. Browning, 1975: The effect of aerosols on the earth-atmosphere albedo. J. Atm. Sci., 32, 1430-1445.

- Herman, Benjamin M., S. Robert Browning and Robert Rabinoff, 1976: The change in earth-atmosphere albedo and radiational equilibrium temperatures due to stratospheric pollution. J. App. Met., 15, 1057-1067.
- Hines, C. O. and I. Halevy, 1975: Reality and nature of a sun-weather correlation. Nature, 258, 313-314.
- Hobbs, P. V., H. Harrison and E. Robinson, 1974: Atmospheric effects of pollutants. Science, 183, 909-915.
- Houghton, David D., John E. Kutzbach, Michael McClintock and David Suchman, 1974: Response of a general circulation model to a sea temperature perturbation. J. Atm. Sci., 31, 857-868.
- Kellogg, William W., James A. Coakley Jr., and Gerald W. Grams, 1975: Effect of anthropogenic aerosols on the global climate. Proc. of the WMO/IAMAP Symposium on Long-Term Climatic Fluctuations, Norwich, 323-330.
- King, J. W., 1973: Solar radiation changes and the weather. Nature, 245, 443-446.
- King, J. W., E. Hurst, A. J. Slater, P. A. Smith and B. Tamkin, 1974: Agriculture and sunspots. Nature, 252, 2-3.
- Kondratyev, K. Ya. and G. A. Nikolsky, 1970: Solar radiation and solar activity. Quart. J. Roy. Met. Soc., 96, 509-522.
- Kraus, E. B., 1973: Comparison between ice age and present general circulations. Nature, 245, 129-133.
- Kukla, G. J., R. K. Matthews and J. M. Mitchell, 1972: The end of the present interglacial. Quaternary Res., 2, 261-269.
- Lacis, Andrew A. and James E. Hansen, 1974: A parameterization for the absorption of solar radiation in the earth's atmosphere. J. Atm. Sci., 31, 118-133.
- Lamb, H. H., 1970: Volcanic dust in the atmosphere: with a chronology and assessment of its meteorological significance. Roy. Phil. Soc. of London, Trans., Series A, 266, 425-533.
- Ledbetter, Michael T. and David A. Johnson, 1976: Increased transport of Antarctic Bottom Water in the Vema Channel during the last ice age. Science, 194, 837-839.
- Lockwood, G. W., 1975: Planetary brightness changes: evidence for solar variability. Science, 190, 560-562.
- London, Julius L., 1957: A study of the atmospheric heat balance. NYU Report AF 19(122)-165.

- Lorenz, Edward N., 1964: The problem of deducing the climate from the governing equations. Tellus, 16, 1-11.
- Lorenz, Edward N., 1968: Climatic determinism. Met. Monographs, 5, Vol. 8. No. 30, 1-3.
- Lorenz, Edward N., 1970: Climatic change as a mathematical problem. J. App. Met., 9, 325-329.
- Lorenz, Edward N., 1976: Nondeterministic theories of climatic change. Quaternary Res., 6, 495-506.
- Luther, Frederick M., 1976: Relative influence of stratospheric aerosols on solar and longwave radiative fluxes for a tropical atmosphere. J. App. Met., 15, 951-955.
- MacCracken, Michael C. and Gerald L. Potter, 1975: Comparative climatic impact of increased stratospheric aerosol loading and decreased solar constant in a zonal climate model. Proc. WMO/IAMAP Symposium on Long-Term Climatic Fluctuations, Norwich, 415-420.
- Machta, Lester and Kosta Telegadas, 1974: Inadvertant large-scale weather modification. Weather and Climate Modification, W. N. Hess, ed., 687-725.
- Manabe, Syukuro and Richard T. Wetherald, 1967: Thermal equilibrium of the atmosphere with a given distribution of relative humidity. J. Atm. Sci., 24, 241-259.
- McCrea, W. H., 1975: Ice ages and the galaxy. Nature, 255, 607-609.
- McGuirk, James P. and Elmar R. Reiter, 1976: A vacillation in atmospheric energy parameters. J. Atm. Sci., 33, 2079-2093.
- Meadows, A. J., 1975: A hundred years of controversy over sunspots and weather. Nature, 256, 95-97.
- Mitchell, J. Murray, 1961: Recent secular changes of global temperature. Ann. New York Acad. of Sci., 95, 235-250.
- Mitchell, J. M., 1963: On the world-wide pattern of secular temperature change. Changes of Climate, Arid Zone research XX, UNESCO, Paris, 161-181.
- Mitchell, J. M., 1967: Climatic variation (instrumental data). The Encyclopedia of Atmospheric Sciences and Astrogeology, Fairbridge ed., Reinhold Publ. Co., New York, 211-213.
- Mitchell, J. Murray, Jr., 1970: A preliminary evaluation of atmospheric pollution as a cause of the global temperature fluctuation of the past century. Global Effects of Environmental Pollution, S. Fred Singer, ed., 139-155.

- Mitchell, J. Murray, Jr., 1971: The effect of atmospheric aerosols on climate with special reference to temperature near the earth's surface. J. App. Met., 10, 703-714.
- Mitchell, J. Murray, 1972: The natural breakdown of the present interglacial and its possible intervention by human activities. Quaternary Res., 2, 436-445.
- Mitchell, J. M., 1974: The global cooling effect of increasing atmospheric aerosols: fact or fiction? Physical and Dynamic Climatology, WMO No. 347, 304-319.
- Mitchell, J. M., 1975: A reassessment of atmospheric pollution as a cause of long-term changes of global temperature. The Changing Global Environment, S. Fred Singer, ed., D. Reidel, Dordrecht-Holland, 149-173.
- Mitchell, J. M., 1976: An overview of climatic variability and its causal mechanisms. Quaternary Res., 6, 481-493.
- Mitchell, J. M., 1977: Carbon dioxide and our future climate. EDS Magazine, to be published.
- Mock, S. J. and W. D. Hibler III, 1976: The 20-yr oscillation in eastern North American temperature records. Nature, 261, 484-486.
- Monin, A. S. and I. L. Vulis, 1971: On the spectra of long-period oscillations of geophysical parameters. Tellus, 23, 337-345.
- Namias, Jerome, 1970: Macroscale variations in sea-surface temperatures in the North Pacific. J. Geophysical Res., 75, 565-582.
- Newell, Reginald E., 1974: Changes in the poleward energy flux by the atmosphere and ocean as a possible cause for ice ages. Quaternary Res., 4, 117-127.
- Newell, Reginald E., John W. Kidson, Dayton G. Vincent and George J. Boer, 1972: The General Circulation of the Tropical Atmosphere, Vol. 1, MIT Press, Cambridge, 258 pp.
- Newell, Reginald E. and Bryan C. Weare, 1976: Factors governing tropospheric mean temperature. Science, 194, 1413-1414.
- Ninkovich, Dragoslav and William L. Donn, 1976: Explosive Cenozoic volcanism and climatic implications. Science, 194, 899-906.
- North, Gerald R., 1975a: Analytical solutions to a simple climate model with diffusive heat transport. J. Atm. Sci., 32, 1301-1307.
- North, Gerald R., 1975b: Theory of energy-balance climate models. J. Atm. Sci., 32, 2033-2043.

- Oliver, Robert C., 1976: On the response of hemispheric mean temperature to stratospheric dust: an empirical approach. J. App. Met., 15, 933-950.
- Oort, Abraham H. and Eugene M. Rasmusson, 1971: Atmospheric circulation statistics. NOAA Professional Paper 5, 323 pp.
- Oort, Abraham H. and Thomas H. VonderHaar, 1976: On the observed annual cycle in the ocean-atmosphere heat balance over the Northern Hemisphere. J. Phys. Ocean., 6, 781-800.
- Otterman, J., 1975: Climatic change by cloudiness linked to the spatial variability of sea surface temperatures. Goddard Space Flight Center, Greenbelt, Maryland, X-910-75-54.
- Payne, Richard E., 1972: Albedo of the sea surface. J. Atm. Sci., 29, 959-970.
- Peterson, James T., 1973: Energy and the weather. Environment, 15, 4-9.
- Pisias, Niklas G., G. Ross Heath and Ted C. Moore, Jr., 1975: Lag times for oceanic responses to climatic change. Nature, 256, 716-717.
- Pollack, James B. and Owen B. Toon, 1974: A study of the effect of stratospheric aerosols produced by SST emissions on the albedo and climate of the earth. Proc. Third Conference on CIAP, Feb., 1974, USDOT, 457-460.
- Pollack, James B., Owen B. Toon and Carl Sagan, 1975: The effect of volcanic activity on climate. Proc. WMO/IAMAP Symposium on Long-Term Climatic Fluctuations, Norwich, 279-285.
- Press, Frank and Peter Briggs, 1975: Chandler Wobble, earthquakes, rotation, and geomagnetic changes. Nature, 256, 270-273.
- Pruppacher, Hans, 1973: The role of natural and anthropogenic pollutants in cloud and precipitation formation. Chemistry of the Lower Atmosphere, S. I. Rasool, ed., Plenum, New York.
- Radke, Lawrence F. and Peter V. Hobbs, 1976: Cloud condensation nuclei on the Atlantic seaboard of the United States. Science, 193, 999-1002.
- Ramanathan, V., 1975: Greenhouse effect due to chlorofluorocarbons: climatic implications. Science, 190, 50-51.
- Ramanathan, V., L. B. Callis and R. E. Boughner, 1976: Sensitivity of surface temperature and atmospheric temperature to perturbations in the stratospheric concentration of ozone and nitrogen dioxide. J. Atm. Sci., 33, 1092-1112.

- Rasool, S. I. and S. H. Schneider, 1971: Atmospheric carbon dioxide and aerosols: effects of large increases on the global climate. Science, 173, 138-141.
- Reck, Ruth A., 1974: Aerosols in the atmosphere: calculations of the critical absorption/backscatter ratio. Science, 186, 1034-1036.
- Reck, Ruth A., 1975: Aerosols and polar temperature changes. Science, 188, 728-730.
- Reitan, Clayton, H., 1974: A climatic model of solar radiation and temperature change. Quaternary Res., 4, 25-38.
- Roads, John Owen, 1977: Numerical experiments on the sensitivity of an atmospheric hydrologic cycle to the equilibrium temperature. Ph.D. thesis, Mass. Inst. Tech., 294 pp.
- Roberts, Walter Orr and Roger H. Olson, 1973: New evidence for effects of variable corpuscular emission of the weather. Rev. Geophys. and Space Phys., 11, 731-740.
- Roosen, Robert G., Robert S. Harrington, James Giles and Iben Browning, 1976: Earth tides, volcanoes and climate change. Nature, 261, 680-682.
- Ruderman, M. A. and J. W. Chamberlain, 1975: Origin of the sunspot modulation of ozone: its implications for stratospheric NO injection. Planet. Space Sci., 23, 247-268.
- Russell, Philip B. and Gerald W. Grams, 1975: Application of soil dust optical properties in analytical models of climate change. J. App. Met., 14, 1037-1043.
- Russell, Philip B. and Richard D. Hake, Jr., 1977: The post-Fuego stratospheric aerosol: lidar measurements, with radiative and thermal implications. J. Atm. Sci., 34, 163-177.
- Sachs, Harvey Maurice, 1976: Evidence for the role of the oceans in climate change: test of Weyl's theory of ice ages. J. Geophysical Res., 81, 3141-3150.
- Sagan, C. and J. B. Pollack, 1967: Anisotropic nonconservative scattering and the clouds of Venus. J. Geophysical Res., 72, 469-477.
- Saltzman, Barry and Anandu D. Vernekar, 1971: An equilibrium solution for the axially symmetric component of the earth's macroclimate. J. Geophysical Res., 76, 1498-1524.
- Sasamori, T., J. London and D. V. Hoyt, 1972: Radiation budget of the Southern Hemisphere. Met. Monographs, Vol. 13, No. 35, 9-23.

- Sawyer, J. S., 1964: Notes on the possible physical causes of long-term weather anomalies. WMO Tech. Note, No. 66, 227-248.
- Schneider, Stephen H., 1972: Cloudiness as a global climatic feedback mechanism: the effects on the radiation balance and surface temperature of variations of cloudiness. J. Atm. Sci., 29, 1413-1422.
- Schneider, Stephen H., 1975: On the carbon dioxide-climate confusion. J. Atm. Sci., 32, 2060-2066.
- Schneider, Stephen H. and Robert E. Dickinson, 1974: Climate modeling. Rev. Geophys. Space Phys., 12, 447-493.
- Schneider, Stephen H. and William W. Kellogg, 1973: The chemical basis for climate change. Chemistry of the Lower Atmosphere, S. I. Rasool, ed., 203-249.
- Schneider, Stephen H. and Clifford Mass, 1975: Volcanic dust, sunspots and temperature trends. Science, 190, 741-746.
- Schove, D. Justin, 1955: The sunspot cycle, 649 B.C. to A.D. 2000. J. Geophysical Res., 60, 127-146.
- Schutz, C. and W. L. Gates, 1971: Global climatic data for surface, 800 mb, 400 mb: January. Rand, R-915-ARPA, 173 pp.
- Schutz, C. and W. L. Gates, 1972a: Supplemental global climatic data: January. Rand, R-915/1-ARPA, 41 pp.
- Schutz, C. and W. L. Gates, 1972b: Global climatic data for surface, 800 mb, 400 mb: July. Rand, R-1029-ARPA, 180 pp.
- Schutz, C. and W. L. Gates, 1973a: Global climatic data for surface, 800 mb, 400 mb: April. Rand, R-1317-ARPA, 192 pp.
- Schutz, C. and W. L. Gates, 1973b: Supplemental global climatic data: January. Rand, R-915/2-ARPA, 38 pp.
- Schutz, C. and W. L. Gates, 1974a: Global climatic data for surface, 800 mb, 400 mb: October. Rand, R-1425-ARPA, 192 pp.
- Schutz, C. and W. L. Gates, 1974b: Supplemental global climatic data: July. Rand, R-1029/1-ARPA, 38 pp.
- Schuermans, C. J. E., 1969: The influence of solar flares on the tropospheric circulation. Medelingen en Verhandelingen, No. 92, 122 pp.
- Sellers, William D., 1969: A global climatic model based on the energy balance of the earth-atmosphere system. J. App. Met., 8, 392-400.

- Sellers, William D., 1973: A new global climatic model. J. App. Met., 12, 241-254.
- Sellers, William D., 1974: A reassessment of the effect of CO<sub>2</sub> variations on a simple global climatic model. J. App. Met., 13, 831<sup>2</sup>-833.
- Sellers, William D., 1976: A two-dimensional global climatic model. Mon. Wea. Rev., 104, 233-248.
- Shapiro, Ralph, 1976: Solar magnetic sector structure and terrestrial atmospheric vorticity. J. Atm. Sci., 33, 865-870.
- Sleeper, H. P., Jr., 1972: Planetary resonances, bi-stable oscillation modes, and solar activity cycles, Northrup Services, Huntsville, NASA, Wash., D.C., NASA CR-2035, 56 pp.
- Sleeper, H. Prescott, Jr., 1974: Natural variations of the climate. Bull. Am. Met. Soc., 55, 864.
- Sleeper, H. Prescott, 1975: Solar activity prediction methods. Northrup Services, Huntsville.
- SMIC, 1971: Inadvertant Climate Modification, MIT Press, Cambridge, 308 pp.
- Somerville, R. C. J., P. H. Stone, M. Halem, J. E. Hansen, J. S. Hogan, L. M. Druyan, G. Russell, A. A. Lacis, W. J. Quirk and J. Tenenbaum, 1974: The GISS model of the global atmosphere. J. Atm. Sci., 31, 84-117.
- Staley, D. O. and G. M. Jurica, 1970: Flux emissivity tables for water vapor, carbon dioxide and ozone. J. App. Met., 9, 365-372.
- Starr, Victor P. and Abraham H. Oort, 1973: Five-year climatic trend for the Northern Hemisphere. Nature, 242, 310-313.
- Stone, Peter H., 1973: The effect of large scale eddies on climatic change. J. Atm. Sci., 30, 521-529.
- Stone, P. H., S. Chow and W. J. Quirk, 1977: The July climate and a comparison of the January and July climates simulated by the GISS general circulation model. Mon. Wea. Rev., 105, 170-194.
- Suarez, Max J. and Isaac M. Held, 1976: Modeling climatic response to orbital parameter variations. Nature, 263, 46-47.
- Tennekes, H., 1973: The logarithmic wind profile. J. Atm. Sci., 30, 234-238.
- Toon, Owen B. and James B. Pollack, 1976: A global average model of atmospheric aerosols for radiative transfer calculations. J. App. Met., 15, 225-246.



- Twomey, S., 1971: The influence of atmospheric particles on cloud and planetary albedo. Preprints, Intern. Conf. on Weather Modification, Am. Met. Soc., 265-266.
- Ulrich, Roger K., 1975: Solar neutrinos and variations in the solar luminosity. Science, 190, 619-624.
- VonderHaar, Thomas H. and Abraham H. Oort, 1973: New estimate of annual poleward energy transport by Northern Hemisphere oceans. J. Phys. Ocean., 3, 169-172.
- Vowinckel, E. and S. Orvig, 1970: The climate of the North Polar Basin. World Survey of Climatology, Vol. 14, H. Landsberg, ed., 129-252.
- Wang, W. C., Y. L. Yung, A. A. Lacis, T. Mo and J. E. Hansen, 1976: Greenhouse effects due to man-made perturbations of trace gases. Science, 194, 685-690.
- Washington, Warren M., 1972: Numerical climatic-change experiments: the effect of man's production of thermal energy. J. App. Met., 11, 768-772.
- Weare, Bryan C., Richard L. Temkin and Fred M. Snell, 1974: Aerosol and climate: some further considerations. Science, 186, 827-828.
- Weertman, Johannes, 1976: Milankovitch solar radiation variations and ice age ice sheet sizes. Nature, 261, 17-20.
- Weickmann, Helmut K. and Rudolf F. Pueschel, 1974: Atmospheric aerosols: residence times, retainment factors and climatic effects. Contributions to Atmospheric Physics, 46, 112-118.
- Welch, Ronald and Wilford Zdunkowski, 1976: A radiation model of the polluted atmospheric boundary layer. J. Atm. Sci., 33, 2170-2184.
- Wetherald, R. T. and S. Manabe, 1975: The effect of changing the solar constant on the climate of a general circulation model. J. Atm. Sci., 32, 2044-2059.
- Weyl, P. K., 1968: The role of oceans in climatic change: a theory of the ice ages. Met. Monogr., 8, 37-62.
- Wiesnet, Donald R. and Michael Matson, 1975: Monthly winter snowline variations in the Northern Hemisphere from satellite records, 1966-75. NOAA Tech. Mem. NESS 74, 21 pp.
- Wilcox, John M., 1976: Solar structure and terrestrial weather. Science, 192, 745-748.

- Wilcox, John M., Leif Svalgaard and Philip H. Scherrer, 1976: On the reality of a sun-weather effect. J. Atm. Sci., 33, 1113-1116.
- Willett, Hurd C., 1962: The relationship of total atmospheric ozone to the sunspot cycle. J. Geophysical Res., 67, 661-670.
- Willett, Hurd C., 1974: Do recent climatic trends portend an imminent ice age? Geofisica Internacional, 14, 265-302.
- Williams, Jill, R. G. Barry and W. M. Washington, 1974: Simulation of the atmospheric circulation using the NCAR global circulation model with ice age boundary conditions. J. App. Met., 13, 305-317.
- Wood, Charles A. and Raymond R. Lovett, 1974: Rainfall, drought and solar cycle. Nature, 251, 594-596.
- Yamamoto, Ryozauro, Tatsuya Iwashima and Makoto Hoshai, 1975: Change of the surface air temperature averaged over the Northern Hemisphere and large volcanic eruptions during the years 1951-1972. J. Met. Soc. Japan, 53, 482-486.
- Zdunkowski, Wilford G., Ronald M. Welch, and Jan Paegle, 1976: One-dimensional numerical simulation of the effects of air pollution on the planetary boundary layer. J. Atm. Sci., 33, 2399-2414.

BIOGRAPHICAL NOTE

I was born in Boston on September 7, 1949, and left a few months later to begin my world travels. My father changed jobs frequently, and I lived successively in Alcoa and Knoxville, Tennessee; Rio de Janeiro and Fortaleza, Brazil; Kansas City, Missouri; Prairie Village, Kansas; and Rye, New York. Next we moved to Bloomington, Indiana, where I lived the longest and was able to attend junior high school and senior high school all in one city. I went to the University of Wisconsin where I protested the Vietnam War and received a B.A. in 1970. I then joined the Peace Corps and worked for two years in the Philippines teaching teachers in the fishery vocational schools how to teach meteorology. One of the best parts of my experience was my trip home through Asia and Europe. I particularly enjoyed Bali, where seeing the results of the eruption of Gunung Agung on the ground may have inspired me to study its effects on climate in this thesis. I returned to the land of my birth in 1972 and have attended MIT since then, receiving an S.M. in 1974. My publications to date are:

Robock, Alan, 1972: Course Outline in Meteorology, (Bureau of Vocational Education, Fishery Education Division, Manila, Philippines), 44 pp.

Bornstein, Robert D. and Alan D. Robock, 1976: Effects of variable and unequal time steps for advective and diffusive processes in simulations of the urban boundary layer. Monthly Weather Review, 104, 260-267.

Robock, Alan, 1975: On the eddy structure of hurricanes. Quart. J. Roy. Met. Soc., 101, 657-663.

Robock, Alan, 1976: Reply [to comments on above paper by J.S.A. Green and H. Riehl]. Quart. J. Roy. Met. Soc., 102, 453-455.